

Department of Precision and Microsystems Engineering

Design and comparison of high speed cable driven parallel pick and place robots, performing a Schönflies motion.

Pim van der Stigchel

Report no : 2021.037
Coach : Dr. P. Tempel
Professor : Dr. Ir. V. van der Wijk
Specialisation : Mechatronic System Design
Type of report : MSc. Thesis
Date : 7 July 2021

Design and comparison of high speed cable driven parallel pick and place robots, performing a Schönflies motion.

by

Pim van der Stigchel

to obtain the degree of Master of Science

at the Delft University of Technology,

Wednesday July 7, 2021.

Student number:	4588010	
Thesis committee:	Prof. dr. ir. J. L. Herder,	TU Delft
	Dr. Ir. V. van der Wijk,	TU Delft
	Dr. P. Tempel,	TU Delft
	Dr. M. Alfeld,	TU Delft

An electronic version of this thesis is available at <http://repository.tudelft.nl/>.



Preface

This report covers a research into the application of cable driven parallel robots in the high speed pick and place industry. It has been written to obtain a masters degree in mechanical engineering at the department of Precision and Microsystems Engineering at the TU Delft.

The core of this thesis consists of two parts, being a literature survey, and a project in which new designs are compared and evaluated. Both parts are present in a paper format and can be read independently. A general discussion and conclusion can be found at the end of the report.

I would like to thank my supervisors Philipp Tempel and Volkert van der Wijk for their support during my thesis. Our regular meetings gave me new insights and positive energy. I would also like to thank the student workshop (IWS) for their guidance during the fabrication of the prototype, and Jos van Driel for his support with the measurement setup and the supplies of the measurement devices. Furthermore, thanks to Just Herder and Matthias Alfeld of the committee for your time and effort to read and grade my report.

Contents

1	Introduction	3
2	Challenges for cable driven parallel robots in the high speed pick and place industry.	6
3	Design, comparison and experimental evaluation of a high speed cable driven parallel pick and place robot, performing a Schönflies motion.	17
4	Discussion	29
5	Conclusions	32
	Bibliography	35
	Appendices	36

Chapter 1

Introduction

Nowadays, a factory can not go without a robot. A robot ensures a constant quality, a high throughput of products, and a flexibility in tasks it can perform. Additionally, a robot can do tasks that humans do not want to do or when it simply outperforms a human. This is also the case when pick and place tasks need to be performed, for instance in the assembly, packaging, bin picking, or the inspection industry [1]. When chocolate bars roll out of the production line and need to be packaged in a box, a pick and place robot can do this task with high accuracy and speed. Also selecting and picking products that do not meet the standard product quality are a common task of these robots. Parallel robots have been widely applied to perform such tasks, due to their high load carrying capacity and their high accuracy [2]. These aspects are common for parallel robots as each leg or kinematic chain is added in parallel, meaning that the stiffness enhances and the load is distributed among more legs. Therefore, the mass of the moving parts can be low which is favourable in high speed pick and place applications. Especially the Delta configuration [3], as shown in figure 1.1, is often used in the high speed pick and place industry. Take for instance the commercially available Delta robots by ABB [4] and Omron [5] that are applied all over the world because of their low cycle time, and high accuracy and repeatability. Cycle times go up to 0.30s on a 25/305/25mm path for 0.1kg payload, with a repeatability of 0.1mm. During this motion, the EE can be fully rotated about the vertical axis with a repeatability of 0.4° .

Another class of Parallel robots are the Cable Driven Parallel Robots (CDPRs), as shown in figure 1.2. These robots actuate the end effector (EE) or moving platform by only cables that are wound on winches, which are located on a frame. Replacing the traditional links of a parallel robot by cables has a number of advantages. The cable masses are low but can still handle large tensile forces, and the cable lengths are hardly limited. This results in cable driven parallel robots with low inertia, low power consumption, and easily scalable workspaces, which makes them attractive for application in the high speed pick and place industry [6, 7]. Several research projects have been performed on CDPRs in high speed and pick and place applications such as the FALCON project by Kawamura et al. [8,9] where a high speed CDPR was designed that can reach accelerations up to 40G and speeds up to 13m s^{-1} for a 150g load. Also the IPAnema family of CDPRs was designed for handling and fast pick and place operations [10,11]. For instance, the IPAnema 1 can reach up to 10m s^{-1} speed and has a maximum acceleration of 100m s^{-2} for payloads up to 3kg. It was proven that this robot is feasible for application in handling and assembly operations by the ISO9283 norm [10]. Likewise, the pick and place CDPR by Zhang et al. [7,12], as shown in figure 1.3, can reach 125 cycles per minute with a precision of 0.12mm on an



Figure 1.1: Delta robot by ABB.

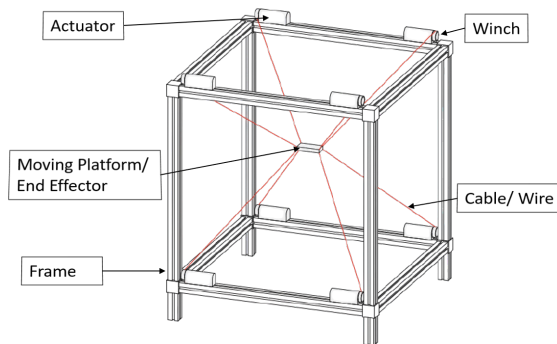


Figure 1.2: Typical layout of a CDRP.

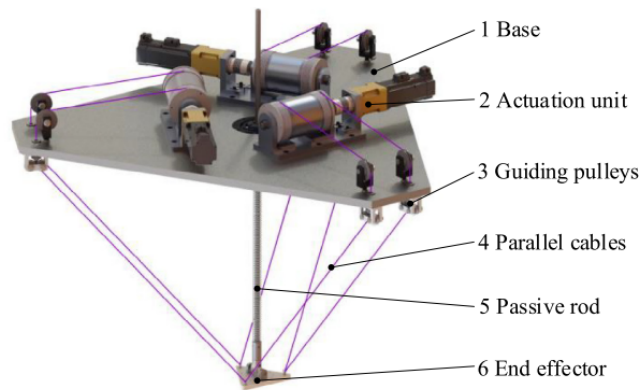


Figure 1.3: High speed CDRP containing a spring rod to tension the cables.

arc shaped 25/305/25mm path with a load of 0.1kg. This was performed by using a compressive spring rod to keep the wires under tension. This design is an evolution of the DeltaBot [13] where the lower limbs of a Delta robot are replaced by cables and a compressive spring rod was put in the centre to keep the cables under tension. In this fashion the inertia of the system is reduced which yields accelerations of 124m s^{-2} and speeds up to 4.1m s^{-1} resulting in 120-150 cycles per minute for a 400g payload on a 25/305/25mm path. Furthermore, the MARIONET CDRP [14] was designed with linear actuators instead of winches allowing for faster motion [15]. Therefore, application of the MARIONET in the pick and place industry was suggested. Finally, the SEGESTA robot [15] was designed for vibration testing and is capable of accelerations up to 200m s^{-2} for a load of 150g.

Despite all these researches, showing high potential of CDRPs in high speed pick and place applications, a CDRP has not yet been applied in the industry. One of the reasons that CDRPs are not yet attractive for this industry is their limited orientation range. In pick and place applications it is often required to not only translate a product, but also reorient it about one axis for proper packaging. This motion is also known as a Schönflies motion. For full product reorientation, a rotation of 180 degrees is required, which can only be achieved with an additional axis on the moving platform [16]. Multiple CDRPs that can perform a rotation of 180 degrees or

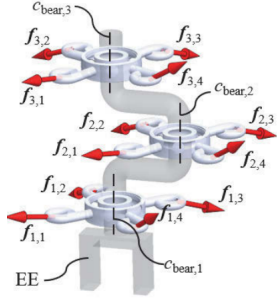


Figure 1.4: Multi-platform design for infinite rotation [19].

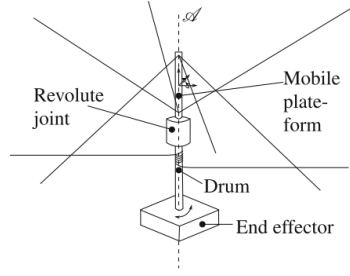


Figure 1.5: Revolute joint and two extra cables to perform large rotations [20].

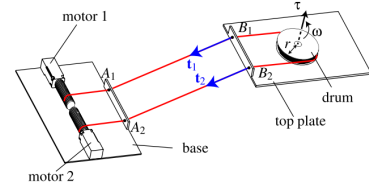


Figure 1.6: Bi actuated cable loop enabling large rotations and translations of the EE [26].

more exist in literature. Pinto et al. added a motor in series to the EE [17]. Other designs use only cables to perform the rotation. For instance by using a multi-platform approach [16, 18, 19], where the EE is shaped as a crankshaft and each of the 3 crankshaft parts are actuated by four cables as shown in figure 1.4. By moving the inner platform relative to the outer platform, an infinite rotation can be achieved. Other solutions use a revolute joint added between the moving platform and the EE and a pair of cables connected to this EE to perform the rotation [20–22], this solution is shown in figure 1.5. Also a passive reconfiguration mechanism for the cable anchor points on the EE is considered to enhance the orientation [23]. However, this solution does not reach 180 degrees of rotation. Additionally, reorientation of the base along a circular track is proposed for full EE reorientation [24]. Finally, bi actuated cable loops have been proposed for performing large rotations [25]. A bi actuated cable loop contains a cable wrapped around a pulley, with both ends connected to an actuator as shown in figure 1.6. In this way the pulley can perform both a translation and a rotation. Combining these cable loops with Omni-wheels on a sphere [26] or a differential like mechanism even multiple rotations are added to the EE [27, 28]. Despite having numerous conceptual solutions for performing a large rotation, none of them were properly designed, modelled, compared or tested for high speed applications.

The goal of this thesis is to make CDPRs more attractive for pick and place tasks by proposing designs of CDPRs for high speed applications that can perform a Schönflies motion including a rotation of at least 180 degrees, and dynamically compare and evaluate them. Chapter 2 contains a literature review paper that identifies the challenges for CDPRs in the high speed pick and place industry and investigates how far these have already been overcome, including the challenge of performing a Schönflies motion containing a rotation of at least 180 degrees. In chapter 3, designs of CDPRs are proposed that can perform a Schönflies motion including a rotation of 180 degrees. These designs are compared on their optimized dynamic workspace, and a prototype is made and experimentally evaluated of the design with the highest potential. This chapter is followed by a general discussion and conclusion in chapters 4 and 5 respectively.

Chapter 2

**Challenges for cable driven
parallel robots in the high speed
pick and place industry.**

Challenges for cable driven parallel robots in the high speed pick and place industry

Pim van der Stigchel

Abstract—Cable driven parallel robots (CDPRs) are not yet applied in the high speed pick and place industry, despite having a high potential. Therefore, this paper identifies why parallel cable robots are not yet applied in the high speed pick and place industry and what should be done to achieve this by performing a literature study. The study showed that three challenges exist for CDPRs in the high speed pick and place industry being; performing a Schönflies motion including a rotation of at least 180 degrees, avoiding collisions between the CDPR and the environment, and vibration attenuation for a higher dynamic performance. Literature showed that multiple solutions for Schönflies motion generation exist, but they increase complexity or cost and are not evaluated on their dynamical performance. Additionally, avoiding collisions with the environment has already been overcome by smart geometrical CDPR design. Furthermore, control methods are considered for vibration attenuation but their performance should increase by the use of more sophisticated models.

Index terms: Cable driven parallel robots - Schönflies motion generation - Collision avoidance - Vibration attenuation

I. INTRODUCTION

Parallel robots have been widely applied in the pick and place industry due to their high load carrying capacity and their high accuracy [1]. These aspects are common for parallel robots as each leg or kinematic chain is added in parallel, meaning that the stiffness enhances and the load is distributed among multiple legs. Therefore, the mass of the moving parts can be low which is favourable in high speed pick and place applications. Especially the Delta configuration [2] is often used in the High Speed Pick and Place industry. The End Effector (EE) of a Delta robot contains three translational degrees of freedom (DOF) and the kinematic chains are actuated by three or four lumped arms, as shown in figure 4. Take for instance the commercially available Delta robots by ABB [3] and Omron [4] that are applied all over the world because of their low cycle time, and high accuracy and repeatability. Cycle times go up to 0.30s on a 25/305/25mm path for 0.1kg payload, with a repeatability of 0.1mm.

Another class of Parallel robots are the Cable Driven Parallel Robots (CDPRs). A typical layout of a CDPR is shown in figure 1, where the EE is driven by only cables that are wound on winches located on a frame. These CDPRs have been researched increasingly since the last couple of decades and show a high potential to be applied in the high speed pick and place industry. Namely, their inertia is low because the cable masses are small. This means they can have high accelerations with relatively little power consumption. Additionally, their load capacity is high since cables can handle large tensile forces, and their translational workspace

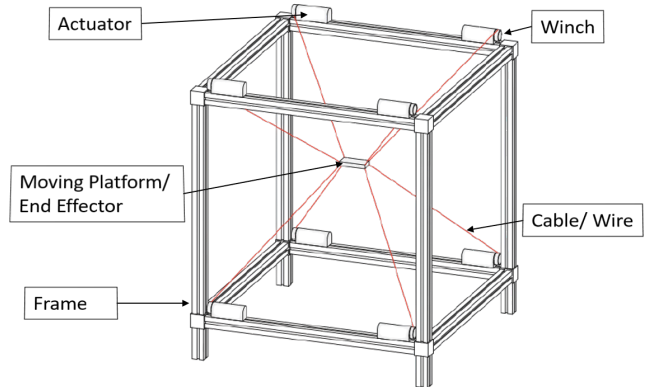


Fig. 1: Typical layout of a CDPR [7].

can be large and is easily scalable [5]. Therefore, CDPRs provide a potential method to improve efficiency and reduce the cost of pick and place robots [6].

Several research projects have been performed on CDPRs in high speed and pick and place applications such as the FALCON project by Kawamura et al. [8], [9] where a high speed CDPR was designed that can reach accelerations up to 40G and speeds up to 13m s^{-1} for a 150g load. Also the IPAnema family of CDPRs was designed for handling and fast pick and place operations [10], [11]. For instance, the IPAnema 1 can reach up to 10m s^{-1} speed and has a maximum acceleration of 100m s^{-2} for payloads up to 3kg. It was proven that this robot is feasible for application in handling and assembly operations by the ISO9283 norm [10]. Likewise, the pick and place CDPR by Zhang et al. [6], [12] can reach 125 cycles per minute with an accuracy of 0.12mm on an arc shaped 25/305/25mm path with a load of 0.1kg. This was performed by using a compressive spring rod to keep the wires under tension, shown in figure 2. This design is an evolution of the DeltaBot [13] where the lower limbs of a Delta robot are replaced by cables and a compressive spring rod was put in the centre to keep the cables under tension. In this fashion the inertia of the system is reduced which yields accelerations of 124m s^{-2} and speeds up to 4.1m s^{-1} resulting in 120-150 cycles per minute for a 400g payload on a 25/305/25mm path. Furthermore, the MARIONET CDPR [14] was designed with linear actuators instead of winches allowing for faster motion [7]. Therefore, application of the MARIONET in the pick and place industry was suggested. Finally, the SEGESTA [7] robot was designed for vibration testing and is capable of accelerations up to 200m s^{-2} for a load of 150g. Despite

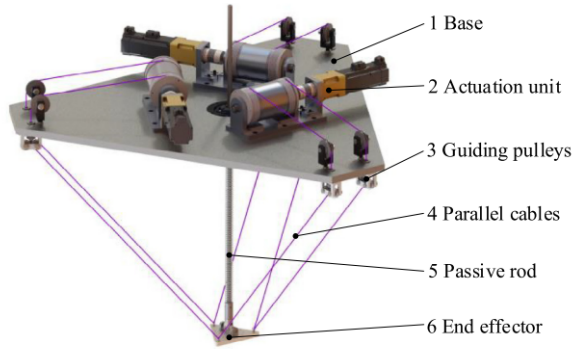


Fig. 2: High speed pick and place CDPR containing a compressive spring rod to keep the wires under tension [6].

all these researches, showing high potential of CDPRs in high speed pick and place applications, a CDPR has not yet been applied in the industry, which is surprisingly!

The goal of this work is to identify why parallel cable robots are not yet applied in the high speed pick and place industry and what should be done to achieve this, by reviewing the existing literature. To reach this goal, challenges for CDPRs in high speed pick and place applications have been identified. Thereafter, existing literature was reviewed to see how far these challenges have already been overcome and what still should be done to overcome these challenges and get the CDPRs applied in the pick and place industry.

Consequently, the paper is structured as follows; first the basics of CDPRs that are needed for the other parts of the paper are given in section II. Then the challenges for CDPRs in high speed pick and place applications are derived and discussed in section III. Next the literature on each challenge is reviewed in sections IV, V, and VI. Finally, a conclusion is given in section VII.

II. BASICS ON PARALLEL CABLE ROBOTICS

A. Classifications

CDPRs can be classified by the number of cables m and the number of controllable degrees of freedom n . Here, the classification is explained according to the book by Andreas Pott [7], where the following classes are determined:

- $m < n < 6$: This class is called incompletely restrained positioning mechanisms (IRPM), since the CDPR is not able to withstand arbitrary applied wrenches in most of the cases.
- $n = m$: Despite being kinematically fully constrained, still a limited range of wrenches can be resisted since the cables can only resist tensile forces. Therefore, this class is also considered belonging to the IRPM robots.
- $n + 1 = m$: This class of robots is called completely restrained positioning mechanisms (CRPM). The robot is fully-constrained, meaning that the applied wrenches are only limited by the minimum and maximum applicable cable forces.
- $n + 1 < m$: This class is called redundantly restrained positioning mechanisms (RRPM). The robot is redun-

dantly constrained, meaning that the applied wrenches are only limited by the minimum and maximum applicable cable forces. The forces have to be distributed among the cables.

Another classification that is often used is *suspended* CDPR. This means that gravity is used to restrain the CDPR instead of cables that are pointing downwards from the EE. Suspended CDPRs can be of all classes discussed above (IRPM, CRPM, RRPM) [7].

B. Motion Patterns

Motion patterns can be used to indicate what DOFs of the EE a CDPR is able to control. These motion patterns are notated with the $n_R n_T$ representation where R and T are used as abbreviations of Rotation and Translation respectively. The n_R and n_T variables indicate the number of rotational and translational DOFs. Verhoeven researched the possible motion patterns a completely restrained CDPR can make [15], which resulted in the following list:

- 1T, linear motion of a body
- 2T, planar motion of a point
- 1R2T, planar motion of a body
- 3T, spatial motion of a point
- 2R3T, spatial motion of a beam
- 3R3T, spatial motion of a body

C. Workspaces

The workspace of a CDPR can be complex. Therefore, subsets of the workspace are often used in literature. Some frequently used geometric descriptions of the workspace subsets are listed below [7]:

- Constant Orientation Workspace: Also called translational workspace contains the positions that belong to the workspace for a fixed orientation of the EE. This workspace is two-dimensional for planar robots and three-dimensional for spatial robots.
- Orientation Workspace: This is a subset of the workspace for one given position of the EE, showing the possible orientations at this position. The dimension of this workspace is one-dimensional for the 1R2T motion pattern, two-dimensional for the 2R3T motion pattern, and three-dimensional for the 3R3T motion pattern.
- Total Orientation Workspace: This workspace subset contains all positions of the EE at which a predetermined set of orientations is feasible. The dimensions of this workspace are the same as for the constant orientation workspace.

To determine if a pose (position and orientation) belongs to the discussed workspaces, several criteria exist. The first criterion is the cable length. The maximum available cable length on the winches limits the reachable poses of the CDPR [7]. A second criterion is the wrench-closure criterion. Wrench-closure means that a pose belongs to the workspace if an arbitrary wrench can be applied to the EE and can be balanced by a positive set of cable forces [5]. Instead of the wrench closure criterion, the wrench feasible criterion

can be used. This criterion is less restrictive and says that a pose belongs to the workspace if a set of predetermined wrenches can be balanced by sets of positive cable forces [5]. To determine if the cable forces are all positive for a certain pose, force distribution calculation algorithms are needed when more cables than degrees of freedom are used. The force distribution can be determined by for instance the closed-form method [16], [17] or the Dijkstra method [18]. These methods can also take minimum and maximum cable forces into account, instead of the positive force requirement. A third criterion that restricts the workspace is known as singularities. These are poses where the CDPR loses or gains controllable DOFs [7]. For purely translational motion patterns no singularities can occur [15]. Also collisions can restrict the workspace and therefore can be seen as a criterion. A pose does not belong to the workspace if a collision occurs at this pose. Collisions can occur between cables, between a cable and the EE, between a cable and the environment, and between the EE and the environment. Going beyond workspace determination, synthesis methods exist. These methods compute the winch positions, or the anchor points of the cables on the frame, for a predetermined workspace [19], [20].

III. CHALLENGES IN HIGH SPEED PICK AND PLACE APPLICATIONS

Three challenges for CDPRs in high speed pick and place applications have been derived. One of the challenges for CDPRs, which also applies to high speed pick and place CDPRs, is their limited orientation workspace [21], [22]. Namely, in pick and place applications it is often required to not only translate but also rotate about the vertical axis to reorient asymmetric products [23], [24]. Full product reorientation requires a minimum rotation angle of 180 degrees. This motion, containing three translational DOFs and one rotational DOF, is known as a Schönflies motion. According to Verhoeven [15], this motion class 1R3T is not part of the motion patterns that CDPRs can produce. Therefore, the Schönflies motion should be performed using the 3R3T or 2R3T classes by proper control or by constraining the unnecessary DOFs. For instance, by connecting two or more cables to one actuator [7]. However, rotations are still limited for CDPRs due to cable-cable collisions and cable-moving platform collisions [25]–[27]. These collisions should be avoided because tension drift in the cables might arise which affects the controllability [28]. Additionally, the orientation workspace is dependent on the applied load on the EE [29]. As mentioned in [24], rotation for conventional redundantly restrained CDPRs is limited to ± 45 degrees. This is not sufficient for pick and place tasks. Therefore, the first challenge for CDPRs in the high speed pick and place industry is: *Performing a Schönflies motion that contains a rotation of at least 180 degrees without interference among cables.*

A second issue for CDPRs in pick and place applications is the collision of their cables with the environment [5], [30]. A typical pick and place environment is shown in figure 3.

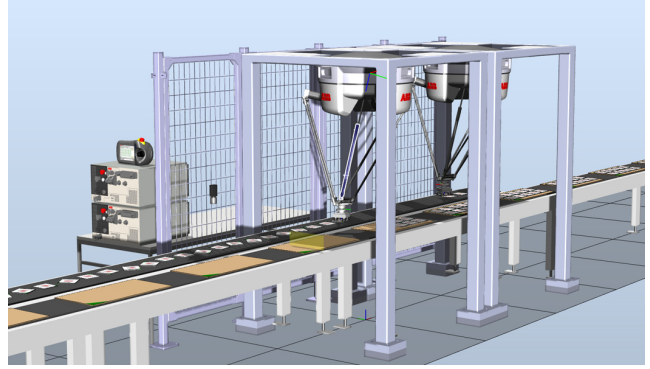


Fig. 3: Typical pick and place environment [3].

It contains conveyor belts or transport lines, and a robot to pick and place a product from one transport line to the other. Collisions with the environment should be avoided because this affects the controllability of the robot and might damage the environment or the robot. In pick and place applications, these collisions could occur between a cable and a conveyor belt or a product [6]. Also collisions with other pick and place robots could occur, but this is disregarded as this is easily avoided by leaving enough space between the robots. Especially for non-suspended CDPRs the risk of collisions with the environment is higher as they have more cables than suspended CDPRs and cables that are both heading down and upwards from the EE. Nevertheless, non-suspended CDPRs should be used in high speed pick and place applications since their acceleration in downward direction can be larger than gravity. Thus, collisions mean that the workspace of the CDPR is limited and could result in the CDPR not being able to pick or place a product without interference. Therefore, the second challenge for CDPRs in high speed pick and place applications is: *Avoiding collisions of the CDPR with the Environment.*

The third challenge is applicable to high speed applications, including high speed pick and place, and involves the stiffness of the CDPR. The stiffness of a CDPR is relatively low compared to rigid link parallel manipulators, due to the flexibility of the cables [31]. Therefore, vibrations are easily induced by changing accelerations, and friction in for instance the pulleys [32]. This has a significant effect on position accuracy, trajectory tracking, settling time, force distribution, and control [32], [33]. So vibrations are of concern when high dynamic performance or high bandwidth is required [34]. Take for instance the pick and place CDPR by Zhang et al. which performance turned out to be limited by vibrations [6]. Accordingly, the third challenge is proposed as: *Attenuation of vibrations for a higher dynamic performance.*

A fourth challenge could be the minimization of the installation space relative to the workspace of the CDPR. Large installation spaces are a common disadvantage of parallel robots [7]. Despite, this disadvantage was not specifically named for high speed pick and place CDPRs. Moreover, optimization methods can be applied to minimize the installation



Fig. 4: FlexPicker Delta robot by ABB [3].

space with respect to the workspace [7], [19]. Consequently, as straight forward methods can be used to overcome this problem and it was not named as a specific problem for high speed pick and place CDPRs, this topic will not be further investigated in this paper.

Likewise, other challenges as force distribution calculation, workspace determination, and CDPR design synthesis are not considered in this paper since they are non specific to high speed pick and place, or seen as part of the basics of CDPRs.

IV. SCHÖNFLIES MOTION GENERATION

The first challenge was identified as: *Performing a Schönflies motion that contains a rotation of at least 180 degrees without interference among cables.* In Delta robots, which usually contain only translational degrees of freedom, a rotation is usually performed by adding a telescopic cardan shaft from the base to the EE for torque transmission [3], [4], see for instance figure 4. Also adding a motor to the EE was used for performing a rotation [35]. Some researches also tried to implement the Schönflies motion by adding a fourth actuated kinematic chain to the Delta robot to overcome the negative dynamic effects of the telescopic cardan shaft and the added motor [23], [36]–[41]. This redundancy is then used to actuate an internal degree of freedom which is converted to a rotation of the EE. However, besides the telescopic cardan shaft and the added motor only the Par4 design [36], [40] made it to the industry [4].

The maximum rotation angle for redundantly restrained CDPRs was identified to be ± 45 degrees by Reichenbach et al. [24] which implies that a Schönflies motion with a rotation larger than 180 degrees can only be achieved by extra actuated axis on the EE [21]. In CDPR researches, several solutions are presented for the generation of a Schönflies motion containing a rotation of at least 180 degrees. A first logical solution is adding a motor in series to the EE [42], see figure 5a. However, this adds inertia to the EE resulting in a lower dynamic performance, smaller workspace or a lower admissible payload [43]. Also a power line has to be

supplied to the EE [22], [25]. Therefore, other solutions are proposed that only use cables to enable a Schönflies motion. For instance by using a multi-platform approach, where the EE is shaped as a crankshaft and each of the 3 crankshaft parts are actuated by four cables [21], [24], [43], see figure 5b. By moving the inner platform relative to the two outer platforms, an infinite rotation can be performed. This rotation can be executed while maintaining tension in the cables and avoiding cable-cable collision. However, this geometry requires twelve cables and actuators which is a disadvantage in terms of cost and complexity [21]. Furthermore, the dynamic performance was not researched yet, so no conclusions can be drawn on high speed applications. Another CDPR design, which involves less cables to perform a Schönflies motion, has a revolute joint connected with one end to the moving platform and with the other end connected to the EE [22], see figure 5c. Two extra cables are coupled to the EE to perform the rotation. Since the torques about the axis through the revolute joint cannot be transferred to the moving platform, the moving platform can be of the 2R3T type. Therefore, this design requires only eight cables in total. However, the cables on the EE increase the risk of interference which has a negative effect on the workspace. The same concept was applied in 2D by Reddy et al. [29], see figure 5d. Here only one extra cable is implemented to control the rotation. If this cable is pulled, the cable unwinds on the EE which leads to a rotation. When the pulling force is released a spring ensures the mechanism to go back to its home position. Furthermore, a revolute joint is applied in a 3D design where eight cables in pairs are wrapped around the EE for the generation of a rotation [44], see figure 5e. Nevertheless, using four cable pairs instead of one to actuate the rotation seems rather inconvenient. Additionally, this paper does not provide a proof of principle in the form of a model or in an experiment. A different approach that does not require extra cables is proposed by Anson et al. [45]. Anson is using a reconfigurable base along a circular track for a higher workspace dexterity and the ability to fully reorient the EE, see figure 5f. Anyhow, a reconfigurable base is considered to raise cost and complexity [22]. Next to the base reconfiguration, also a passive reconfiguration mechanism on the EE is considered to enhance the orientation workspace [46], see figure 5g. This concept was tested on a 2D robot. However, rotations did not meet the 180 degrees requirement. In addition to these researches, some even go beyond the Schönflies motion and add multiple rotations to the mobility of the EE. This was mostly achieved by the use of bi-actuated cable loops [47]. A bi-actuated cable loop contains a cable wrapped around a pulley, with both ends connected to an actuator. In this way the pulley can perform a translation and a rotation. This concept was applied in combination with Omni-wheels on a sphere to gain three rotational DOFs [26], see figure 5h. Cable loops were also applied in a CDPR with an embedded tilt-roll wrist [25], [48], see figure 5i. Here the cable loops actuate a differential-like mechanism, adding two rotational DOFs to the EE. These two designs of CDPRs are both suspended CDPRs, meaning that they need

modifications before they can be applied in the high speed pick and place industry. Additionally, designs comprising cable loops are sensitive to parasitic inclinations when under-actuated [49]. Cable loops have also been researched in robots other than CDPRs, because of their low inertia and their ability to provide high transmission ratios [50], [51]. Another CDPR that goes beyond the Schönflies motion is the FAST CDPR, which is the largest suspended CDPR ever built [52]. This robot has a Steward-Gaugh mechanism [1] added to its moving platform to fine tune the pose of the EE, including rotations. Obviously, this is not an option for high speed motions since the CDPR is suspended and the Steward-Gaugh platform adds a relatively large amount of mass to the moving platform.

This literature overview shows that numerous solutions exist for generation of a Schönflies motion. Firstly adding an actuator in series seems the easiest solution, but is disregarded by the researches due to added inertia and necessary power supply. Nevertheless, these disadvantages are only named but never confirmed in literature by models or experiments on CDPRs. Secondly, using cables or reconfigurable bases for rotation can lead to a higher risk of interference, added cost, and complexity. Finally, none of the proposed solutions have been designed, modeled, compared or tested dynamically. This should be the case before any of these solutions can be applied in the high speed pick and place industry.

V. CABLE-ENVIRONMENT COLLISION AVOIDANCE

The second challenge was described as: *Avoiding collisions of the CDPR with the Environment*. Four methods have been identified in literature to overcome this challenge. A first method is called collision free path planning. This method is applied by Lahouar et al. [53] where a path planning algorithm is proposed for a suspended CDPR, given a start and end point of its path and containing an obstacle in between. From the starting point the depth mode is activated which is a straight line to the end point. When an upcoming collision is detected the algorithm goes to width mode to find an alternative path. Collisions between cables and the environment, and EE and the environment are considered and detected by modelling the cables and objects as line-segments and polyhedrons respectively, and calculating the minimum distance between them. This method ensures that a path is found if it exists, however not in the most efficient way. Also, Bury et al. [54] proposed an algorithm that can detect collisions along a path in a continuous fashion. Taking not only auto-collisions between cables into account, but also collision of cables between other bodies of the robot and the environment. Another approach that uses visual guidance for path planning without collisions is proposed by Pinto et al [42]. The idea is to apply this technique on construction sites for automated construction of architectural projects, as shown in figure 5a. In [28], a path planning method is proposed for the use in cluttered environments. Here, the rapidly exploring random trees (RRT) method [55] is used for path planning, including the Gilbert-Johnson-Keerthi (GJK) [56] method for fast collision detection.

A second method for avoiding collisions of a CDPR with the environment is a variation on path planning. However, in this method not the path but the anchor points of the cables on the base frame are adapted to avoid collisions. In [57] the shortest distance between cables is calculated along a path and if this distance gets below a predetermined threshold, the concerned cables' anchor point is moved to avoid a collision. Unfortunately, this method has yet only implemented cable-cable collisions and is not considering the environment. In [58] the environment has been taken into account. Moreover, an optimised reconfiguration strategy was studied to achieve the least amount of reconfigurations along a path. Another reconfiguration concept is reorienting the EE instead of the anchor points for collision avoidance [44]. However, a full proof of concept was not given. Yet another approach that disregards reconfiguration and uses relaxation of redundant cables is suggested [59]. Reconfiguration of the anchor points is disregarded since this cancels the low inertia of the cable robots and adds complexity. Therefore, the redundancy of a CDPR is used to relax one of the cables when a collision is imminent. Nevertheless, this concept has shown to be instable due to sudden variations in cable tensile forces.

Methods as reconfiguration and path planning might not be desirable for avoiding collisions in pick and place applications, because the low inertia is cancelled and complexity is added by reconfiguration, and path planning is mainly effective in complex or unknown environments. In pick and place applications the environment is not complex or unknown, since only conveyor belts and the products on these belts are present. A box could be drawn around the conveyor belts and the products as a non complex obstacle. Therefore, a third method for collision avoidance would be more desirable for pick and place applications, which is collision free workspace determination. In this workspace any path can be taken without collision. A frequently used method for collision free workspace determination is a geometric method created by Perrault et al. [27]. This method finds regions of cable-cable interference based on the simple principle that a cable, or geometrically seen a line, must lie in the same plane as another cable for a possible collision. Also detection of interference regions between the EE and cables are based on the same principle by dividing the edges of the EE in line segments. A recently proposed more efficient collision free workspace determination method, where a CAD file of the EE geometry can be provided, was proposed in [60]. Unfortunately, these methods do not take collisions with the environment into account. A research that does take all sorts of collisions, including collisions with the environment, into account was written by Aref et al. [61] and uses box based algorithms [62] to determine collision areas of an object with the CDPR. Another paper that geometrically determines the interference regions of cables with a cylindrical object is proposed in [30]. This is a promising method to be used in collision free workspace determination with objects other than cylinders. Also Wang et al. [63] suggested a method for collision free wrench feasible workspace determination for planar CDPRs by using the topological constraint and the

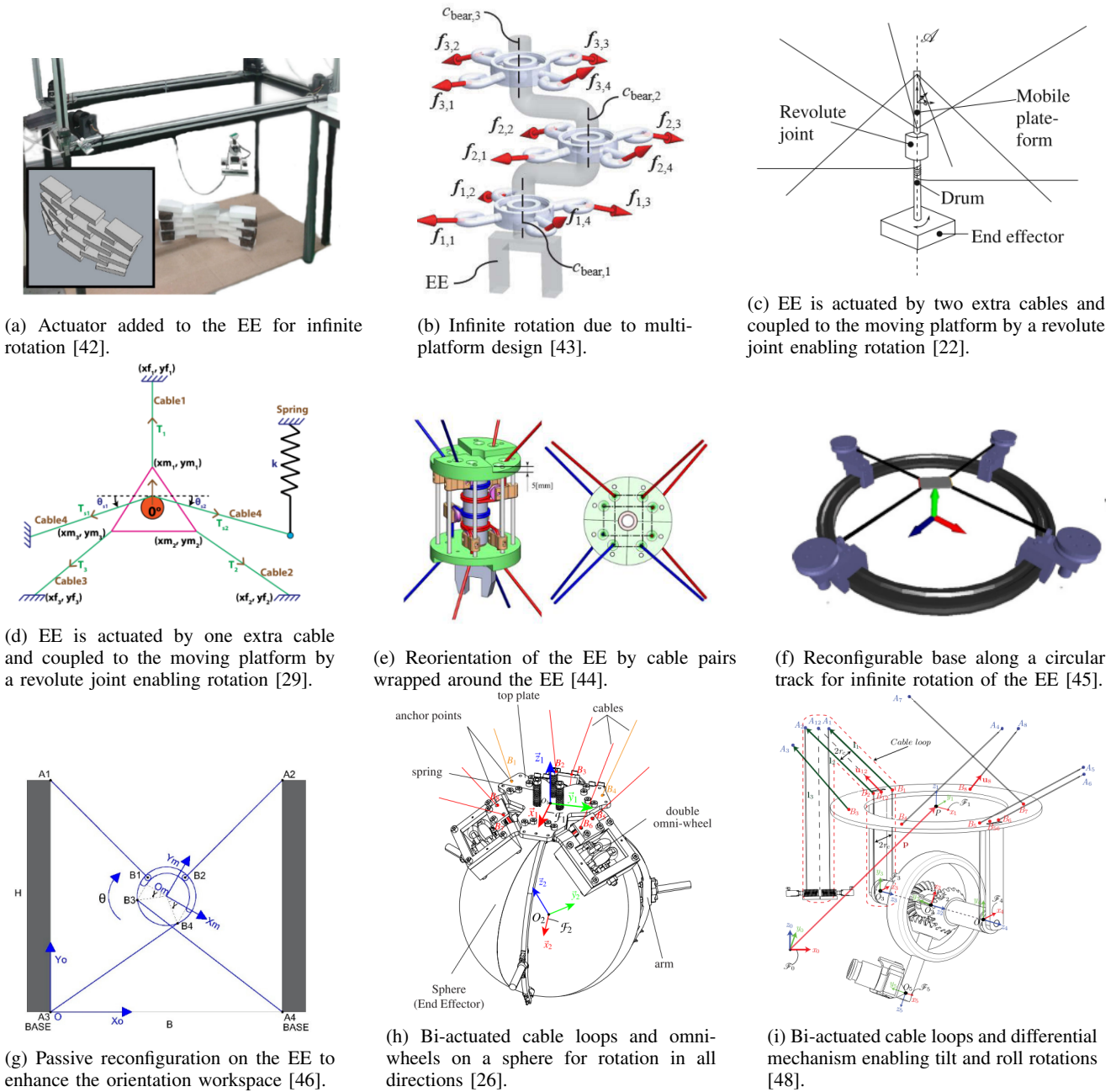


Fig. 5: CDRP designs from literature where the EE can perform large rotations.

critical support lines of an obstacle. Furthermore, a method for calculation of the maximum 3D printable workspace was given [64]. The maximum 3D printable workspace contains the space where a part can be printed without collision between cables and the part, and is calculated by evaluating each 2D layer individually. Nevertheless, this method is not applicable to spaces where the complete object is already present.

Numerous approaches for collision free workspace determination have been discussed. However, only determining the collision free workspace might not be sufficient since the

region of interest might still be in an interference region. Therefore, synthesis methods should be applied. Nevertheless, these methods were not found in literature applied on collision free workspaces. Only one synthesis method was found, which uses the minimization of collisions on given paths to determine the location of the cable anchor points [20]. A completely different approach to avoid collisions between the environment was shown by the FALCON robot [9], the FALCON-IPAnema robot [7], and the robot by Zhang et al. [6], whose geometries were designed such that no collisions with a conveyor belt or products under the EE

can happen. The potential of these designs in a high speed application were already shown by Kawamura et al. [9] and Zhang et al. [6]. Therefore, using these designs seems the most feasible solution for collision avoidance in the high speed pick and place industry and this challenge can be considered overcome. The geometries of these designs are shown in figures 2, 6, and 7.

VI. VIBRATION ATTENUATION

Another challenge for CDPRs in high speed applications is how to deal with vibrations, or in other words: *Attenuation of vibrations for a higher dynamic performance*. Several methods are known from literature for vibration attenuation, being transient wrench compensation, and control or input shaping [32], [65]. Wrench compensation can be performed in two ways. The first way is to use the wires and increase the tension in the wires, named bias tension. This concept was applied by the well known high speed FALCON robot to enhance its stiffness [8], [9]. Also Nguyen et al. [66] showed that increasing the lower bound of the wire tension already improves the stiffness. Anyhow, this method leads to an increase in power consumption and wear in the pulleys [33], [67]. Moreover, the stiffness of the EE is not only a function of the tension but also of the position in the workspace, and an increase in tension does not necessarily mean a monotonic increase in stiffness [68]. So proper cable force control is required. A second method for wrench compensation is external wrench compensation, meaning that actuators are added to the EE. This concept is for instance applied by using reaction wheels [69]. However, these reaction wheels can only compensate for torques thus angular vibrations. Since both forces and torques need to be compensated, another external wrench compensation concept was suggested. In this concept, arms are added to the EE [65]. When the arms are accelerated in opposing angular directions, forces can be compensated, and when actuated in the same angular direction, torques can be compensated. Other systems for external wrench compensation use cold gas thrusters [70], or a multi-rotor system [71]. External wrench compensation is in all shown cases applied to suspended CDPRs, since they are not capable of using bias tension because no tension can be applied in downward direction. Furthermore, adding actuators increases the inertia of the EE which is not desirable for high speed pick and place applications since the available wires can also be used for wrench compensation.

A second method for vibration attenuation is using control or input shaping. For accurate control, an accurate model of the system is required. In most CDPR control applications, the axial linear spring model is used to model the cables that are connected to the EE. This model was shown to be quite accurate when the cable masses are low and sufficient tension force is present [33]. Also transversal vibrations have shown to have minor effect on the EE vibrations [34]. However, in high speed applications a more accurate model might be necessary. This can be achieved by taking nonlinear spring behaviour of the cables into account [8] or by taking cable

mass and thereby taking cable dynamics into account. As cable dynamics influence the dynamics of the EE by adding new resonances [32], [33]. These vibrations of the EE due to cable dynamics are analysed using a finite element model or a dynamic stiffness method [66], [72]. Also including friction [73] and the auxiliary winch parts dynamics [7] can make a model more accurate.

Now having discussed the models, control methods applied on CDPRs can be distracted from the literature. In [74] a robust PID controller was applied to damp vibrations and ensure positive cable forces at all times, using an axial linear spring cable model and winch position measurement by an encoder. This controller was shown to be stable and could attenuate vibrations. An extension to this method was proposed by Baklouti et al. [31] who uses PID feedback control and elasto-dynamic model based feed forward control for a better trajectory tracking performance and better vibration attenuation. Also sliding mode controllers were suggested, which are known for their high response speed, a good transient response, and their insensitivity to parameter changes and external disturbances. Sliding mode control is based on changing the structure of the controller to gain a desired response [73], [75]. Another paper proposes a new dynamic model where the unwanted vibration equations are decoupled from its desired equations of motion in the form of a linear parametric varying (LPV) system [76]. This model can than be used for simple $LPV - H_\infty$ control to attenuate vibrations. An experiment shows that the $LPV - H_\infty$ controller has less error on a given trajectory than PD and sliding mode control. Additionally, the use of modal control was proposed since each mode can be controlled by a simple single-input single-output (SISO) controller designed by the root locus method [67], [77]. This requires the model to be linearized about a certain point, whereafter it is transferred into modal space and ready for the use in the control method. Thus, this controller is only stable for a static or a slowly varying position of the EE and not applicable to the high speed industry. Finally, a cascade controller is proposed using both visual feedback and encoder feedback in the winches for determining the EE pose [78]. The actuator position feedback is used in a fast inner control loop and the visual EE pose feedback is used in a slower outer control loop. This method was shown to be effective for vibration attenuation and has the potential to include friction in the model.

Almost all controllers that are discussed show potential for usage in the high speed pick and place industry. Some of them have even been implemented in a high speed CDPR [6], [9]. However, a more comparable dynamic performance with the Delta robot is still required for application of CDPRs in the industry. Therefore, more sophisticated models that include cable dynamics, friction, and auxiliary winch parts should be used in future control methods. Moreover, there is no holistic approach yet for vibration attenuation in CDPRs [73]. Thus, methods should be compared to find the method with the highest performance.

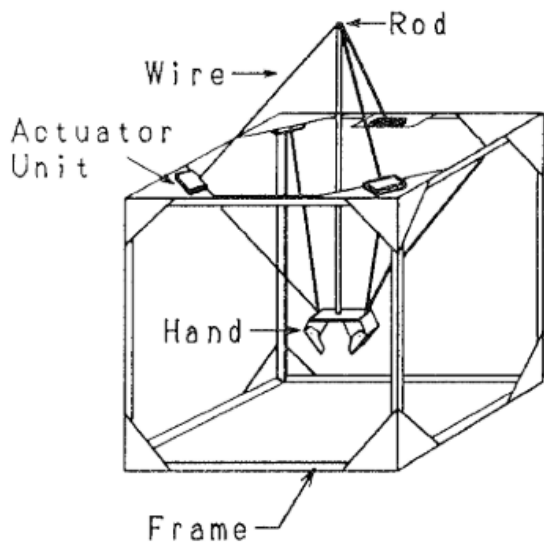


Fig. 6: High speed FALCON robot, which geometry is designed to avoid collisions with the environment [8].

VII. CONCLUSIONS

This paper identified and analysed the challenges for CDPRs in the high speed pick and place industry by performing a literature study. The identified challenges are; performing a Schönflies motion that contains a rotation of at least 180 degrees, avoiding collisions of the CDPR with the environment, and vibration attenuation for a higher dynamic performance. Literature showed that several solutions exist to perform large rotations, but none of them have been designed, modeled, compared or tested for dynamic applications. Additionally, four methods were found to avoid collisions with the environment being; collision free path planning, reconfiguration of the base, collision free workspace determination, and geometric design. Here geometric design was shown to be the most efficient solution for pick and place applications. Therefore, the second challenge can be considered overcome. Literature on the third challenge revealed that wrench compensation and control can be used for vibration attenuation. Bias tension wrench compensation can be applied but increases wear and power consumption, and a holistic control approach needs to be found including cable dynamics, friction, and auxiliary winch parts in the model to reach a comparable dynamic performance with a Delta robot.

Cable driven parallel robots have not been applied in the high speed pick and place industry since there has not been a design that has a comparable performance with a Delta robot as the Flexpicker [3]. Current designs are limited by vibrations, which needs to be remedied with more sophisticated models to improve the control. Moreover, strategies for performing large rotations of the EE have not been applied in high speed CDPRs. This would make CDPRs more attractive for the high speed pick and place industry.

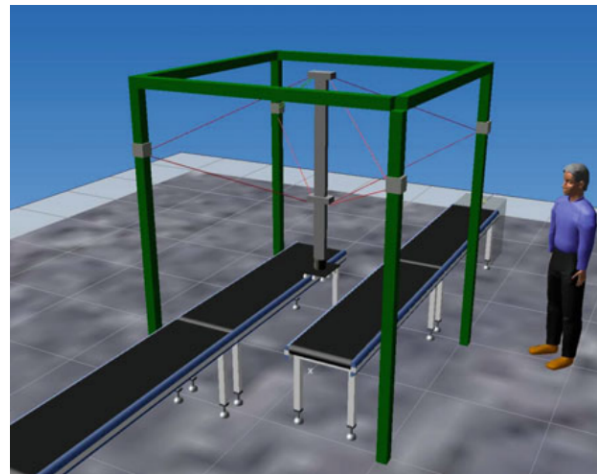


Fig. 7: FALCON-IPanema robot, which geometry is designed to avoid collisions with the environment [7].

ACKNOWLEDGEMENTS

The author would like to thank Philipp Tempel and Volkert van der Wijk for their guidance and support during the project.

REFERENCES

- [1] Bruno Siciliano and Oussama Khatib. *Springer handbook of robotics*. Springer, 2016.
- [2] François Pierrot, C Reynaud, and Alain Fournier. Delta: a simple and efficient parallel robot. *Robotica*, 8(2):105–109, 1990.
- [3] ABB. ROBOTICS IRB 360 FlexPicker ©, 2020.
- [4] Omron. Omron: Industrial Robotics Automation Catalog - Product Datasheets, 2020.
- [5] Clément Gosselin. Cable-driven parallel mechanisms: state of the art and perspectives. *Mechanical Engineering Reviews*, 1(1):DSM0004–DSM0004, 2014.
- [6] Zhaokun Zhang, Zhufeng Shao, and Liping Wang. Optimization and implementation of a high-speed 3-dofs translational cable-driven parallel robot. *Mechanism and Machine Theory*, 145:103693, 2020.
- [7] Andreas Pott and Tobias Bruckmann. *Cable-driven parallel robots: Theory and Application*. Springer, 2018.
- [8] S Kawamura, W Choe, S Tanaka, and SR Pandian. Development of an ultrahigh speed robot falcon using wire drive system. In *Proceedings of 1995 IEEE International Conference on Robotics and Automation*, volume 1, pages 215–220. IEEE, 1995.
- [9] Sadao Kawamura, Hitoshi Kino, and Choe Won. High-speed manipulation by using parallel wire-driven robots. *Robotica*, 18(1):13–21, 2000.
- [10] Andreas Pott, Hendrick Mütterich, Werner Kraus, Valentine Schmidt, Philipp Miermeister, and Alexander Verl. Ipanema: a family of cable-driven parallel robots for industrial applications. In *Cable-Driven Parallel Robots*, pages 119–134. Springer, 2013.
- [11] Andreas Pott. Forward kinematics and workspace determination of a wire robot for industrial applications. In *Advances in Robot Kinematics: Analysis and Design*, pages 451–458. Springer, 2008.
- [12] Zhaokun Zhang, Zhufeng Shao, Liping Wang, and Albert J Shih. Optimal design of a high-speed pick-and-place cable-driven parallel robot. In *Cable-Driven Parallel Robots*, pages 340–352. Springer, 2018.
- [13] Robert Dekker, Amir Khajepour, and Saeed Behzadipour. Design and testing of an ultra-high-speed cable robot. *International Journal of Robotics and Automation*, 21(1):25–34, 2006.

- [14] Jean-Pierre Merlet. Kinematics of the wire-driven parallel robot marionet using linear actuators. In *2008 IEEE International Conference on Robotics and Automation*, pages 3857–3862. IEEE, 2008.
- [15] Richard Verhoeven. *Analysis of the workspace of tendon-based Stewart platforms*. PhD thesis, University Duisburg-Essen, 2004.
- [16] Andreas Pott, Tobias Bruckmann, and Lars Mikelsons. Closed-form force distribution for parallel wire robots. In *Computational Kinematics*, pages 25–34. Springer, 2009.
- [17] Andreas Pott. An improved force distribution algorithm for over-constrained cable-driven parallel robots. In *Computational Kinematics*, pages 139–146. Springer, 2014.
- [18] Mahir Hassan and Amir Khajepour. Minimum-norm solution for the actuator forces in cable-based parallel manipulators based on convex optimization. In *Proceedings 2007 IEEE International Conference on Robotics and Automation*, pages 1498–1503. IEEE, 2007.
- [19] Tobias Bruckmann, Lars Mikelsons, Thorsten Brandt, Manfred Hiller, and Dieter Schramm. Design approaches for wire robots. In *International Design Engineering Technical Conferences and Computers and Information in Engineering Conference*, volume 49040, pages 25–34, 2009.
- [20] Simon Perreault and Clément M Gosselin. Cable-driven parallel mechanisms: Application to a locomotion interface. *Journal of Mechanical Design*, 130(10), 2008.
- [21] Andreas Pott and Philipp Miermeister. Workspace and interference analysis of cable-driven parallel robots with an unlimited rotation axis. In *Advances in Robot Kinematics*, pages 341–350. Springer, 2018.
- [22] Alexis Fortin-Côté, Céline Faure, Laurent Bouyer, Bradford J McFadyen, Catherine Mercier, Michaël Bonenfant, Denis Laurendeau, Philippe Cardou, and Clément Gosselin. On the design of a novel cable-driven parallel robot capable of large rotation about one axis. In *Cable-Driven Parallel Robots*, pages 390–401. Springer, 2018.
- [23] Guanglei Wu, Zirong Lin, Wenkang Zhao, Sida Zhang, Huiping Shen, and Stéphane Caro. A four-limb parallel schönflies motion generator with full-circle end-effector rotation. *Mechanism and Machine Theory*, 146:103711, 2020.
- [24] Thomas Reichenbach, Philipp Tempel, Alexander Verl, and Andreas Pott. On kinetostatics and workspace analysis of multi-platform cable-driven parallel robots with unlimited rotation. In *IFTOMM International Symposium on Robotics and Mechatronics*, pages 79–90. Springer, 2019.
- [25] Saman Lessanibahri, Philippe Cardou, and Stéphane Caro. Kinetostatic modeling of a cable-driven parallel robot using a tilt-roll wrist. In *International Conference on Cable-Driven Parallel Robots*, pages 109–120. Springer, 2019.
- [26] Marceau Métilion, Saman Lessanibahri, Philippe Cardou, Kévin Subrin, and Stéphane Caro. A cable-driven parallel robot with full-circle end-effector rotations. In *The ASME 2020 International Design Engineering Technical Conferences & Computers and Information in Engineering Conference IDETC/CIE 2020*, 2020.
- [27] Simon Perreault, Philippe Cardou, Clément M Gosselin, and Martin J-D Otis. Geometric determination of the interference-free constant-orientation workspace of parallel cable-driven mechanisms. *Journal of Mechanisms and Robotics*, 2(3), 2010.
- [28] Jeong-Hyeon Bak, Sung Wook Hwang, Jonghyun Yoon, Jong Hyeon Park, and Jong-Oh Park. Collision-free path planning of cable-driven parallel robots in cluttered environments. *Intelligent Service Robotics*, 12(3):243–253, 2019.
- [29] M Vikranth Reddy, NC Praneet, and GK Ananthasuresh. Planar cable-driven robots with enhanced orientability. In *International Conference on Cable-Driven Parallel Robots*, pages 3–12. Springer, 2019.
- [30] Antoine Martin, Stéphane Caro, and Philippe Cardou. Geometric determination of the cable-cylinder interference regions in the workspace of a cable-driven parallel robot. In *Cable-Driven Parallel Robots*, pages 117–127. Springer, 2018.
- [31] Sana Baklouti, Eric Courteille, Philippe Lemoine, and Stéphane Caro. Vibration reduction of cable-driven parallel robots through elastodynamic model-based control. *Mechanism and Machine Theory*, 139:329–345, 2019.
- [32] Han Yuan, Eric Courteille, Marc Gouttefarde, and Pierre-Elie Hervé. Vibration analysis of cable-driven parallel robots based on the dynamic stiffness matrix method. *Journal of Sound and Vibration*, 394:527–544, 2017.
- [33] Han Yuan, Eric Courteille, and Dominique Deblaise. Static and dynamic stiffness analyses of cable-driven parallel robots with non-negligible cable mass and elasticity. *Mechanism and Machine Theory*, 85:64–81, 2015.
- [34] Xiumin Diao and Ou Ma. Vibration analysis of cable-driven parallel manipulators. *Multibody system dynamics*, 21(4):347–360, 2009.
- [35] Omron. Delta robot 3 axes + 1 rot, 2020.
- [36] Vincent Nabat, María de la O Rodriguez, O Company, Sébastien Krut, and F Pierrot. Par4: very high speed parallel robot for pick-and-place. In *2005 IEEE/RSJ International Conference on intelligent robots and systems*, pages 553–558. IEEE, 2005.
- [37] Songtao Liu, Tian Huang, Jiangping Mei, Xueman Zhao, Panfeng Wang, and Derek G Chetwynd. Optimal design of a 4-dof scara type parallel robot using dynamic performance indices and angular constraints. *Journal of Mechanisms and Robotics*, 4(3), 2012.
- [38] Sébastien Krut, Olivier Company, Vincent Nabat, and Francois Pierrot. Heli4: a parallel robot for scara motions with a very compact traveling plate and a symmetrical design. In *2006 IEEE/RSJ International Conference on Intelligent Robots and Systems*, pages 1656–1661. IEEE, 2006.
- [39] David Corbel, Marc Gouttefarde, François Pierrot, et al. Actuation redundancy as a way to improve the acceleration capabilities of 3t and 3t1r pick-and-place parallel manipulators. *Journal of Mechanisms and Robotics*, 2(4), 2010.
- [40] Fugui Xie and Xin-Jun Liu. Design and development of a high-speed and high-rotation robot with four identical arms and a single platform. *Journal of Mechanisms and Robotics*, 7(4), 2015.
- [41] Jiao Mo, Zhu-Feng Shao, Liwen Guan, Fugui Xie, and Xiaoqiang Tang. Dynamic performance analysis of the x4 high-speed pick-and-place parallel robot. *Robotics and Computer-Integrated Manufacturing*, 46:48–57, 2017.
- [42] Andry Maykol Pinto, Eduardo Moreira, José Lima, José Pedro Sousa, and Pedro Costa. A cable-driven robot for architectural constructions: a visual-guided approach for motion control and path-planning. *Autonomous Robots*, 41(7):1487–1499, 2017.
- [43] Thomas Reichenbach, Philipp Tempel, Alexander Verl, and Andreas Pott. Static analysis of a two-platform planar cable-driven parallel robot with unlimited rotation. In *International Conference on Cable-Driven Parallel Robots*, pages 121–133. Springer, 2019.
- [44] Toru Makino and Takashi Harada. Cable collision avoidance of a pulley embedded cable-driven parallel robot by kinematic redundancy. In *Proceedings of the 4th International Conference on Control, Mechatronics and Automation*, pages 117–120, 2016.
- [45] Michael Anson, Aliakbar Alamdari, and Venkat Krovi. Orientation workspace and stiffness optimization of cable-driven parallel manipulators with base mobility. *Journal of Mechanisms and Robotics*, 9(3), 2017.
- [46] Marco Alexander Carpio Alemán, Roque Saltaren, Alejandro Rodriguez, Gerardo Portilla, and Juan Diego Placencia. Rotational workspace expansion of a planar cdpr with a circular end-effector mechanism allowing passive reconfiguration. *Robotics*, 8(3):57, 2019.
- [47] Tam Nhat Le, Hiroki Dobashi, and Kiyoshi Nagai. Configuration of redundant drive wire mechanism using double actuator modules. *ROBOMECH Journal*, 3(1):25, 2016.
- [48] Saman Lessanibahri, Philippe Cardou, and Stéphane Caro. A cable-driven parallel robot with an embedded tilt-roll wrist. *Journal of Mechanisms and Robotics*, 12(2), 2020.
- [49] Saman Lessanibahri, Philippe Cardou, and Stéphane Caro. Parasitic inclinations in cable-driven parallel robots using cable loops. *Procedia CIRP*, 70:296–301, 2018.
- [50] Daniel Krebs, Gunnar Borchert, and Annika Raatz. Simulation and design of an orientation mechanism for assembly systems. *Procedia CIRP*, 44:245–250, 2016.
- [51] Peyman Karimi Eskandary and Jorge Angeles. The virtual screw: Concept, design and applications. *Mechanism and Machine Theory*, 128:349–358, 2018.
- [52] Rui Yao, Hui Li, and Xinyu Zhang. A modeling method of the cable driven parallel manipulator for fast. In *Cable-Driven Parallel Robots*, pages 423–436. Springer, 2013.
- [53] Samir Lahouar, Erika Ottaviano, Said Zeghoul, Lotfi Romdhane, and Marco Ceccarelli. Collision free path-planning for cable-driven parallel robots. *Robotics and Autonomous Systems*, 57(11):1083–1093, 2009.
- [54] Diane Bury, Jean-Baptiste Izard, Marc Gouttefarde, and Florent Lamiereux. Continuous collision detection for a robotic arm mounted on a cable-driven parallel robot. *arXiv preprint arXiv:1909.10857*, 2019.

- [55] Steven M LaValle. Rapidly-exploring random trees: A new tool for path planning. 1998.
- [56] Elmer G Gilbert, Daniel W Johnson, and S Sathiy Keerthi. A fast procedure for computing the distance between complex objects in three-dimensional space. *IEEE Journal on Robotics and Automation*, 4(2):193–203, 1988.
- [57] Khaled Youssef and Martin J-D Otis. Reconfigurable fully constrained cable driven parallel mechanism for avoiding interference between cables. *Mechanism and Machine Theory*, 148:103781, 2020.
- [58] Lorenzo Gagliardini, Stéphane Caro, Marc Gouttefarde, and Alexis Girin. A reconfiguration strategy for reconfigurable cable-driven parallel robots. In *2015 IEEE international conference on robotics and automation (ICRA)*, pages 1613–1620. IEEE, 2015.
- [59] Martin J-D Otis, Simon Perreault, Thien-Ly Nguyen-Dang, Patrice Lambert, Marc Gouttefarde, Denis Laurendeau, and Clément Gosselin. Determination and management of cable interferences between two 6-dof foot platforms in a cable-driven locomotion interface. *IEEE Transactions on Systems, Man, and Cybernetics-Part A: Systems and Humans*, 39(3):528–544, 2009.
- [60] Marc Fabritius, Christoph Martin, and Andreas Pott. Calculation of the cable-platform collision-free total orientation workspace of cable-driven parallel robots. In *International Conference on Cable-Driven Parallel Robots*, pages 137–148. Springer, 2019.
- [61] Mohammad M Aref and Hamid D Taghirad. Geometrical workspace analysis of a cable-driven redundant parallel manipulator: Kntu cdrpm. In *2008 IEEE/RSJ International Conference on Intelligent Robots and Systems*, pages 1958–1963. IEEE, 2008.
- [62] Deng-wu Ma, Wen Ye, and Ying LI. Survey of box-based algorithms for collision detection. *Journal of System Simulation*, 18(4):1058–1061, 2006.
- [63] Bingyao Wang, Bin Zi, Sen Qian, and Dan Zhang. Collision free force closure workspace determination of reconfigurable planar cable driven parallel robot. In *2016 Asia-Pacific Conference on Intelligent Robot Systems (ACIRS)*, pages 26–30. IEEE, 2016.
- [64] Marc Fabritius, Christoph Martin, and Andreas Pott. Calculation of the collision-free printing workspace for fully-constrained cable-driven parallel robots. In *Mechanisms and Robotics Conference*, volume 42, pages 1–9. American Society of Mechanical Engineers, 2018.
- [65] Maximilian Lesellier, Loic Cuvillon, Jacques Gangloff, and Marc Gouttefarde. An active stabilizer for cable-driven parallel robot vibration damping. In *2018 IEEE/RSJ International Conference on Intelligent Robots and Systems (IROS)*, pages 5063–5070. IEEE, 2018.
- [66] Sy Nguyen-Van, Kwan-Woong Gwak, Duc-Hai Nguyen, Soon-Geul Lee, and Byoung Hun Kang. A novel modified analytical method and finite element method for vibration analysis of cable-driven parallel robots. *Journal of Mechanical Science and Technology*, 34(9):3575–3586, 2020.
- [67] Loic Cuvillon, Xavier Weber, and Jacques Gangloff. Modal control for active vibration damping of cable-driven parallel robots. *Journal of Mechanisms and Robotics*, 12(5), 2020.
- [68] Hao Xiong and Xiumin Diao. The effect of cable tensions on the stiffness of cable-driven parallel manipulators. In *2017 IEEE International Conference on Advanced Intelligent Mechatronics (AIM)*, pages 1185–1190. IEEE, 2017.
- [69] Xavier Weber, Loic Cuvillon, and Jacques Gangloff. Active vibration canceling of a cable-driven parallel robot using reaction wheels. In *2014 IEEE/RSJ International Conference on Intelligent Robots and Systems*, pages 1724–1729. IEEE, 2014.
- [70] Hugo Sellet, Imane Khayour, Loic Cuvillon, Sylvain Durand, and Jacques Gangloff. Active damping of parallel robots driven by flexible cables using cold-gas thrusters. In *2019 International Conference on Robotics and Automation (ICRA)*, pages 530–536. IEEE, 2019.
- [71] Yue Sun, Matthew Newman, Arthur Zygielbaum, and Benjamin Terry. Active vibration damping of a cable-driven parallel manipulator using a multitorotor system. In *International Conference on Cable-Driven Parallel Robots*, pages 403–414. Springer, 2019.
- [72] Christian Schenk, Carlo Masone, Philipp Miermeister, and Heinrich H Bühlhoff. Modeling and analysis of cable vibrations for a cable-driven parallel robot. In *2016 IEEE International Conference on Information and Automation (ICIA)*, pages 454–461. IEEE, 2016.
- [73] Christian Tobias Schenk. *Modelling and Control of a Cable-Driven Parallel Robot - Methods for Vibration Reduction and Motion Quality Improvement*. PhD thesis, University Stuttgart, 2019.
- [74] MA Khosravi and Hamid D Taghirad. Stability analysis and robust pid control of cable driven robots considering elasticity in cables. *AUT Journal of Electrical Engineering*, 48(2):113–126, 2016.
- [75] So-Ryeok Oh, Kalyan K Mankala, Sunil K Agrawal, and James S Albus. Dynamic modeling and robust controller design of a two-stage parallel cable robot. *Multibody System Dynamics*, 13(4):385–399, 2005.
- [76] Hamed Jamshidifar, Saeid Khosravani, Baris Fidan, and Amir Khajepour. Vibration decoupled modeling and robust control of redundant cable-driven parallel robots. *IEEE/ASME Transactions on Mechatronics*, 23(2):690–701, 2018.
- [77] Xavier Weber, Loic Cuvillon, and Jacques Gangloff. Active vibration canceling of a cable-driven parallel robot in modal space. In *2015 IEEE International Conference on Robotics and Automation (ICRA)*, pages 1599–1604. IEEE, 2015.
- [78] Jeremy Begey, Loic Cuvillon, Maximilien Lesellier, Marc Gouttefarde, and Jacques Gangloff. Dynamic control of parallel robots driven by flexible cables and actuated by position-controlled winches. *IEEE Transactions on Robotics*, 35(1):286–293, 2018.

Chapter 3

Design, comparison and experimental evaluation of a high speed cable driven parallel pick and place robot, performing a Schönflies motion.

Design, comparison, and experimental evaluation of a high speed cable driven parallel pick and place robot, performing a Schönflies motion.

Pim van der Stigchel

Abstract—Cable driven parallel robots (CDPRs) show potential for application in the high speed pick and place industry. A pick and place operation can be described as a Schönflies motion, containing three translations and a rotation up to 180 degrees about one axis for full product reorientation. The rotations of CDPRs are restrained and require an additional actuated axis on the moving platform to perform a rotation of 180 degrees. Literature showed several CDPR concept solutions that can perform a large rotation, but they were not properly designed, modelled, compared or tested for high speed applications. This paper proposes three design variations that can perform this motion and are compared on their optimized dynamic workspace volume, which is based on the accelerations during an adept cycle. The concept design that comprises a cable loop for product orientation shows the largest dynamic workspace for the smallest cable forces. A prototype of this design was made and evaluated on the adept cycle in a forward dynamic model, and in an experimental setup. The evaluation showed stable end effector motion and rotation, providing the design to be suitable for high speed pick and place tasks. Still, stiffness should be improved to reach a better repeatability.

Index terms: Cable driven parallel robot - Schönflies motion generation - Pick and Place task - Dynamic workspace optimization

I. INTRODUCTION

A pick and place motion can be described by a Schönflies motion, which contains three independent translations and one rotation up to 180 degrees about the vertical body fixed axis. This motion is required in the high speed pick and place industry since products need to be translated and reoriented for sorting and packaging. Parallel robots, like the Delta robot [1], have been widely applied in the pick and place industry to perform this motion since they possess advantageous properties, being a high load carrying capacity and high accuracy [2]. Moreover, the moving mass of these robots is low since the load is distributed among multiple legs or kinematic chains, and the actuators are fixed on the base of the robot. This results in high accelerations and speeds, leading to low pick and place cycle times. Take for instance the commercially available Delta robots by ABB [3] or Omron [4], with cycle times up to 0.30s on a 25/305/25mm path for 0.1kg payload, and a repeatability of 0.1mm. The rotation of the payload is performed by an added actuator on the end effector (EE) [5], a telescopic cardan shaft from the robot base to the EE [3], [4], or by adding a fourth kinematic chain which enables an extra degree of freedom [6], [7]. Another class of parallel robots that shows high potential for application in the high speed pick and place industry are the cable driven parallel robots (CDPRs). A typical layout

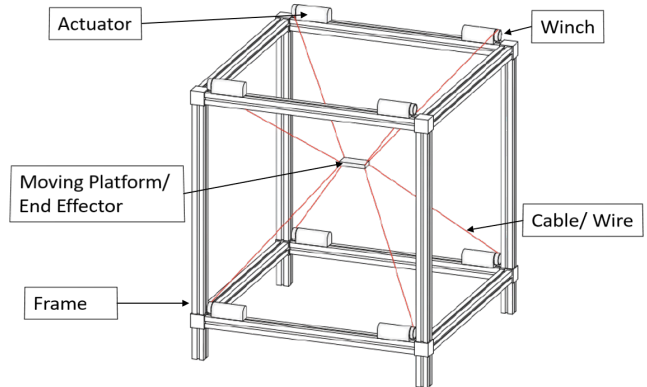


Fig. 1: Typical layout of a CDPR [10].

of a CDPR is shown in figure 1, where the EE or moving platform is driven by only cables that are wound on winches located on a frame. The potential of these robots is high since their inertia is low due to low cable masses. This means they can have high accelerations and velocities with relatively little power consumption. Additionally, their load capacity is high because cables can handle large tension forces, and their translational workspace can be large and is easily scalable [8]. Therefore, CDPRs provide a potential method to improve efficiency and reduce the cost of pick and place robots [9].

This potential is supported by multiple researches like the FALCON project by Kawamura et al. [11], [12] where a high speed CDPR was designed that can reach accelerations up to 40G and speeds up to 13m s^{-1} for a 150g load. Also the IPAnema family of CDPRs was designed for handling and fast pick and place operations [13], [14]. For instance, the IPAnema 1 can reach up to 10m s^{-1} speed and has a maximum acceleration of 100m s^{-2} for payloads up to 3kg. It was proven that this robot is feasible for application in handling and assembly operations by the ISO9283 norm [13]. Likewise the pick and place CDPR by Zhang et al. [9], [15] can reach 125 cycles per minute with an accuracy of 0.12mm on an arc shaped 25/305/25mm path with a load of 0.1kg. This was performed by using a compressive spring rod to keep the wires under tension. This design is an evolution of the DeltaBot [16] where the lower limbs of a Delta robot are replaced by cables and a compressive spring rod was put in the centre to keep the cables under tension. In this fashion the inertia of the system is reduced which yields accelerations of 124m s^{-2} and speeds up to 4.1m s^{-1} , resulting in 120-150 cycles per minute for a 400g payload on a 25/305/25mm path. Finally, the SEGESTA [10] robot was

designed for vibration testing and is capable of accelerations up to 200m s^{-2} for a load of 150g.

However, none of these CDPRs can perform a full Schönflies motion since their orientation space is limited [17], [18]. The maximum rotation angle for redundantly restrained CDPRs was identified to be ± 45 degrees by Reichenbach et al. [19] which implies that a Schönflies motion with a rotation larger than or equal to 180 degrees can only be achieved by an extra actuated axis on the EE [17]. Multiple CDPRs that can perform a rotation of 180 degrees or more exist in literature. Pinto et al. added a motor in series to the EE [20]. Other designs use only cables to perform the rotation. For instance by using a multi-platform approach [17], [19], [21], where the EE is shaped as a crankshaft and each of the 3 crankshaft parts are actuated by four cables as shown in figure 2. By moving the inner platform relative to the outer platform, an infinite rotation can be achieved. Other solutions use a revolute joint added between the moving platform and the EE and a pair of cables connected to this EE to perform the rotation [18], [22], [23], this solution is shown in figure 3. Also a passive reconfiguration mechanism for the cable anchor points on the EE is considered to enhance the orientation [24]. However, this solution does not reach 180 degrees of rotation. Additionally, reorientation of the base along a circular track is proposed for full EE reorientation [25]. Finally, bi actuated cable loops have been proposed for performing large rotations [26]. A bi actuated cable loop contains a cable wrapped around a pulley, with both ends connected to an actuator as shown in figure 4. In this way the pulley can perform both a translation and a rotation. Combining these cable loops with Omni-wheels on a sphere [27] or a differential like mechanism even multiple rotations are added to the EE [28], [29]. Despite having numerous conceptual solutions for performing a large rotation, none of them were properly designed, modelled, compared or tested for high speed applications.

The goal of this paper is to propose designs of CDPRs for high speed applications that can perform a Schönflies motion including a rotation of at least 180 degrees, and dynamically compare and evaluate them. For this goal, a benchmark is presented together with criteria for an optimal design in section II. Based on this benchmark and criteria three concept designs were derived from literature in section III. The equations of motion are derived for these concepts in section IV, and a method to compute the dynamic workspace is discussed in section V. The concepts are optimized and compared on their dynamic workspace in section VI. A prototype was build of the concept with the highest potential and evaluated in an experimental setup and a forward dynamic model in section VII. Finally, a conclusion is drawn in section VIII.

II. BENCHMARK DESIGN AND CRITERIA

This section presents a benchmark design, which is a state of the art industrial Delta robot. This benchmark is used to compare the CDPR designs with and show how competitive they are compared to Delta robots, and what should still

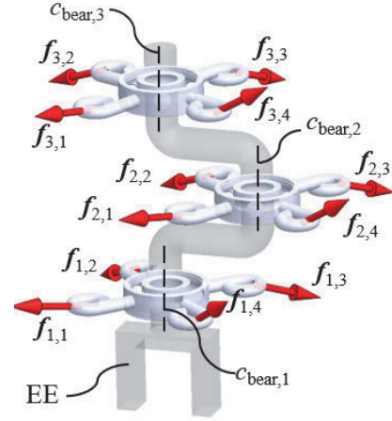


Fig. 2: Multi-platform design for infinite rotation [21].

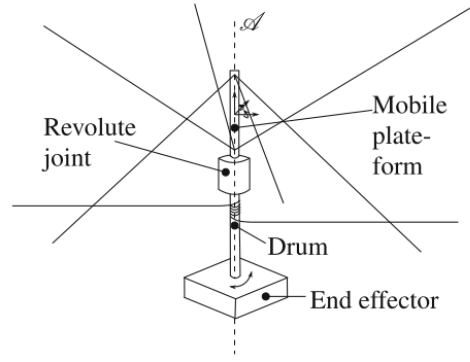


Fig. 3: Revolute joint between moving platform and EE and two extra cables for large rotations [18].

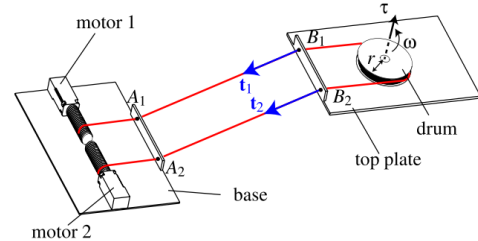


Fig. 4: Bi actuated cable loop enabling large rotations and translations of the EE [27].

improve to be attractive for high speed pick and place tasks. The Flexpicker IRB 360-1/1600 Delta robot [3] was selected as a benchmark design, since this robot is currently one of the fastest Delta robots with a relatively large workspace, and because it can perform full product reorientation. I.e. it can reach a 0.35s cycle time on a 25/305/25mm path for 0.1kg payload, and can fully rotate this payload. The position repeatability is given as 0.1mm, and the angular repeatability as 0.4° . Additionally, this robot has a workspace with a diameter of 1440mm and a height of 350mm requiring an estimated 2m cubic installation space.

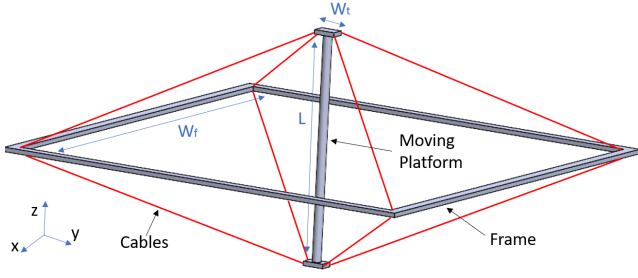


Fig. 5: Selected architecture for the concepts having a 2D frame and a rod shaped moving platform.

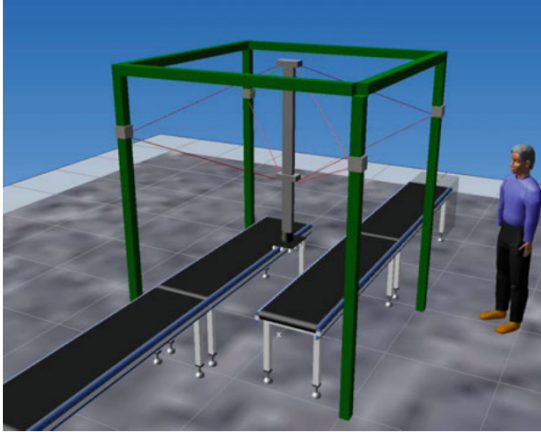


Fig. 6: FALCON-IPanema design, shown in a pick and place situation [10].

From the presented benchmark it can be derived that the CDPR designs should have a low inertia such that high accelerations and speeds can be reached with low power consumption. Furthermore, the workspace of the design should be large for a benchmark installation space and the EE should at least reach 180° for full product reorientation. In order to keep complexity and cost low, so the design remains attractive for use in the industry, a minimal number of actuators should be used. Finally, the stiffness should be high to suppress vibrations and reach the benchmark repeatability.

III. CONCEPT DESIGNS

Based on the literature presented in section I and the criteria in section II, a thorough concept generation and selection has been performed as discussed in appendices 1, 2, and 3. Three concept designs have been derived that show potential for further optimization in section VI.

The architecture for the three concepts is chosen to be the same and is based on the design by Kawamura [11], [12] and the Falcon-Ipanema design proposal by Pott [10], as shown in figure 5. This architecture shows a 2D frame and a moving platform that is shaped as a beam or rod, which is chosen since it has convenient properties for pick and place tasks. Namely, the moving platform will be non-

suspended meaning that accelerations higher than gravity can be achieved. Additionally, collisions of the cables with the environment are avoided, see figure 6, and a high stiffness is generated [10]. Moreover, Kawamura already showed that this architecture is applicable in high speed applications according to the data presented in section I. In each concept design a rotation mechanism is added to this architecture.

In the first concept a motor is added to the moving platform, as shown in figure 7. It is argued that adding the mass of the motor reduces the dynamic performance, the workspace size, or the admissible payload [21]. However, this solution has never been compared to other solutions and this solution bears great mechanical simplicity. Therefore, this concept shows potential for further optimization and comparison.

The second concept is derived from the cable loop mechanisms discussed in section I [26]–[29], and is combined with the selected architecture as shown in figure 8. Here the two cables of the cable loop act as one cable to manipulate the moving platform, but also actuate the rotation of the EE. The moving platform has six degrees of freedom and the rotation adds one degree of freedom. According to Verhoeven [30], the number of cables m need to be larger than the number of degrees of freedom n to fully constrain the CDPR, $n + 1 \leq m$. So this design requires only eight cables. Additionally, this concept shows potential since it adds little inertia to the moving platform and has a non complex mechanical design. The third concept is derived from the design by Fortin-Coté et al. [18], and is shown in figure 9. This design seems to overlap with the cable loop design in concept 2. However, this design decouples the torques of the EE from the moving platform by allowing the cable guides to rotate with respect to the vertical body fixed axis. Therefore, the moving platform only needs to be constrained for 5 degrees of freedom having a 2R3T motion pattern [30]. Thus only six cables are required to fully constrain the moving platform and two additional cables are required for the rotation. This concept as well shows potential since it adds little inertia to the moving platform and has a non complex mechanical design.

For concept 1 seven cables would be sufficient to fully constrain the moving platform. However, eight cables will be applied in this paper such that a fair comparison with the other concepts can be performed.

IV. EQUATIONS OF MOTION

For each of the concepts we can set up the equations of motion (EOM), starting from equation 1 [31].

$$\begin{bmatrix} M_p \mathbf{E} & \mathbf{0} \\ \mathbf{0} & \mathbf{I} \end{bmatrix} \cdot \begin{bmatrix} \ddot{\mathbf{r}} \\ \ddot{\boldsymbol{\phi}} \end{bmatrix} + \begin{bmatrix} \mathbf{0} \\ \dot{\boldsymbol{\phi}} \times (\mathbf{I} \dot{\boldsymbol{\phi}}) \end{bmatrix} - \begin{bmatrix} \mathbf{f}_e \\ \boldsymbol{\tau}_e \end{bmatrix} = \mathbf{A}^T \cdot \mathbf{f} \quad (1)$$

This equation is based on the Newton-Euler equations, where M_p is the mass and \mathbf{I} the inertia tensor of the moving platform and EE. \mathbf{r} contains the position of the moving platform and $\boldsymbol{\phi}$ the orientation. \mathbf{f}_e and $\boldsymbol{\tau}_e$ contain the external forces and moments respectively, including gravitational forces. The dynamics and external wrenches need to be balanced with forces and torques applied by the cable forces \mathbf{f} . The cable

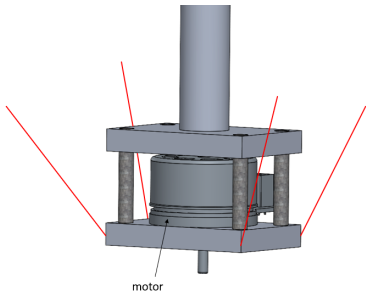


Fig. 7: Concept 1, a motor is added for rotation of the EE.

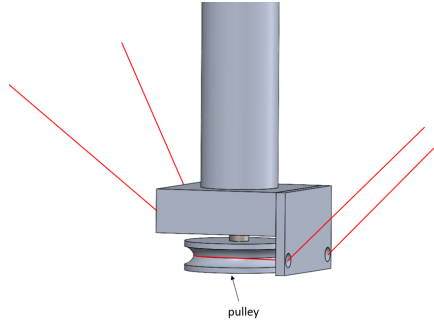


Fig. 8: Concept 2, a cable loop mechanism is added for the rotation of the EE.

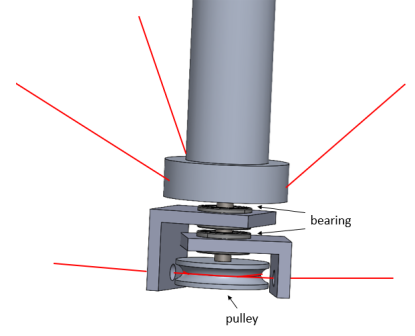


Fig. 9: Concept 3, two added cables actuate the EE rotation via a pulley.

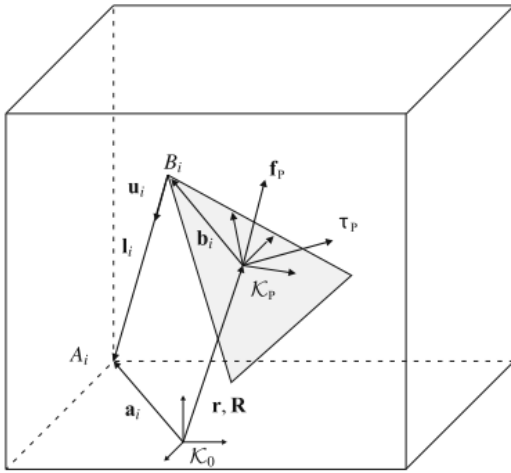


Fig. 10: General kinematic representation of a parallel cable robot [10].

forces are converted to forces and torques on the moving platform by the transpose of the structure matrix A^T , which is based on the kinematics as shown in figure 10.

$$A^T = \begin{bmatrix} \mathbf{u}_1 & \dots & \mathbf{u}_m \\ \mathbf{b}_1 \times \mathbf{u}_1 & \dots & \mathbf{b}_m \times \mathbf{u}_m \end{bmatrix} \quad (2)$$

Here \mathbf{u}_i is a unit vector pointing from the moving platform along a cable and \mathbf{b}_i is the cable anchor point on the platform. \mathbf{u}_i is computed according to

$$\mathbf{l}_i = \mathbf{a}_i - \mathbf{r} - \mathbf{R} \cdot \mathbf{b}_i \quad (3)$$

$$\mathbf{u}_i = \frac{\mathbf{l}_i}{\|\mathbf{l}_i\|_2} \quad (4)$$

Where \mathbf{l}_i is a vector representing the cable, \mathbf{a}_i the cable anchor point on the frame, and \mathbf{R} the rotation matrix between the body and the world frame.

In each of the concepts a rotation mechanism is added which affects the EOM. An angular acceleration of the EE can be added as an external torque to the EOM for concept 1

$$\boldsymbol{\tau}_e = \begin{bmatrix} 0 \\ 0 \\ (I_l + I_m) \cdot \ddot{\theta} \end{bmatrix} \quad (5)$$

Here I_m is the internal inertia of the motor and I_l is the inertia of the payload that can be attached to the motor axis. θ is the angle of the payload or EE. For concept 2 one can not add the angular accelerations of the EE as external wrenches since the cable forces apply this acceleration. Therefore, an extra degree of freedom needs to be added to the EOM in equation 1 as an extra row [28], [29].

$$(I_l + I_p) \cdot \ddot{\theta} = \begin{bmatrix} 0 & 0 & 0 & 0 & 0 & 0 & -D_p/2 & D_p/2 \end{bmatrix} \cdot \mathbf{f} \quad (6)$$

Here D_p is the diameter of the pulley and I_p the inertia of the pulley. Equation 6 can as well be used for concept 3. However, as discussed in section III the moving platform of concept 3 has a 2R3T motion pattern. Therefore, the final row of equation 1 can be replaced with equation 6. Additionally, for every pose \mathbf{b}_i changes for the cables that perform the rotation of the EE. They are computed according to the method given by Fortin-Coté et al. [18].

V. DYNAMIC WORKSPACE COMPUTATION

In the criteria in section II it was described that a large workspace for a comparable installation space with the Flexpicker, and low pick and place cycle times are desired. Therefore, each of the concept designs from section III is optimized in section VI for its dynamic workspace volume and compared with the other concept designs. The dynamic workspace is defined as the set of poses of the moving platform at which a predefined set of accelerations is feasible [32]. This means that the cable forces lie within a defined minimum and maximum cable force while performing the accelerations. In this paper the acceleration set is based on the accelerations that are performed during an adept cycle. This adept cycle is a trajectory that is often used for the comparison and evaluation of pick and place robots, as showed in section I. The trajectory is shown in figure 11 and has a 25/305/25mm translation. During this translation the orientation of the moving platform remains constant and the EE rotates 180°. Taking the benchmark cycle time of 0.35s and using a 4-5-6-7-polynomial to relate time with position [33], results in a smooth acceleration profile depicted in figure 12. The instances where the acceleration in one of the directions is maximal are determined as the dynamic

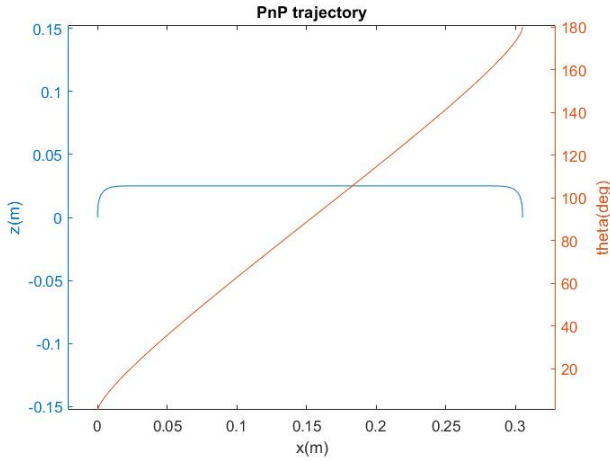


Fig. 11: Adept cycle pick and place trajectory having a 25mm translation in z-direction, a 305mm translation in x-direction, and a 180° EE rotation about the z-axis.

acceleration set. In this way the dynamic workspace shows the space where the CDPR is able to perform the adept cycle with a cycle time of 0.35s.

The Hull method [14] is used to compute the dynamic workspace. This method starts with a unit sphere with its centre at the estimated workspace centre \mathbf{m} . The surface of this unit sphere is triangulated and from the centre \mathbf{m} to each vertex a vector \mathbf{v}_i is drawn. This results in lines, given in equation 7, along which line searches are performed by a regula falsi method.

$$\mathbf{h}_i = \mathbf{m} + \lambda_i \cdot \mathbf{v}_i \quad (7)$$

At each line search evaluation the acceleration set is inserted into the EOM from section IV in both x and y direction, and the cable forces are computed. If the cable forces fall within the set cable force limits, the pose belongs to the dynamic workspace. In this way each line search finds $\lambda_{i,f}$ for which the cable forces are just within the set limits and the triangulated sphere is expanded to the dynamic workspace. To solve the EOM from section IV for the cable forces, the improved closed form method is used [34]. This method is required since the CDPRs are redundantly actuated, more cables than degrees of freedom are used.

VI. OPTIMIZATION

The dynamic workspace volume is optimized by the particle swarm method, from the Matlab optimization toolbox [35]. This method is able to find the global minimum for a non convex and non smooth cost function. Since the maximum dynamic workspace volume is desired, the cost function is the inverse of the dynamic workspace volume

$$f_{cost} = -V_{dyn} \quad (8)$$

V_{dyn} is computed as described in section V and optimized for variables that determine the geometry of the concepts. The geometry of a concept determines the mass of the moving

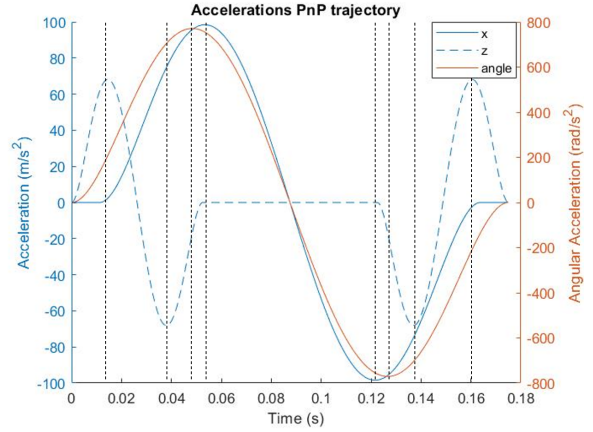


Fig. 12: Accelerations required to perform the adept cycle with a cycle time of 0.35s. The black vertical lines indicate the accelerations taken for the dynamic workspace computation.

Variable	Lower bound (m)	Upper bound (m)
W_f	0.5	2
L	0.05	1
W_t	0.02	0.2
D_p	0.02	0.2
D_{in}	0	0.05
D_{out}	0	0.05

TABLE I: List of optimization variables including bounds.

platform and the cable arrangement, which influences the EOM as described in section IV. The length of the rod L , and the inner D_{in} and outer diameter D_{out} of the rod are selected as variables for each concept. Also the width of the frame W_f is selected as a variable, and is considered being square. For concepts 2 and 3 the pulley diameter D_p is selected as an additional variable to optimize for. A larger diameter means more inertia, but a lower required cable force to perform the angular accelerations of the EE. Finally, the width of the top plate W_t of concept 1 and 2 are selected as variable since the moments about the local z-axis are not decoupled. A larger W_t means a better resistance against torques from the EE, but again more mass is added for a larger W_t . The remaining parameters that determine the geometry are considered to be constant to save computation time in the optimization. L , W_f , and W_t are shown in figure 5 and an overview of the selected variables is given in table I including their bounds. The bounds of the variables are required to remain within the installation space as described in section II and to limit the optimization time. In addition to the bounds, constraints are required to ensure the strength of the concepts. Namely, D_{in} , D_{out} and L are not limited with respect to each other and a low mass is desired for a large V_{dyn} . This will result in an unrealistically slender rod. Therefore, the following constraints are imposed concerning deformation and buckling of the rod. Where each of the constraints should be smaller or equal to zero $g_i \leq 0$.

1) *Buckling*:

$$g_1 = \frac{f_c \cdot L^2}{\pi^2 \cdot E \cdot I_r} - 1$$

Here f_c is the maximum compressive force that occurs in the rod including a safety factor of 3, E the Young's modulus, and I_r the bending factor of inertia of the rod.

2) *Compression*:

$$g_2 = \frac{f_c \cdot L}{A \cdot E \cdot \delta_c} - 1$$

Here A is the cross-sectional area of the rod, and δ_c is the maximum compression of the rod. The maximum compression of the rod is set to 0.1mm to ensure accurate EE positioning.

3) *Bending due to acceleration*:

$$g_3 = \frac{5 \cdot q \cdot L^4}{384 \cdot E \cdot I_r \cdot \delta_b} - 1$$

This constraint models the rod as a beam with a distributed load q applied on it, resulting from the maximum acceleration that occurs in x or y direction a_m and the density of the rod ρ : $q = a_m \cdot A \cdot \rho$. The maximum allowed bending deformation δ_b is calculated based on δ_c by Pythagoras, because δ_c influences the EE position.

4) $D_{in} < D_{out}$:

$$g_4 = \frac{D_{in} \cdot 1.05}{D_{out}} - 1$$

5) *Angular deformation*:

$$g_5 = \frac{T \cdot L}{G \cdot I_T \cdot \psi_T} - 1$$

Here T is the maximum torque that occurs in the rod including a safety factor of 3, G the shear modulus, I_T the torsion moment of inertia, and ψ_T the maximum angular deformation of the rod. The maximum angular deformation is set to 0.4° to ensure accurate EE positioning. This constraint is only taken into account for concepts 1 and 2 since the torques are decoupled from the main body in concept 3.

The constraints are added to f_{cost} as a barrier function as shown in equation 9, where p is the penalization factor.

$$f_{cost} = -V_{dyn} + p \cdot \sum_i (\max(0, g_i))^2 \quad (9)$$

All parts of the concepts are considered to be made of aluminium with a density of $\rho_{al} = 2700 \text{kg m}^{-3}$, except for the motor in concept 1. This motor was selected to be a lightweight Maxon EC-45-flat-80W, which has a mass of 0.15kg and is able to generate the required torque to accelerate the payload. The payload has a mass of 0.1 kg, following the benchmark as described in section II, and an inertia of $I_z = 2.8 \cdot 10^{-4} \text{kg m}^2$. Furthermore, cable force bounds are selected. A minimum cable force of $f_{min} = 10\text{N}$ was selected to provide stiffness, and a maximum cable force was set to $f_{max} = 100\text{N}$ which could be provided by a realistic motor torque and drum size.

	Concept 1	Concept 2	Concept 3
W_f (m)	2.00	2.00	2.00
L (m)	1.00	1.00	1.00
W_t (mm)	30.0	23.6	x
D_p (mm)	x	20.2	47.0
D_{in} (mm)	17.4	16.9	10.0
D_{out} (mm)	19.3	18.6	12.3
V_{dyn} (m ³)	0.213	0.288	0.165
M_p (kg)	0.575	0.266	0.278

TABLE II: Optimization results.

	Concept 1	Concept 2	Concept 3
W_f (m)	2.00	2.00	2.00
L (m)	1.00	1.00	1.00
W_t (mm)	35.1	32.4	x
D_p (mm)	x	20.0	46.6
D_{in} (mm)	26.1	14.8	10.2
D_{out} (mm)	27.4	17.1	13.0
V_{dyn} (m ³)	0.413	0.374	0.224
M_p (kg)	0.580	0.306	0.296

TABLE III: Optimization results for $f_m = 125\text{N}$.

A. Results

Optimization of the concepts results in the dynamic workspaces as shown in figures 13 and 14. Here the workspaces are shown for the centre of mass of the moving platform. The resulting parameter values that are linked to this workspace, the total mass of the concepts, and the actual workspace volume are given in table II. Concept 1 shows a conveniently shaped dynamic workspace. This concept also has a mass that is about twice as large compared to the other concepts and still has a relatively large dynamic workspace. This means that the cable configuration of concept 1 handles its mass efficiently. Still, a large mass can negatively influence the vibrations and repeatability. Concept 2 has the largest dynamic workspace volume, that covers almost all of the workspace of concept 1, and has a protrusion in the direction of the cable loop. This is logical since the parallel cables of the cable loop provide more force than a single cable. Concept 3 has the smallest workspace, which is also inconveniently shaped compared to the benchmark workspace. This is caused by the rotation cables being decoupled from the motion of the moving platform. They do not aid the motion as the cable loop in concept 2. Therefore, the force of only six cables is available to perform the adept cycle which results in a smaller dynamic workspace. Also the cable attachment points on the square frame, as shown in figure 13a, contribute to the inconvenient shape of the workspace. Furthermore, the dynamic workspace volumes of all concepts do not reach the volume of the benchmark volume, being 0.570m^3 . A larger dynamic workspace could be reached by higher cable forces or by a larger installation space since L and W_f are currently at their upper bound. Optimizing for a higher maximum cable force of $f_{max} = 125\text{N}$ results in volumes as shown in table III. It is noted that the workspace volume of concept 1 is larger than concept 2, which means that efficient cable configuration becomes more prominent than mass for high cable forces. However, when higher torques are required for the rotation of the payload,

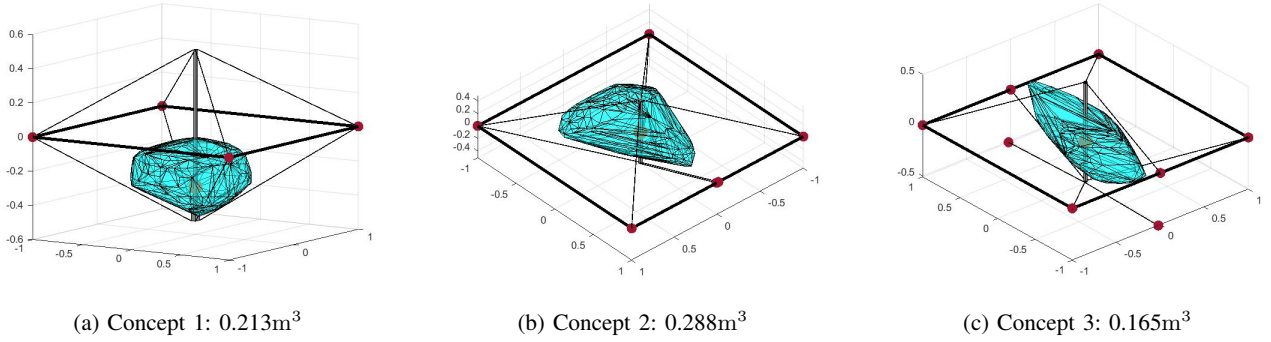


Fig. 13: Optimized workspace volumes and architectures of the concepts, showing that concept 2 has the largest dynamic workspace volume.

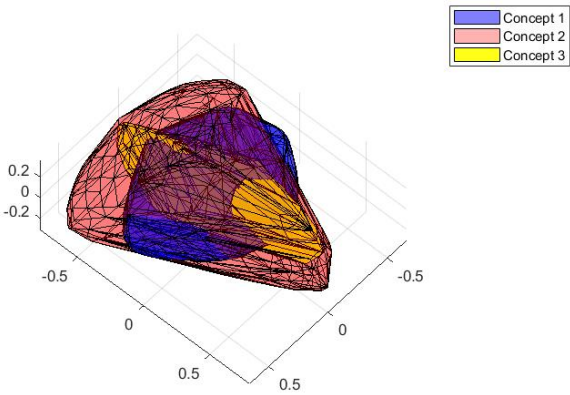


Fig. 14: This figure shows an overlap of the 3 optimized workspaces.

concept 2 does not need to be adapted. On the contrary, concept 1 needs a different motor with a larger mass, which leads to a smaller workspace. Since concept 2 has the largest workspace for the smallest cable forces and does not require adaptation for higher angular accelerations, it was selected as the concept with the most potential for application in the high speed pick and place industry. Therefore, a prototype of concept 2 was made and evaluated in section VII.

VII. PROTOTYPE

A. Design

Concept 2 was selected for experimental evaluation and build into a prototype. The design of the moving platform of the prototype is depicted in figure 15, containing close-ups of the top and bottom. At the top, cables are attached by clamping two aluminium plates on each other. These plates have a thickness of 5mm each, and a width and depth of 55mm and 25mm respectively. This clamping method is also applied at the bottom. An aluminium tube is connecting the top and bottom of the moving platform and has a length of 1m, with an inner and outer diameter of 18mm and 20mm

Cable	$a_{ix}(m)$	$a_{iy}(m)$	$a_{iz}(m)$	$b_{ix}(m)$	$b_{iy}(m)$	$b_{iz}(m)$
1	-1.173	0.939	0.060	-0.019	0.013	0.475
2	1.173	0.939	0.104	0.019	0.013	0.475
3	1.223	-0.939	0.060	0.019	-0.013	0.475
4	-1.223	-0.939	0.104	-0.019	-0.013	0.475
5	-1.173	-0.939	-0.104	-0.019	-0.021	-0.475
6	-1.223	0.939	-0.060	-0.019	0.021	-0.475
7	1.223	0.939	-0.104	0.028	0.015	-0.493
8	1.173	-0.939	-0.060	0.028	-0.015	-0.493

TABLE IV: Coordinates of the cable attachment point on the frame a and on the moving platform b .

respectively. The bottom of the moving platform is a u-shaped aluminium part, having a width of 53mm, a depth of 42mm, and a height of 47mm. This part houses two roller bearings which support the axis, and two eyelets that guide the cable of the cable loop to the teflon pulley which has a smallest diameter of 22mm. This pulley is glued on a steel 6mm diameter axis with a length of 65mm, that transfers the torque from the cable loop to the EE. The EE is again made of 5mm thick aluminium, having a width and depth of 66mm and 10mm. This results in a total mass of 0.377kg, taking both the EE and moving platform into account.

The moving platform is build into a frame with sizes of 2.5m by 2m, as shown in figure 16. Here it is shown that the servo motors and drums are located on the floor, and the 3mm Dyneema cables are guided by pulleys to the moving platform. This results in the a and b coordinates as given in table IV. The actuation and control unit is a CNC Beckhoff system, which requires cable lengths as input. It measures the cable lengths by absolute encoders, and controls the cable lengths with a PID controller. Thus to perform a motion, the motion coordinates are first transferred to joint coordinates and then inserted into the control system with G-code. Note that the frame is tilted with respect to gravity and how one would expect to see it in a pick and place application. This is the case because the frame and hardware of the CarISA CDPR [36] were used. Since the CDPR is fully constrained, this hardly affects the results.

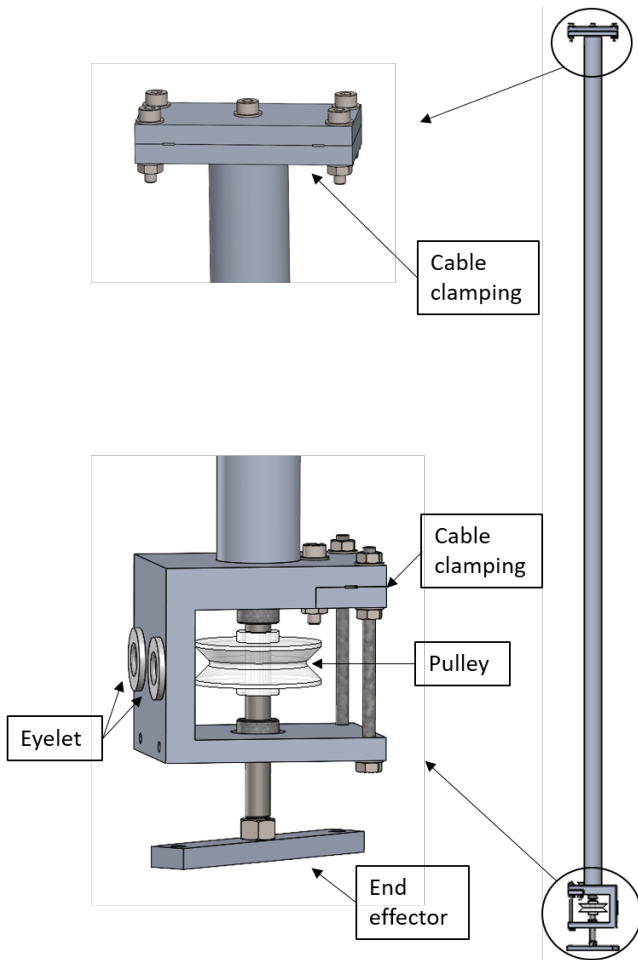


Fig. 15: Design of the moving platform of the prototype.

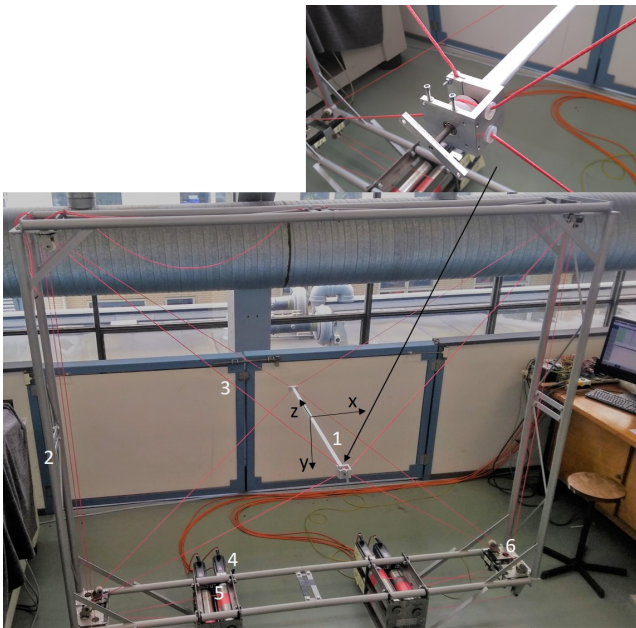


Fig. 16: Prototype of the robot. 1: moving platform, 2: frame, 3: cable, 4: servo motor, 5: drum, 6: guiding pulley

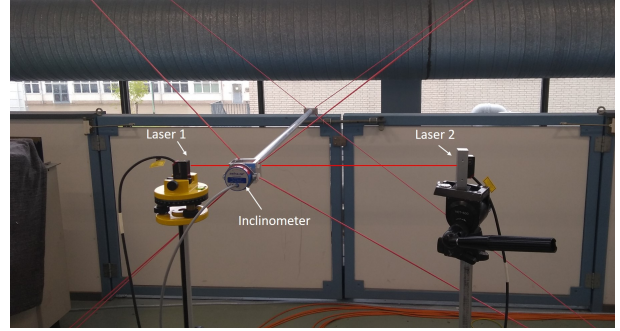


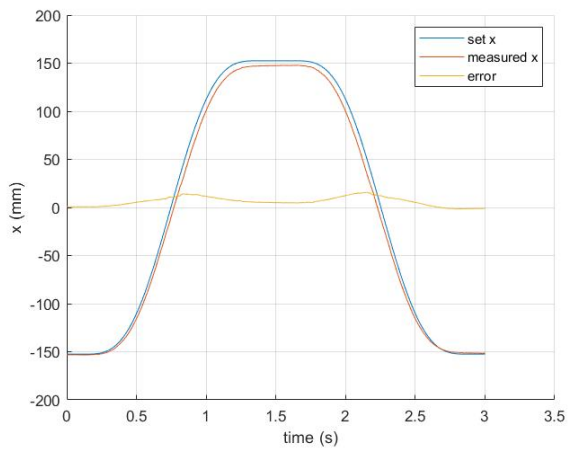
Fig. 17: Prototype of the robot in an experimental setup.

B. Evaluation

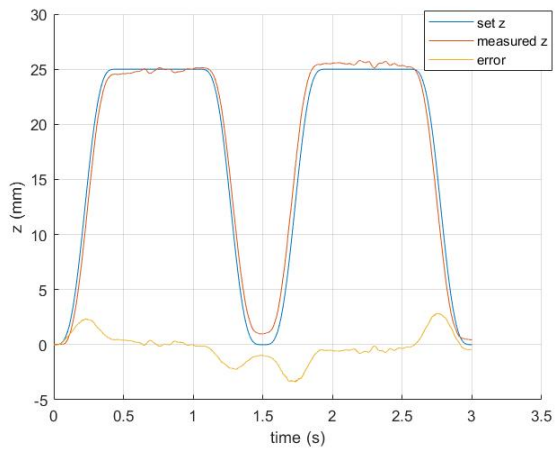
To verify that the design can perform a pick and place Schönflies motion in a stable manner, and to compare it with the benchmark design, the adept cycle has been applied on the prototype. The adept cycle as given in figure 11 is applied, starting from $x = -152.5\text{mm}$, and with a cycle time of 3s due to hardware limitations. The error between the intended and the actual trajectory is measured along the trajectory, and the measurement is repeated for 24 times to obtain the repeatability halfway the trajectory.

Two laser sensors (optoNCDT ILD1420-200) are aimed at the lower part of the moving platform, as indicated in figure 17, to measure the position in x -direction. These lasers have a range of 200mm, which is not sufficient to measure the complete 305mm translation. Therefore, the second laser takes over when the first laser is out of range. The position in z -direction is measured by mounting one laser at the moving platform and aiming it at a mirror that is parallel to the x - y -plane. Additionally, an inclinometer (Seika NG4i) is attached to the EE to measure the angle. This results in an measured versus applied trajectory, as shown in figure 18.

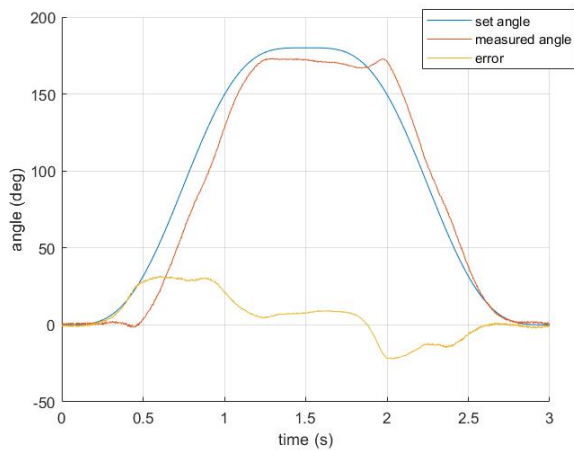
The resulting error is also shown in this figure and is maximally 15.84mm in x -direction, and 2.84mm in z -direction. Halfway the adept cycle, at the instance where a product would be placed, the errors are 4.96mm (3.3%) in x -direction and 0.98mm in z -direction. The main cause of these position errors are the inaccuracies in the determination of the cable attachment points a and b . These inaccuracies result from inaccuracies in the prototype fabrication and the guiding pulleys at the frame with inherently non fixed cable attachment points. A better calibration procedure and including pulley kinematics to compute the cable lengths should be sufficient to overcome these issues. The position repeatability was computed to be 0.46mm, which does not meet the benchmark precision of 0.1mm. An increase in stiffness is required to reduce vibrations and reach a better repeatability. The stiffness could be enhanced by a higher initial cable force [12]. However, this robot is not able to measure cable forces, which is required for accurate determination of the pretension. Changing the architecture or configuration of the robot could also result in a higher stiffness [37], for instance by using crossing cables as applied to the CaRISA robot [36].



(a) x-direction

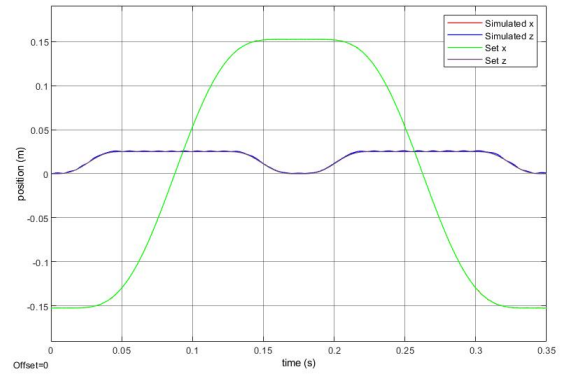


(b) z-direction

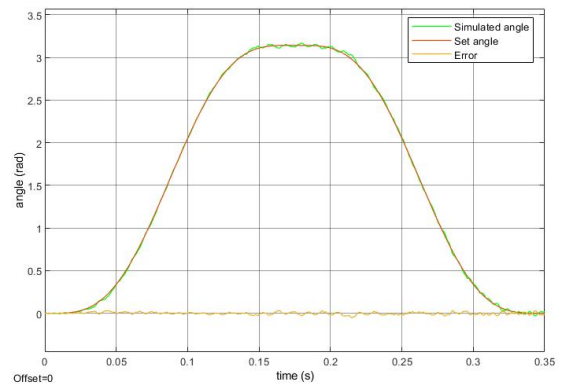


(c) Angle of the EE.

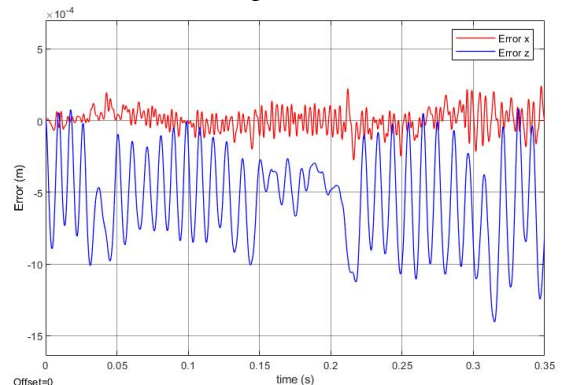
Fig. 18: Measured versus applied trajectory of the prototype, showing stable motion and rotation of the EE and errors of 4.96mm, 0.98mm, and 7.81° halfway the adept cycle.



(a) Position of the moving platform.



(b) Angle of the EE.



(c) Error of the moving platform position.

Fig. 19: Simulated versus applied trajectory of the prototype, showing vibrations of 0.5mm and 1° amplitude.

The maximum error in the angle is 31.89°, and 7.81° (4.3%) halfway the adept cycle, which is relatively high. This is caused again by the inaccuracies in a and b , which have an even stronger effect on the angle. Namely, an error of 1mm in cable length already results in an angular error of 4.3° due to the small pulley diameter. Therefore, one might want to use a larger pulley diameter in future designs to reduce the error amplification. The motors contribute to the angular error as well, since they are at their performance limit. The cables of the cable loop have the largest change in length of all cables, which results in higher cable accelerations.

These accelerations are hardly met, which results in the angle lagging behind. The angular repeatability is 0.41° , which almost meets the benchmark repeatability of 0.4° .

Since the measurements can not be obtained for the benchmark cycle time, a forward dynamic model in Matlab/Simscape is also used for the evaluation of the design. This is a feed forward model, based on the model by Tempel et al. [38], that only models the moving platform and the cables. The moving platform and EE are modelled as rigid bodies and the cables are modelled as springs according to

$$f_{c,i} = \begin{cases} \frac{E_c \cdot A_c}{L_{c,i}} \cdot (L_{c,i} - L_{set,i}) & \text{if } f_{c,i} \leq 0 \\ 0 & \text{otherwise} \end{cases} \quad (10)$$

Here A_c is the cross section of the cable, and $E_c = 95\text{GPa}$ the Young's modulus of the Dyneema material [10]. The differences between the cable lengths $L_{c,i}$ and the set cable lengths $L_{set,i}$ from the trajectory result in the cable forces $f_{c,i}$ which are imposed on the moving platform. Inserting the adept cycle with a cycle time of 0.35s results in a modeled trajectory versus the intended trajectory as shown in figure 19. Here the vibrations have an amplitude of about 0.5mm and 1° , which solely result from the stiffness of the design. This confirms that the stiffness should be enhanced in future designs to meet the benchmark repeatability.

VIII. CONCLUSIONS

This paper proposes three new CDPR design variations that are able to perform a Schönflies motion, including a rotation of at least 180 degrees. Additionally, a method to dynamically compare these designs is introduced, and one design is experimentally evaluated on the adept cycle.

The three design variations contain a 2D frame and a rod shaped moving platform. Each of the designs has a different rotation mechanism, being a motor (concept 1), a cable loop (concept 2), and a torque decoupling cable loop (concept 3). These design variations have been optimized for their dynamic workspace, which is the space where they can perform the accelerations of an adept cycle with a cycle time of 0.35s, given a maximum installation space. Concept 2 shows the largest dynamic workspace volume for the smallest cable forces, thus the least power consumption. Concept 1 has a competitive workspace size and has the most efficient cable configuration, but it has the highest mass and is the least adaptable to higher (angular) accelerations. Concept 3 has the smallest and most inconveniently shaped dynamic workspace, it would require additional cables to be competitive. Additionally, the workspace volumes do not yet reach the workspace volume of a benchmark Delta robot. The CDPR designs would require a larger installation space or higher available cable forces.

As concept 2 shows the highest potential to be applied in the high speed pick and place industry, a prototype of this design was made and evaluated in an experimental setup and a forward dynamic model by application of the adept cycle. Application of the adept cycle in the experimental setup with a cycle time of 3s results in an error of 4.96mm and 7.81° , and a repeatability of 0.46mm and 0.41° halfway

the cycle. Inserting the adept cycle with a 0.35s cycle time in the forward dynamic model shows vibrations with an amplitude of 0.5mm and 1° . The results show that the design can perform a stable motion and EE rotation, providing the design to be suitable for high speed pick and place tasks. However, a better calibration procedure should be applied to reduce the error and future designs should improve their stiffness to reach the benchmark repeatability.

ACKNOWLEDGEMENTS

The author would like to thank Philipp Tempel and Volkert van der Wijk for their guidance and support during the project.

REFERENCES

- [1] François Pierrot, C Reynaud, and Alain Fournier. Delta: a simple and efficient parallel robot. *Robotica*, 8(2):105–109, 1990.
- [2] Bruno Siciliano and Oussama Khatib. *Springer handbook of robotics*. Springer, 2016.
- [3] ABB. ROBOTICS IRB 360 FlexPicker ©, 2020.
- [4] Omron. Omron: Industrial Robotics Automation Catalog - Product Datasheets, 2020.
- [5] Omron. Delta robot 3 axes + 1 rot, 2020.
- [6] Vincent Nabat, María de la O Rodriguez, O Company, Sébastien Krut, and F Pierrot. Par4: very high speed parallel robot for pick-and-place. In *2005 IEEE/RSJ International Conference on intelligent robots and systems*, pages 553–558. IEEE, 2005.
- [7] Fugui Xie and Xin-Jun Liu. Design and development of a high-speed and high-rotation robot with four identical arms and a single platform. *Journal of Mechanisms and Robotics*, 7(4), 2015.
- [8] Clément Gosselin. Cable-driven parallel mechanisms: state of the art and perspectives. *Mechanical Engineering Reviews*, 1(1):DSM0004–DSM0004, 2014.
- [9] Zhaokun Zhang, Zhufeng Shao, and Liping Wang. Optimization and implementation of a high-speed 3-dofs translational cable-driven parallel robot. *Mechanism and Machine Theory*, 145:103693, 2020.
- [10] Andreas Pott and Tobias Bruckmann. *Cable-driven parallel robots: Theory and Application*. Springer, 2018.
- [11] S Kawamura, W Choe, S Tanaka, and SR Pandian. Development of an ultrahigh speed robot falcon using wire drive system. In *Proceedings of 1995 IEEE International Conference on Robotics and Automation*, volume 1, pages 215–220. IEEE, 1995.
- [12] Sadao Kawamura, Hitoshi Kino, and Choe Won. High-speed manipulation by using parallel wire-driven robots. *Robotica*, 18(1):13–21, 2000.
- [13] Andreas Pott, Hendrick Mütherich, Werner Kraus, Valentine Schmidt, Philipp Miermeister, and Alexander Verl. Ipanema: a family of cable-driven parallel robots for industrial applications. In *Cable-Driven Parallel Robots*, pages 119–134. Springer, 2013.
- [14] Andreas Pott. Forward kinematics and workspace determination of a wire robot for industrial applications. In *Advances in Robot Kinematics: Analysis and Design*, pages 451–458. Springer, 2008.
- [15] Zhaokun Zhang, Zhufeng Shao, Liping Wang, and Albert J Shih. Optimal design of a high-speed pick-and-place cable-driven parallel robot. In *Cable-Driven Parallel Robots*, pages 340–352. Springer, 2018.
- [16] Robert Dekker, Amir Khajepour, and Saeed Behzadipour. Design and testing of an ultra-high-speed cable robot. *International Journal of Robotics and Automation*, 21(1):25–34, 2006.
- [17] Andreas Pott and Philipp Miermeister. Workspace and interference analysis of cable-driven parallel robots with an unlimited rotation axis. In *Advances in Robot Kinematics*, pages 341–350. Springer, 2018.
- [18] Alexis Fortin-Côté, Céline Faure, Laurent Bouyer, Bradford J McFadyen, Catherine Mercier, Michaël Bonenfant, Denis Laurendeau, Philippe Cardou, and Clément Gosselin. On the design of a novel cable-driven parallel robot capable of large rotation about one axis. In *Cable-Driven Parallel Robots*, pages 390–401. Springer, 2018.

- [19] Thomas Reichenbach, Philipp Tempel, Alexander Verl, and Andreas Pott. On kinetostatics and workspace analysis of multi-platform cable-driven parallel robots with unlimited rotation. In *IFTOMM International Symposium on Robotics and Mechatronics*, pages 79–90. Springer, 2019.
- [20] Andry Maykol Pinto, Eduardo Moreira, José Lima, José Pedro Sousa, and Pedro Costa. A cable-driven robot for architectural constructions: a visual-guided approach for motion control and path-planning. *Autonomous Robots*, 41(7):1487–1499, 2017.
- [21] Thomas Reichenbach, Philipp Tempel, Alexander Verl, and Andreas Pott. Static analysis of a two-platform planar cable-driven parallel robot with unlimited rotation. In *International Conference on Cable-Driven Parallel Robots*, pages 121–133. Springer, 2019.
- [22] M Vikranth Reddy, NC Praneet, and GK Ananthasuresh. Planar cable-driven robots with enhanced orientability. In *International Conference on Cable-Driven Parallel Robots*, pages 3–12. Springer, 2019.
- [23] Toru Makino and Takashi Harada. Cable collision avoidance of a pulley embedded cable-driven parallel robot by kinematic redundancy. In *Proceedings of the 4th International Conference on Control, Mechatronics and Automation*, pages 117–120, 2016.
- [24] Marco Alexander Carpio Alemán, Roque Saltaren, Alejandro Rodríguez, Gerardo Portilla, and Juan Diego Placencia. Rotational workspace expansion of a planar cdpr with a circular end-effector mechanism allowing passive reconfiguration. *Robotics*, 8(3):57, 2019.
- [25] Michael Anson, Aliakbar Alamdari, and Venkat Krovi. Orientation workspace and stiffness optimization of cable-driven parallel manipulators with base mobility. *Journal of Mechanisms and Robotics*, 9(3), 2017.
- [26] Tam Nhat Le, Hiroki Dobashi, and Kiyoshi Nagai. Configuration of redundant drive wire mechanism using double actuator modules. *ROBOMECH Journal*, 3(1):25, 2016.
- [27] Marceau Métillon, Saman Lessanibahri, Philippe Cardou, Kévin Subrin, and Stéphane Caro. A cable-driven parallel robot with full-circle end-effector rotations. In *The ASME 2020 International Design Engineering Technical Conferences & Computers and Information in Engineering Conference IDETC/CIE 2020*, 2020.
- [28] Saman Lessanibahri, Philippe Cardou, and Stéphane Caro. Kinetostatic modeling of a cable-driven parallel robot using a tilt-roll wrist. In *International Conference on Cable-Driven Parallel Robots*, pages 109–120. Springer, 2019.
- [29] Saman Lessanibahri, Philippe Cardou, and Stéphane Caro. A cable-driven parallel robot with an embedded tilt-roll wrist. *Journal of Mechanisms and Robotics*, 12(2), 2020.
- [30] Richard Verhoeven. *Analysis of the workspace of tendon-based Stewart platforms*. PhD thesis, University Duisburg-Essen, 2004.
- [31] Tobias Bruckmann, Lars Mikelsons, Thorsten Brandt, Manfred Hiller, and Dieter Schramm. Wire robots part ii: Dynamics, control & application. 2008.
- [32] Lorenzo Gagliardini, Marc Gouttefarde, and Stéphane Caro. Determination of a dynamic feasible workspace for cable-driven parallel robots. In *Advances in Robot Kinematics 2016*, pages 361–370. Springer, 2018.
- [33] J-F Gauthier, J Angeles, and S Nokleby. Optimization of a test trajectory for scara systems. In *Advances in robot kinematics: Analysis and design*, pages 225–234. Springer, 2008.
- [34] Andreas Pott. An improved force distribution algorithm for over-constrained cable-driven parallel robots. In *Computational Kinematics*, pages 139–146. Springer, 2014.
- [35] Mathworks. Particle swarm optimization, 2020.
- [36] Philipp Tempel, Matthias Alfeld, and Volkert van der Wijk. Design and analysis of cable-driven parallel robot carisa: A cable robot for inspecting and scanning artwork. In *Symposium on Robot Design, Dynamics and Control*, pages 136–144. Springer, 2020.
- [37] Hao Xiong and Xiumin Diao. The effect of cable tensions on the stiffness of cable-driven parallel manipulators. In *2017 IEEE International Conference on Advanced Intelligent Mechatronics (AIM)*, pages 1185–1190. IEEE, 2017.
- [38] Philipp Tempel, Philipp Miermeister, Armin Lechler, and Andreas Pott. Modelling of kinematics and dynamics of the ipanema 3 cable robot for simulative analysis. In *Applied Mechanics and Materials*, volume 794, pages 419–426. Trans Tech Publ, 2015.

Chapter 4

Discussion

The first part of this thesis showed that three challenges exist for CDPRs to be applied in the high speed pick and place industry, being the performance of a Schönflies motion that contains a rotation of at least 180 degrees for full product reorientation, cable-environment collision avoidance, and vibration attenuation. Literature showed that several solutions exist to perform large rotations, however none of the solutions were designed, modelled compared or tested for dynamic applications. Additionally, methods to avoid collisions with the environment were identified as collision free path planning, collision free workspace determination, and smart geometric design. Collision free path planning was shown to be efficient in unknown or complex environments, but a pick and place environment is considered not to be unknown nor being complex. Collision free workspace determination is a more efficient method to avoid collisions, but the region of interest could still lie outside this workspace. Therefore synthesis methods would be needed to obtain the required collision free workspace, these methods do not yet exist in literature. A better solution was proposed by smart geometrical design, making use of a 2D frame and a rod or beam shaped moving platform, to avoid collisions. This design was as well applied in the concept designs in the second part of this thesis. The third challenge can be solved by bias tension wrench compensation or control. However, bias tension increases the power consumption and wear of the robot, and an increase in tension does not necessarily lead to a monotonic increase in stiffness [29]. The proposed control methods show potential to attenuate vibrations. However, more sophisticated models need to be implemented to reach a sufficient dynamic performance by including cable dynamics, friction, and auxiliary winch parts. Moreover, no holistic control approach is yet available for CDPRs [30]. Therefore, control methods should be compared and evaluated to find the best approach.

The second paper focused on the first challenge that was found in the literature review, by comparing three new concepts that have potential to perform a Schönflies motion in the high speed pick and place industry. These concepts use a motor, a cable loop, and a torque decoupling cable loop to perform the rotation, and have been selected from a larger group of concepts based on the criteria as shown in appendices 1, 2, and 3. Despite having performed a thorough concept selection, other rotation principles as described in the appendices and chapter 1 might also have potential for high speed motions. Therefore, one may want to include them in future comparisons.

The three selected concepts are compared and optimized for their dynamic workspace volume, which is computed based on the accelerations of the adapt cycle. This makes it a task based comparison. Such a comparison has not been performed before on dynamic cable driven parallel

robots and has shown to be a convenient method to compare cable driven robots when both workspace size and dynamics are of interest. Using a different trajectory might result in other workspace volumes, which is a disadvantage of a task based comparison. However, when using a different trajectory one can not do a comparison with a state of the art Delta robot. Moreover, when the accelerations are about the same magnitude, this will have little impact. The payload, cable force bounds, and the allowed installation space will also influence the workspace volume. Ideally, one would exactly want to know which concept has the largest workspace for which of these parameter values. However, this will take an unrealistically amount of optimization time. Some investigations on these parameters have been performed in appendix 4, showing that a higher maximum cable force has the same effect on the workspace volume as a lower acceleration set, and a larger installation space or mass results in the same relation between the concepts' workspace volumes. Still, these investigations were not all performed by optimizations so this can only be taken as an indication. Additionally, comparing the exact workspace volume might not be the optimal method, because a workspace could have a large volume but an inconvenient workspace shape. Therefore, one might want to consider the overlapping volume with an intended workspace to be the volume to optimize for in future work. Nevertheless, this paper showed that the concepts with the largest volumes also have the most convenient volumes. So the results will not be affected by this statement. The optimization of the workspace volumes was performed for 6 variables that determine the mass and cable configuration of the CDPR. Including more geometric variables can influence the optimization results. However, this will strongly increase computation time for a small expected difference in the results, as the variables that have the strongest effect on mass and cable configuration were already used.

Optimization and comparison of the concepts revealed that concept 2 has the largest dynamic workspace volume for the smallest cable forces, thus the least power consumption. This concept is followed by concept 1 which has a competitive dynamic workspace volume, and even a larger dynamic workspace volume when higher cable forces are allowed. Yet this robot has a mass that is twice as large as the other concepts, which means that its cable configuration is more efficient. In literature, adding a motor was mostly disregarded because its mass would reduce the workspace size [19], which makes it less attractive with respect to only using cables to perform rotations. The motor mass of course does reduce the workspace size, but the cable configuration is shown to be just as important. Still, the motor mass does reduce the dynamic performance in terms of vibrations. Additionally, when larger angular accelerations of the end effector are required, a stronger and heavier motor is needed contrary to the other concepts that do not need adaptation. Nevertheless, in low speed applications, a motor is an option to consider. The third concept showed the smallest and most inconveniently shaped workspace volume since the cables that perform the rotation do not aid the translational motions. The force of only six cables is available to perform the translations of the adapt cycle. This concept would require additional cables to compete with the other dynamic workspace volumes. However, more cables means more actuators which makes the robot more costly and less attractive for the industry. Despite concept 1 and 2 showing a large dynamic workspace volume, they do not meet the benchmark workspace volume. To reach the benchmark Delta robot workspace volume, the maximum allowable cable forces or installation space should be larger. Larger cable forces can be acquired with stronger motors. A larger installation space would make the solutions less attractive for the industry. Therefore, one might want to consider this as an additional challenge for CDPRs in the high speed pick and place industry and apply optimization methods to obtain the intended workspace volume with the smallest installation space.

Concept 2 was fabricated as a prototype and evaluated on the adapt cycle in an experimental setup and in a forward dynamic model. The feed forward model is only taking the cables as

springs into account. Ideally, one would also want to take actuators, winches, cable dynamics, friction, and damping into account. However, including these components in the model is either a gap in literature or corresponding values were unknown. Therefore, the feed forward model gives a simplified view with regard to reality.

The experimental setup showed relatively large errors between the intended trajectory and the measured prototype trajectory. These errors mainly result from inaccuracies in the determination of the cable attachment points, which causes the actual cable lengths to deviate. The cable anchor points deviate due to inaccurate fabrication and because the cable guiding pulleys on the frame inherently have non constant cable attachment points. A better calibration procedure and taking pulley kinematics into account would reduce the error. The repeatability was determined to be relatively close to the benchmark repeatability for a cycle time of 3s, but still not equal to or better than the benchmark Delta robot. At a benchmark cycle time of 0.35s this repeatability will not improve, which is confirmed by the feed forward model. The pick and place CDPR by Zhang et al. [7] also shows better performance, as it reaches a repeatability of 0.12mm, and an error of 0.3mm halfway the cycle for a 0.48s cycle time. Therefore, the stiffness should improve in future designs to meet the benchmark repeatability and attenuate the vibrations which is again the third challenge as discussed in the first part of this thesis. Vibrations can be attenuated by bias tension in the cables and control methods as discussed above. Bias tension will increase wear and power consumption, and the prototype should have force sensors to be able to apply and measure the bias tension. Furthermore, other architectures can also be considered and compared to increase the stiffness. Yet one should be aware that while considering other architectures the second challenge of collision avoidance might reopen.

The proposed designs can also be of interest for other areas of application. For instance in rehabilitation [20], assembly operations, or art scanning [31], as large rotations are also required for fully constrained CDPRs in these fields. Additionally, the proposed designs can also be easily adapted if rotations about other axes are required, or even multiple cable loops or motors can be added when multiple large rotations are required.

Chapter 5

Conclusions

This thesis was written to make CDPRs more attractive for high speed pick and place tasks. Challenges for CDPRs in the pick and place industry were obtained by a literature review, and three design variations were proposed that are able to perform a Schönflies motion, including a rotation of at least 180 degrees. Additionally, a method to dynamically compare these designs was introduced, and one design was build as a prototype and experimentally evaluated.

A literature review identified three challenges for the application of cable driven parallel robots in the high speed pick and place industry, being the performance of a Schönflies motion that contains a rotation of at least 180 degrees for full product reorientation, cable-environment collision avoidance, and vibration attenuation. Literature showed that several conceptual solutions exist for performing large rotations, but none of them have been designed, modelled, compared, or tested for dynamic applications. Furthermore, the challenge of collision avoidance with the environment is considered to be overcome by smart geometrical design. Additionally, vibrations can be attenuated by bias tension wrench compensation and control. Bias tension increases power consumption and wear, and a holistic control approach needs to be found including cable dynamics, friction, and auxiliary winch parts in the model to reach high dynamic performances.

Three CDPR design variations were proposed that are able to perform a Schönflies motion including a rotation of at least 180 degrees. The designs were compared on their dynamic workspace, based on the accelerations during an adept cycle. This comparison revealed that adding a motor or a cable loop to perform large rotations results in reasonably sized dynamic workspaces with potential to reach the workspace size of a Delta robot by applying higher cable forces or allowing a larger installation space. Additionally, a prototype of the cable loop concept was fabricated and evaluated on a typical pick and place trajectory including an end effector rotation of 180 degrees. This showed a stable motion and end effector rotation, and potential for application in the high speed pick and place industry when accurate calibration is performed. However, to meet the repeatability of commercially available Delta robots the stiffness of the designs should increase to reduce vibrations, which is again the third challenge as identified in the literature review.

In conclusion, conceptual CDPRs that can perform large rotations were proposed in literature but none of them were designed, modelled, compared or tested for high speed applications. This thesis filled this gap by proposing and dynamically comparing three design variations that can perform a Schönflies motion including a rotation of at least 180 degrees, and by experimentally evaluating one of the design variations. Thereby, making CDPRs more attractive for high speed pick and place tasks.

Bibliography

- [1] Robotics Online Marketing Team. Pick and place robots: What are they used for and how do they benefit manufacturers?, Mar 2018.
- [2] Bruno Siciliano and Oussama Khatib. *Springer handbook of robotics*. Springer, 2016.
- [3] François Pierrot, C Reynaud, and Alain Fournier. Delta: a simple and efficient parallel robot. *Robotica*, 8(2):105–109, 1990.
- [4] ABB. ROBOTICS IRB 360 FlexPicker , 2020.
- [5] Omron. Omron: Industrial Robotics Automation Catalog - Product Datasheets, 2020.
- [6] Clément Gosselin. Cable-driven parallel mechanisms: state of the art and perspectives. *Mechanical Engineering Reviews*, 1(1):DSM0004–DSM0004, 2014.
- [7] Zhaokun Zhang, Zhufeng Shao, and Liping Wang. Optimization and implementation of a high-speed 3-dofs translational cable-driven parallel robot. *Mechanism and Machine Theory*, 145:103693, 2020.
- [8] S Kawamura, W Choe, S Tanaka, and SR Pandian. Development of an ultrahigh speed robot falcon using wire drive system. In *Proceedings of 1995 IEEE International Conference on Robotics and Automation*, volume 1, pages 215–220. IEEE, 1995.
- [9] Sadao Kawamura, Hitoshi Kino, and Choe Won. High-speed manipulation by using parallel wire-driven robots. *Robotica*, 18(1):13–21, 2000.
- [10] Andreas Pott, Hendrick Mütherich, Werner Kraus, Valentine Schmidt, Philipp Miermeister, and Alexander Verl. Ipanema: a family of cable-driven parallel robots for industrial applications. In *Cable-Driven Parallel Robots*, pages 119–134. Springer, 2013.
- [11] Andreas Pott. Forward kinematics and workspace determination of a wire robot for industrial applications. In *Advances in Robot Kinematics: Analysis and Design*, pages 451–458. Springer, 2008.
- [12] Zhaokun Zhang, Zhufeng Shao, Liping Wang, and Albert J Shih. Optimal design of a high-speed pick-and-place cable-driven parallel robot. In *Cable-Driven Parallel Robots*, pages 340–352. Springer, 2018.
- [13] Robert Dekker, Amir Khajepour, and Saeed Behzadipour. Design and testing of an ultrahigh-speed cable robot. *International Journal of Robotics and Automation*, 21(1):25–34, 2006.

- [14] Jean-Pierre Merlet. Kinematics of the wire-driven parallel robot marionet using linear actuators. In *2008 IEEE International Conference on Robotics and Automation*, pages 3857–3862. IEEE, 2008.
- [15] Andreas Pott and Tobias Bruckmann. *Cable-driven parallel robots: Theory and Application*. Springer, 2018.
- [16] Andreas Pott and Philipp Miermeister. Workspace and interference analysis of cable-driven parallel robots with an unlimited rotation axis. In *Advances in Robot Kinematics*, pages 341–350. Springer, 2018.
- [17] Andry Maykol Pinto, Eduardo Moreira, José Lima, José Pedro Sousa, and Pedro Costa. A cable-driven robot for architectural constructions: a visual-guided approach for motion control and path-planning. *Autonomous Robots*, 41(7):1487–1499, 2017.
- [18] Thomas Reichenbach, Philipp Tempel, Alexander Verl, and Andreas Pott. On kinetostatics and workspace analysis of multi-platform cable-driven parallel robots with unlimited rotation. In *IFTToMM International Symposium on Robotics and Mechatronics*, pages 79–90. Springer, 2019.
- [19] Thomas Reichenbach, Philipp Tempel, Alexander Verl, and Andreas Pott. Static analysis of a two-platform planar cable-driven parallel robot with unlimited rotation. In *International Conference on Cable-Driven Parallel Robots*, pages 121–133. Springer, 2019.
- [20] Alexis Fortin-Côté, Céline Faure, Laurent Bouyer, Bradford J McFadyen, Catherine Mercier, Michaël Bonenfant, Denis Laurendeau, Philippe Cardou, and Clément Gosselin. On the design of a novel cable-driven parallel robot capable of large rotation about one axis. In *Cable-Driven Parallel Robots*, pages 390–401. Springer, 2018.
- [21] M Vikranth Reddy, NC Praneet, and GK Ananthasuresh. Planar cable-driven robots with enhanced orientability. In *International Conference on Cable-Driven Parallel Robots*, pages 3–12. Springer, 2019.
- [22] Toru Makino and Takashi Harada. Cable collision avoidance of a pulley embedded cable-driven parallel robot by kinematic redundancy. In *Proceedings of the 4th International Conference on Control, Mechatronics and Automation*, pages 117–120, 2016.
- [23] Marco Alexander Carpio Alemán, Roque Saltaren, Alejandro Rodriguez, Gerardo Portilla, and Juan Diego Placencia. Rotational workspace expansion of a planar cdpr with a circular end-effector mechanism allowing passive reconfiguration. *Robotics*, 8(3):57, 2019.
- [24] Michael Anson, Aliakbar Alamdari, and Venkat Krovi. Orientation workspace and stiffness optimization of cable-driven parallel manipulators with base mobility. *Journal of Mechanisms and Robotics*, 9(3), 2017.
- [25] Tam Nhat Le, Hiroki Dobashi, and Kiyoshi Nagai. Configuration of redundant drive wire mechanism using double actuator modules. *ROBOMECH Journal*, 3(1):25, 2016.
- [26] Marceau Métillon, Saman Lessanibahri, Philippe Cardou, Kévin Subrin, and Stéphane Caro. A cable-driven parallel robot with full-circle end-effector rotations. In *The ASME 2020 International Design Engineering Technical Conferences & Computers and Information in Engineering Conference IDETC/CIE 2020*, 2020.

- [27] Saman Lessanibahri, Philippe Cardou, and Stéphane Caro. Kinetostatic modeling of a cable-driven parallel robot using a tilt-roll wrist. In *International Conference on Cable-Driven Parallel Robots*, pages 109–120. Springer, 2019.
- [28] Saman Lessanibahri, Philippe Cardou, and Stéphane Caro. A cable-driven parallel robot with an embedded tilt-roll wrist. *Journal of Mechanisms and Robotics*, 12(2), 2020.
- [29] Hao Xiong and Xiumin Diao. The effect of cable tensions on the stiffness of cable-driven parallel manipulators. In *2017 IEEE International Conference on Advanced Intelligent Mechatronics (AIM)*, pages 1185–1190. IEEE, 2017.
- [30] Christian Tobias Schenk. *Modelling and Control of a Cable-Driven Parallel Robot - Methods for Vibration Reduction and Motion Quality Improvement*. PhD thesis, University Stuttgart, 2019.
- [31] Philipp Tempel, Matthias Alfeld, and Volkert van der Wijk. Design and analysis of cable-driven parallel robot carisa: A cable robot for inspecting and scanning artwork. In *Symposium on Robot Design, Dynamics and Control*, pages 136–144. Springer, 2020.

Appendices

The appendices contain additional information on the project for the ones that are interested or proceeding with the project. The appendices start at the next page, having the following content:

1. List of requirements and criteria
2. Concept generation
3. Concept selection
4. Optimization investigation
5. Cable loop criteria, concepts and concept selection
6. Strength analysis
7. Clamping design test
8. Calibration of CaRISA
9. Repeatability measurements
10. Simulink model of the forward dynamic model
11. Matlab scripts

Appendix 1: List of requirements and criteria

At the start of the project a list of requirements and criteria was set up. The criteria are used to compare the concepts. In this appendix the requirements and criteria are given as a summation.

Requirements

- 1. The cycle time of the end effector along a 25/305/25mm path should be equal or lower than 0.35s for a 0.1kg payload.** This cycle time is chosen since this is comparable with the cycle times of a delta robot. The cycle time of the flexpicker is 0.35 seconds, which is taken as a benchmark robot.
- 2. The end effector should be able to perform a rotation about its local z-axis of at least 180 degrees.** This is the goal of the project and therefore one of the most important requirements.
- 3. The end effector rotation around its local z-axis should be performed within half of the cycle time.** To reorient products during a pick and place task, the robot should be able to perform the reorientation between a pick and a place. So half of the cycle time. Otherwise the product will not be fully reoriented at its placed position or the cycle time will increase.
- 4. The wrench feasible, collision free, and singularity free workspace of the parallel cable robot should include the same cylinder as the benchmark robot, with a 1440mm diameter and a height of 350mm.** The workspace of common delta robots are cylindrically shaped. A state of the art delta robot is the flexpicker by ABB robotics. The flexpicker has a workspace size of 1440mm diameter and a height of 350mm for a maximum payload of 1kg. This is taken as a benchmark for the parallel cable robot, the workspace of the parallel cable robot should be at least as large.
- 5. The position repeatability of the end effector should be at least 0.1 mm.** The position repeatability of common delta robots in the industry as the flexpicker or the Hornett by Omron have a position repeatability of 0.1mm. This was taken as a benchmark.
- 6. The angular repeatability of the end effector should be at least 0.4°.** The angular repeatability of common delta robots in the industry as the flexpicker or the Hornett by Omron have an angular repeatability of 0.4 degrees. This was taken as a benchmark.
- 7. The maximum installation space of the parallel cable robot is a cube having 2m long sides.** This installation space is comparable to a delta robot such as the flexpicker. To be attractive for the industry, the installation space should not be larger.

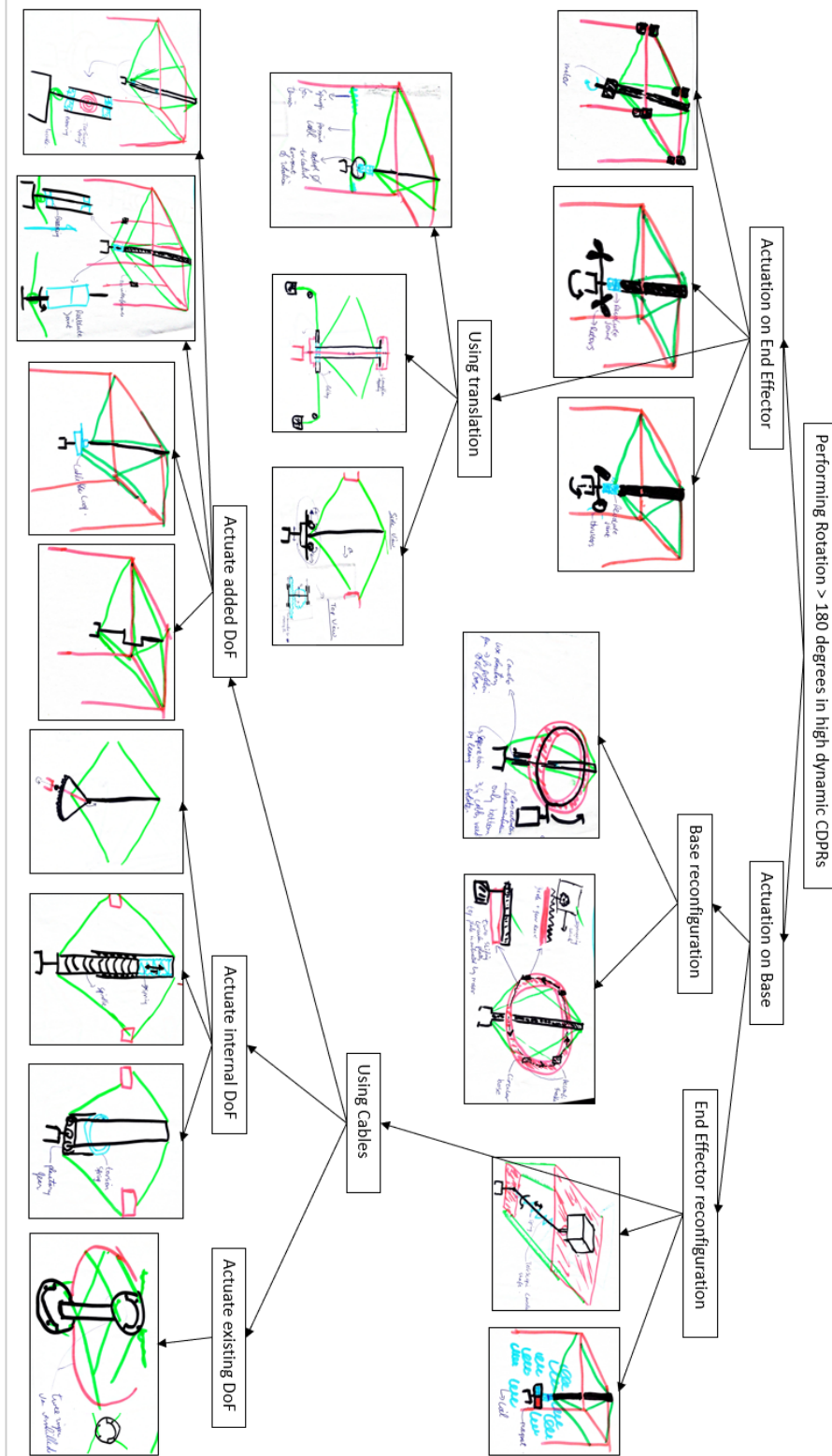
Criteria

1. Inertia / Moving mass. Lower inertia means higher accelerations and likely a smaller cycle time. Or it means less/smaller actuators for the same accelerations reducing the cost and complexity.
2. Rotation, the larger the rotation capability the more preferred the design is. Because better product reorientation can be performed.
3. Workspace size, a large workspace size is favourable since products can be picked and placed over larger distances.
4. Number of actuators, less actuators means less cost and less complexity in actuation.
5. Complexity in mechanical design, a less complex mechanical design is favourable.
6. Stiffness of mechanical design, a higher stiffness means that the likelihood to reach the repeatability requirements is larger.

In the concept selection phase the weights for the criteria can be given as follows. The most important criteria are the Inertia and the moving mass, since this is strongly connected with the high speed goal. The inertia and the moving mass need to be low to reach the highest accelerations with the lowest power consumption. The rotation criterion is also important for the goal, however when the 180 degrees is met there is not much benefit when a concept can rotate more. The workspace size is mainly important in the next phase, in this phase the concepts with a clear disadvantage in workspace shape or size can be penalized in this phase. The number of actuators is less important than the Inertia and moving mass since this is more of a wish than important for the goal. Less cables means less actuators and thus less cost which makes the cable robot more attractive for the industry. The complexity and the stiffness in the mechanical design is considered of equal importance, but less important than the inertia. A less complex design means easier fabrication and likely also a less complex model. Furthermore, stiffness (including play) is important to reach the repeatability requirements.

Appendix 2: Concept generation

In this appendix, a summary of the concept generation phase is given in the shape of a figure where all concepts are sketched and split into categories. The concepts were deviated from existing concepts in literature and new concepts were devised.



Appendix 3: Concept selection

In this appendix, each concept is evaluated based on the criteria and three concepts are selected for further optimization. Each concept gets a grade on each criteria and each criterium is weighted, this results in the final score and the three concepts for further optimization.

Inertia (rotation)

For the inertia we can calculate the exact inertia for each concept. However this is based on the exact dimensions of the EE and the moving platform. These values are not available yet and will be in the next phase. In this phase we will look at the amount of rotating parts and compare the concepts based on that.

Inertia	Grade
Very low	5
Low	4
Medium	3
High	2
Very High	1

Concept	Grade	Note
A	4	Inertia is low, only the EE and the inside of the motor need to rotate.
B	1	The inertia is very high, the complete moving platform needs to rotate and the actuation units need to move along a circular path. Also the motors that actuate the cables and the motors that actuate the rotation do move themselves during rotation.
C	2	The inertia is high, the complete moving platform needs to rotate and one of the circular plates needs to rotate as well with the cable actuators on them.
D	3	The inertia is medium, the complete moving platform needs to rotate and one of the circular plates needs to rotate as well with the cable actuators on them. However, the plate only has to rotate for about 45 degrees due to the planetary gear.
E	3	The inertia is medium, the EE and the cardan shaft rotate during rotation.
F	4	The inertia is low, only the EE and the cable guidance rotates during rotation.
G	4	The inertia is low, only the EE and the cable guidance rotates during rotation.

H	4	The inertia is low, only the EE and the cable pulleys rotate during rotation.
I	3	The inertia is medium, the complete moving platform and EE need to rotate during a rotation.
J	4	The inertia is low, only the EE needs to rotate and the short part of the planetary gear. Moreover, this part only needs to rotate about 45 degrees in half of the cycle time.
K	3	The inertia is medium, the complete moving platform and the EE rotate during a rotation.
L	3	The inertia is medium, the complete inner shaft and the pulley is rotating during a rotation.

Moving mass (translation)

For the moving mass we can calculate the exact mass for each concept. However this is based on the exact dimensions of the EE and the moving platform. These values are not available yet and will be in the next phase. In this phase we will look at the amount of moving parts and compare the concepts based on that.

Moving mass	Grade
Very low	5
Low	4
Medium	3
High	2
Very High	1

Concept	Grade	Note
A	2	Moving mass is high, the motor, the EE and the moving platform move during a translation. Moreover the moving platform needs to be strong enough to capture the torques from the motor which makes the moving platform have more mass.
B	4	Moving mass is Low, the moving platform including the EE are the only moving parts in a translation. The moving platform needs to be strong enough to capture the torques from rotational acceleration which makes the moving platform have more mass.
C	4	Moving mass is Low, the moving platform including the EE are the only moving parts in a translation. The moving platform needs to be strong enough to capture the torques from rotational acceleration which makes the moving platform have more mass.
D	3	Moving mass is medium, the moving platform including the EE

		and the planetary gear are the only moving parts in a translation. The moving platform needs to be strong enough to capture the torques from rotational acceleration which makes the moving platform have more mass.
E	3	Moving mass is medium, the cardan shaft is a pendulum during translation and the moving platform and the EE are also moving masses.
F	4	Moving mass is Low, the moving platform including the EE are the only moving parts in a translation. The moving platform needs to be strong enough to capture the torques from rotational acceleration which makes the moving platform have more mass.
G	5	Moving mass is very low, the only parts that have to move are the EE the moving platform and the cable guidance. The moving platform does not need to be strong enough for torques since they are decoupled from the EE.
H	5	Moving mass is very low, the only parts that have to move are the EE the moving platform and the cable guidance.
I	4	Moving mass is Low, the moving platform including the EE are the only moving parts in a translation. The moving platform needs to be strong enough to capture the torques from rotational acceleration which makes the moving platform have more mass.
J	3	Moving mass is medium, the EE , the moving platform and the planetary gear need to move during translation. The moving platform needs to be strong enough to capture the torques from rotational acceleration which makes the moving platform have more mass.
K	4	Moving mass is low, the moving platform including the EE are the only moving parts in a translation. The moving platform needs to be strong enough to capture the torques from rotational acceleration which makes the moving platform have more mass.
L	2	The moving mass is high, both the inner shaft and the outer tube need to move during a translation. Also the friction couplings and the actuation of those are considered moving masses.

Rotation range

Rotation Range	Grade
∞°	5
$>180^\circ$	4
$\sim 180^\circ$	1

Concept	Grade	Note
A	5	Rotation of a rotary electrical motor can be infinite.
B	5	Rotation can be infinite since the actuation units can continue rotating along the circular base.
C	5	Rotation can be infinite. The motor that actuates the rotation of the base can rotate infinitely.
D	5	Rotation can be infinite. The motor that actuates the rotation of the base can rotate infinitely.
E	5	Rotation can be infinite. Motor rotation can be infinite and therefore the EE rotation as well since they are coupled by the cardan shaft.
F	4	Rotation can be larger than 180 degrees. The cable length is limiting the rotation.
G	4	Rotation can be larger than 180 degrees. The cable length is limiting the rotation.
H	4	Rotation can be larger than 180 degrees. The cable length is limiting the rotation.
I	5	Rotation can be infinite. The rotation is not limited by the cable length.
J	4	Rotation can be larger than 180 degrees depending on the transmission ratio of the planetary gear. This range of transmission is considered 3:1 to 10:1. A cdpr can do ~90 degrees so more than 180 degrees can be met.
K	1	Rotation is about 180 degrees as shown in the paper on passive reconfiguration.
L	1	The rotation range is dependent on the diameter of the pulley and on the travelled distance. If the pick and place distance is very short the minimum rotation of 180 degrees might not be reached.

Workspace Size

We can not say a lot about the workspace size since this depends on the mass of the moving platform and EE, the cable configuration, the number of cables, and the min and max cable tension. These aspects will be considered in the next phase of the project where 3 concepts are chosen. We can do some initial estimates on the workspace shape in most cases. All concepts will get five points at first, however when it is known that the workspace will be significantly smaller than the others or inconveniently shaped it will get less points (3 or 1).

Concept	Grade	Note
A	5	Same base as the most concepts so the shape will be the same.
B	5	Same shape and base assuming that the moving base does not influence the workspace
C	5	Same shape and base assuming that the moving base does not influence the workspace
D	5	Same shape and base assuming that the moving base does not influence the workspace
E	3	Workspace is limited by the length of the cardan shaft end therefore most likely smaller than the other workspaces.
F	5	Same base as the most concepts so the shape will be the same.
G	5	Same base as the most concepts so the shape will be the same.
H	5	Same base as the most concepts so the shape will be the same.
I	5	Workspace is shown in paper and is considered large with regard to the frame size.
J	5	Workspace shape is probably shaped like the others because the cable configuration is the same, the rotation workspace could limit this somewhat but that is not certain since only a small rotation is required.
K	3	Workspace shape will probably be inconveniently shaped as shown in the paper, due to the inconvenient orientation workspace.
L	5	The workspace size will be regularly shaped as the other concepts.

Number of actuators

# actuators	grade
5-6	5
7-8	4
9-10	3
11-12	2
>13	1

Concept	Grade	Note
A	3.5	8 or 9 actuators are needed, with 8 cables more symmetric workspace. Additionally to the cable actuators, one actuator for the rotation on the EE.
B	2	11 or 12 actuators are needed, with 8 cables more symmetric workspace. For each cables two actuators are needed, one for the cable actuation and one for the reconfiguration.
C	3.5	8 or 9 actuators are needed, with 8 cables more symmetric workspace. Additionally to the cable actuators, one actuator for the rotation of the base.
D	3.5	8 or 9 actuators are needed, with 8 cables more symmetric workspace. Additionally to the cable actuators, one actuator for the rotation of the base.
E	5	5 actuators, where 4 actuators for the cables and 1 for the rotation.
F	3.5	8 or 9 actuators are needed, with 8 cables more symmetric workspace and torques can be resisted. Additionally to the cable actuators, one actuator for the rotation on the EE.
G	4	8 actuators are needed. Additionally to the cable actuators, two actuators for the rotation on the EE. 6 actuators for the cables of the moving platform and 2 for the EE actuation.
H	4	8 actuators are needed for this concept.
I	2	12 actuators are needed, for each cable one actuator.
J	4	8 cables and actuators are needed to account for the torques on both parts.
K	4	8 actuators are needed for this concept.
L	4	7 actuators, 6 for the translation of the main body and one for the friction couplings

Mechanical Complexity

Complexity	Grade
Very low	5
Low	4
Medium	3
High	2
Very High	1

Concept	Grade	Note
A	5	Mechanical complexity is very low, only motor connection to the moving platform.
B	1	Mechanical complexity is very high since each actuator unit (2 cable actuators and 1 orientation on frame actuator) has to move on a circular guid and a circular gear rack in combination with a gear wheel on the actuator unit controls the position of the actuator unit.
C	2	Mechanical complexity is high. The moving ring needs to be coupled to the circular base by a guide (including bearings). A circular gear rack needs to be present on this guide such that one actuator on the base can control the orientation position.
D	1	Mechanical complexity is very high. The moving ring needs to be coupled to the circular base by a guide (including bearings). A circular gear rack needs to be present on this guide such that one actuator on the base can control the orientation position. Also a planetary gear needs to be implemented in the EE.
E	2	Mechanical complexity is high. A cardanshaft needs to be implemented between the base and the EE for torque transmission. This cardan shaft also needs to be telescopic, and applying pressure between the EE and the base so a spring is also included in the shaft.
F	3	Mechanical complexity is medium. A bearing between the EE and the moving platform is needed. Also a torsion spring is needed between the moving platform and the EE and a guidance for the wire around the EE.
G	3	Mechanical complexity is medium. A guidance for the wires on the EE for rotation is needed and a bearing between the EE and the moving platform. As shown in the paper by Fortin-Coté.
H	4	Mechanical complexity is low. The cables of the cable loop must be guided by extra pulleys or eyelets.
I	4	Mechanical complexity is low. Only 3 bearings are needed on every cable attachment point, and the EE must be shaped.
J	4	Mechanical complexity is low. Only a planetary gear is needed between the two moving parts of the EE. This planetary gear can be bought as a standard part. Furthermore, the cables can be in a standard configuration.
K	4	Mechanical complexity is Low. A circular slot is needed and an attachment mechanism for the cables in this slot.
L	1	Mechanical complexity is very high, we need an inner tube and outer tube connected by bearings and also makes relative sliding in local z direction possible. Also the outer tube is connected by

		a bearing to the pulley. Then there is a friction coupling that can switch the attachment of the EE
--	--	---

Mechanical Stiffness

The mechanical stiffness is not determined in a quantitative way in this phase, since the exact geometry of the system should be known. The concepts are compared on the basic cable configuration and the play that can occur in the parts.

Concept	Grade	Note
A	4	The stiffness is high, the cable configuration is the same as in most of the other concepts. The only part where extra play can be introduced is in the motor.
B	2	The stiffness is low, the cables need to transmit the rotations to the EE. Furthermore there will be play in the gear rack.
C	2	The stiffness is low, the cables need to transmit the rotations to the EE. Furthermore there will be play in the gear rack.
D	2	The stiffness is low, the cables need to transmit the rotations to the EE. Furthermore there will be play in the gear rack also the planetary gear will have some play.
E	2	The stiffness is low, the stiffness depends mainly on the spring in the cardan shaft. Also there will be play in the cardan couplings.
F	2	The stiffness will be low, the angular stiffness depends on the spring. A force on the spring will result in a deformation of the spring.
G	4	The stiffness will be high, the stiffness depends on the cables' stiffnesses which have high stiffnesses.
H	4	The stiffness will be high, the stiffness depends on the cables' stiffnesses which have high stiffnesses.
I	4	The stiffness will be high, the stiffness depends on the cables' stiffnesses which have high stiffnesses.
J	3	The stiffness will be medium, the stiffness depends mainly on the cables. Also the play in the planetary gear reduces the rotational stiffness.
K	4	The stiffness will be high, the stiffness depends on the cables' stiffnesses which have high stiffnesses.
L	2	The stiffness will be low since the cables that actuate the rotation are not actively actuated. Furthermore the repeatability will also be low since the breaking time(friction coupling) is very important for the amount of rotation. The maximum acceleration is also influenced by the counter masses.

	Inertia	Mass	Rotation Range	Workspace	# Actuators	Mech Complexity	Mech Stiffness	SCORE
A	4	2	5	5	3.5	5	4	58
B	1	4	5	5	2	1	2	40
C	2	4	5	5	3.5	2	2	48
D	2	3	5	5	3.5	1	2	43
E	3	3	5	3	5	2	3	51
F	4	4	3	5	3.5	3	3	54
G	4	5	3	5	4	4	4	62
H	4	5	3	5	4	4	4	62
I	3	4	5	5	2	4	4	56
K	3	3	3	3	4	3	3	47
L	3	4	1	3	4	3	4	48
weight	3	3	2	1	2	2	2	

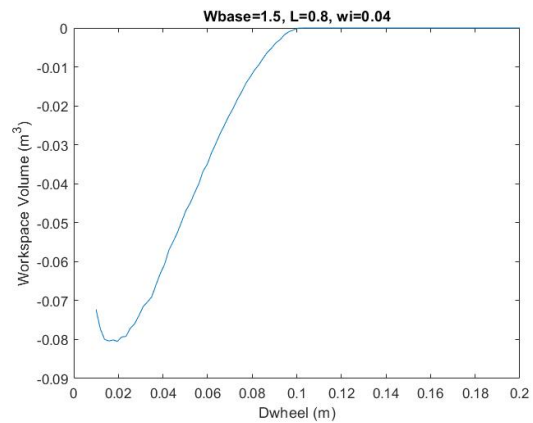
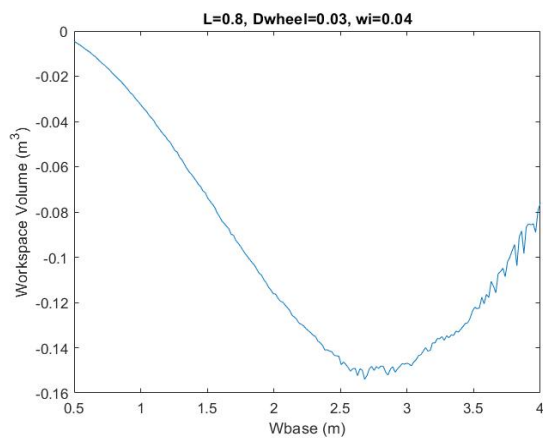
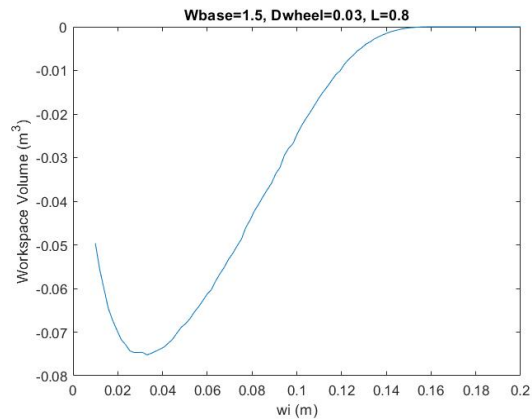
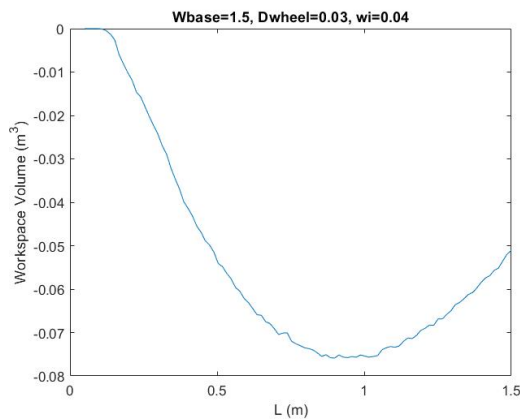
This figure shows the score table resulting from all previous tables. Concepts A, G, and H were selected for further optimization since they have the highest score.

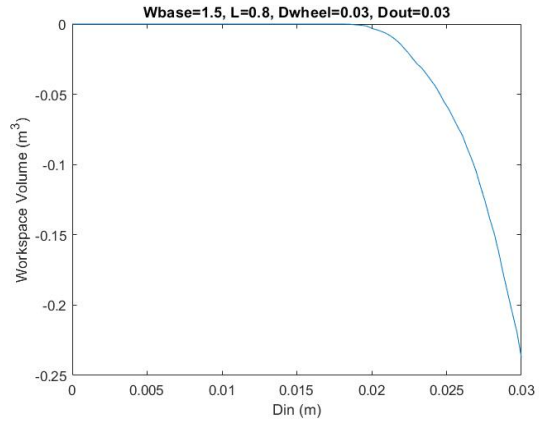
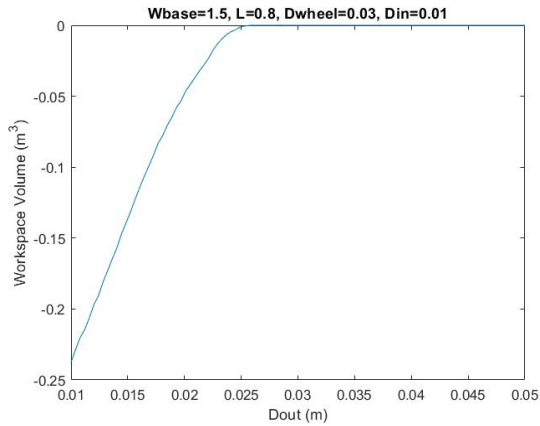
Appendix 4: Optimization investigation

In this appendix the optimization is further investigated. First an initial problem investigation is performed, which was used for the selection of the optimization algorithm. Then the optimization results are further investigated by varying parameters. Finally some remaining optimization results, that were not shown in the paper, are given.

Initial problem investigation

The initial problem investigation changes one variable while the others are fixed, and finds the resulting value of the cost function. This gives an indication of what properties the cost function has for the variables.



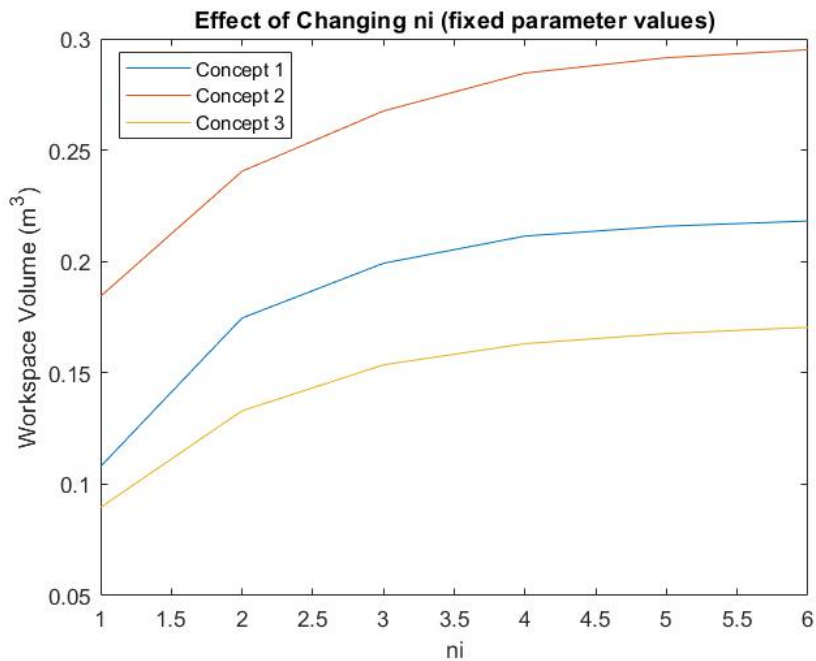


The figures show non convex and non smooth behavior, therefore an optimizer must be selected that can handle these properties and find the global optimum. Additionally, the variables Din and Dout are not bounded by themselves, therefore constraints are required as shown in the paper.

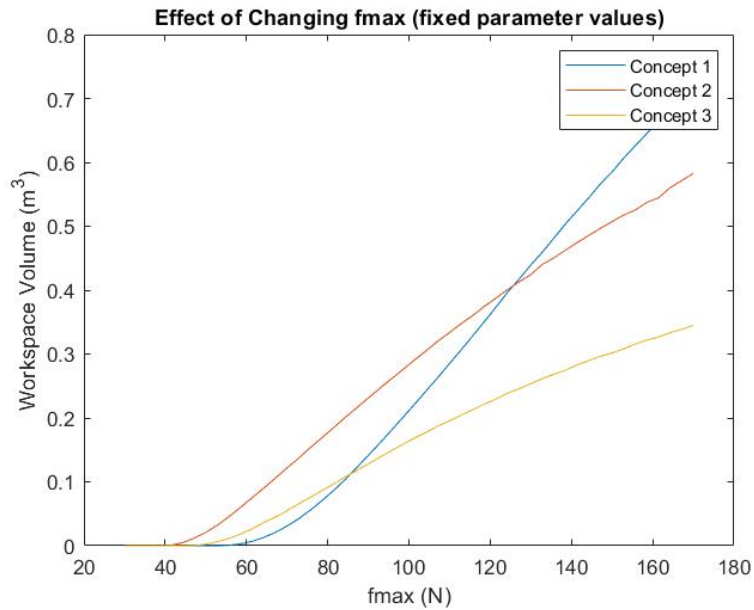
Optimization results investigation

In this part the optimization results are further investigated. The investigations that are performed do not use optimization as this would require a vast amount of time. The graphs show a variation of a parameter while the others are constant.

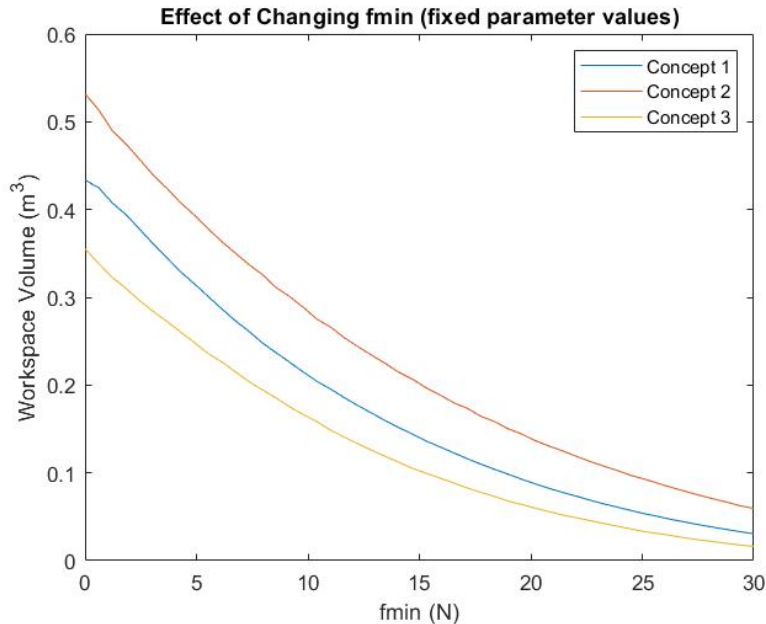
First the variable ni is determined for which the volume converges. The ni value determines the number of triangulations of the hull, more triangulations means more linesearches and more computation time but a too small ni would give an incorrect workspace volume.



After ni~4 the computed volume remains relatively constant, therefore ni=4 was chosen for the optimizations.

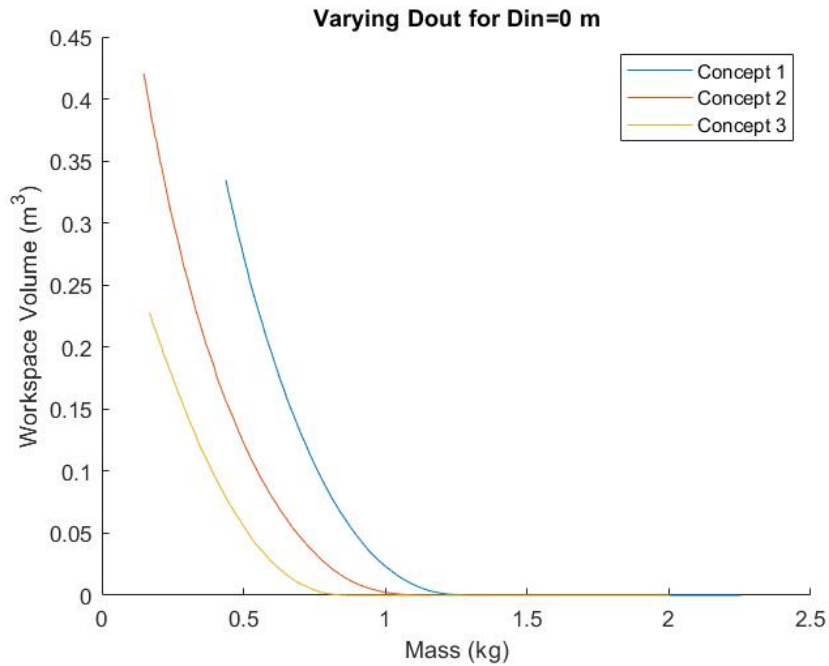


A higher maximum cable force f_{max} shows that the effect of the mass is less prominent, meaning that the cable configuration becomes more prominent. In this figure it is visible that the cable configuration of concept 1 is better than that of concept 2. Therefore the volume of concept 1 is higher than concept 2 for a certain f_{max} . However, in this case an optimization is not performed. Meaning that for a higher f_{max} also larger D_{out} is required. Therefore the mass becomes again more prominent and the point that the volume of concept 1 being larger than concept 2 shifts a bit to the right.

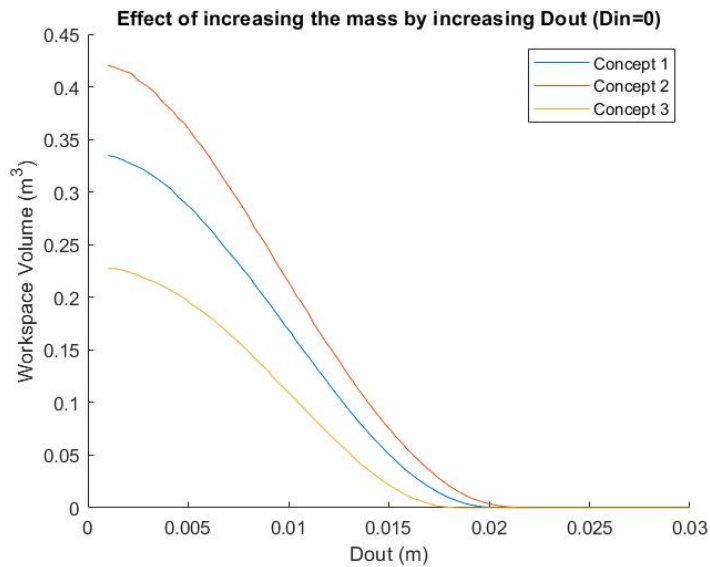


A larger f_{min} shows that the workspace volumes decrease but the relation between the concepts remains approximately the same.

Also the effect of increasing mass is investigated for fixed variable values. This increase in mass is performed by increasing D_{out} . This does not influence the cable configuration, thus only influences the mass. This results in the figures as given below.



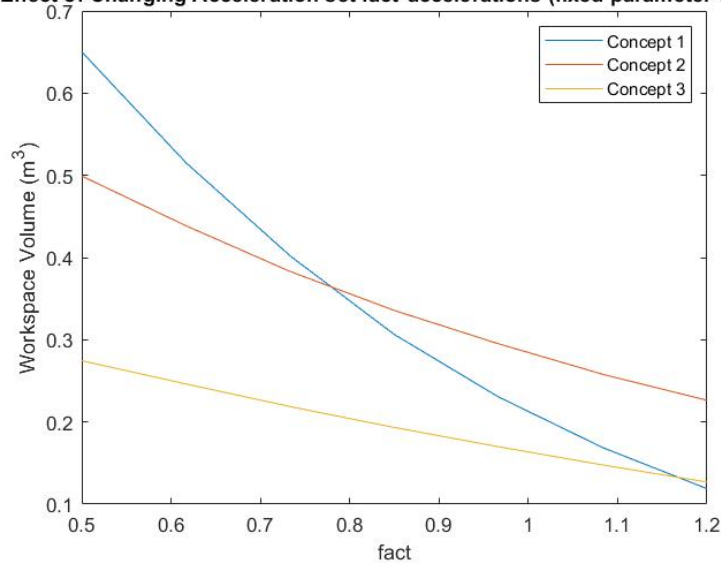
This figure shows that when the mass of the concepts is equal, the volume of concept 1 is the largest. This confirms that the cable configuration of concept 1 is better and more efficiently uses its mass.



Increasing Dout results in a larger mass and a decrease in volume. We can see that concept 2 is always above the other two concepts and concept 1 always above concepts 3 for the given variable values.

Finally, the effect of changing the acceleration set with a factor is investigated as well for fixed variable values. The result is shown in the figure below.

Effect of Changing Acceleration set fact*accelerations (fixed parameter values)



This result shows about the same result as increasing the f_{max} . When the required accelerations become lower, the mass of the concept becomes less important and the cable configuration more important. The cable configuration of concept 1 is better than the configuration of concept 2. We can see that from $fact < \sim 0.8$ the volume of concept 1 is larger than that of concept 2. This means that for a higher cycle time concept 1 might be favourable. However, when accelerations are lower one might reduce the cable forces to save energy and then concept two becomes more interesting again.

Remaining optimization results

Some optimization results were not shown in the paper, since they were not important for the global outline and story of the paper. These results will be given here.

The bounds for the width of the frame and the tube were set to 4m and 2m respectively. This results in the following variables and volumes. Concept 2 still has the largest volume.

	Concept 1	Concept 2	Concept 3
Wf (m)	3.9963	4.0000	3.9996
L (m)	1.5615	1.3216	1.2315
Wt (m)	0.0302	0.0201	x
Dp (m)	x	0.0202	0.0411
Din (m)	0.0242	0.0192	0.0102
Dout (m)	0.0254	0.0207	0.0123
Vdyn (m ³)	0.7723	1.1520	0.6663

Mass (Kg)	0.6443	0.3007	0.2802
-----------	--------	--------	--------

The constraints usually use a safety factor of $S=3$ to multiply with the maximum force or torque that occurs in the rod. Now a safety factor of $S=6$ is used. This results in an increase in mass since the rods are stronger and have more material, and a reduction in workspace size. Still the same order of workspace sizes is measured. The usual bounds are used.

	Concept 1	Concept 2	Concept 3
Wf (m)	2.0000	2.0000	1.9991
L (m)	0.9275	0.8641	0.8332
Wt (m)	0.0300	0.0202	x
Dp (m)	x	0.0202	0.0422
Din (m)	0.0225	0.0204	0.0098
Dout (m)	0.0245	0.0226	0.0134
Vdyn (m ³)	0.1733	0.2064	0.1205
Mass (Kg)	0.6180	0.3123	0.3037

Appendix 5: Cable loop criteria, concepts and concept selection

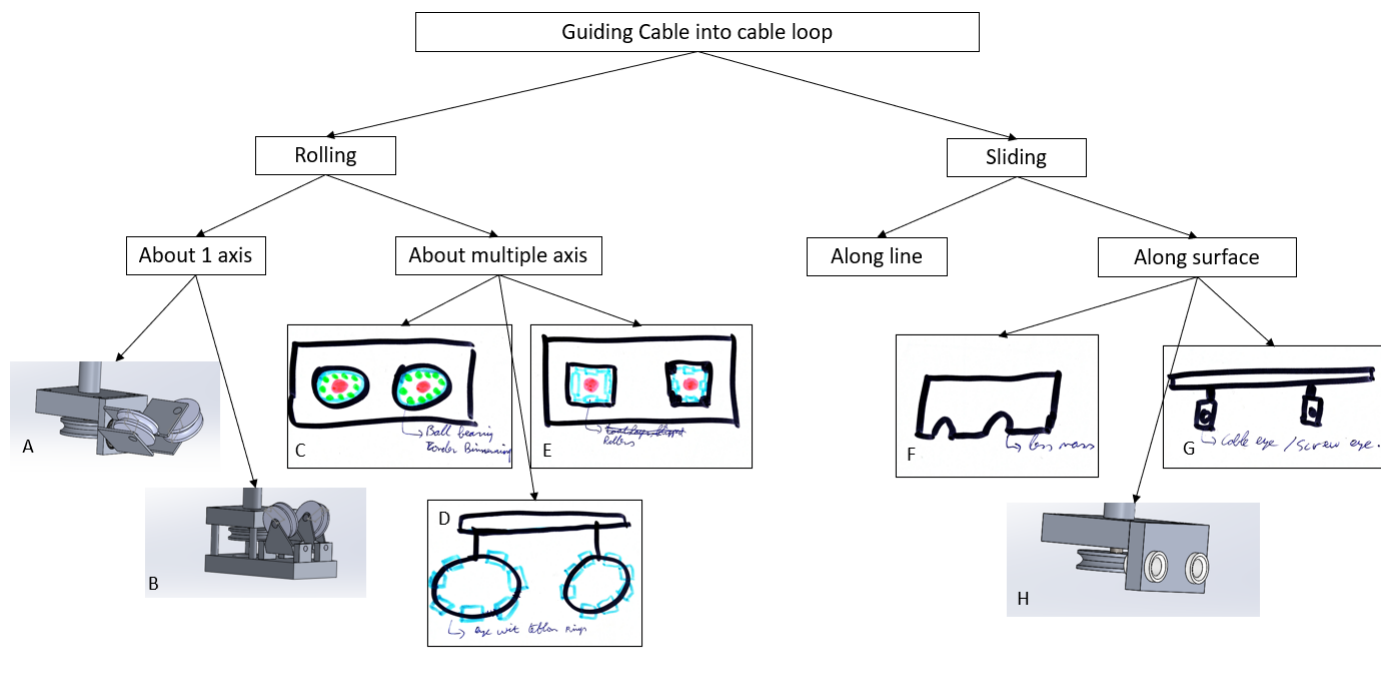
Since concept 2 was selected for further investigation in a prototype, multiple cable loop designs were considered. This appendix shows the criteria, concept generation, and concept selection for the cable loop design.

Criteria:

1. **Mass/Inertia:** When mass is added, cable forces increase, workspace size decreases, and dynamics/ vibrations are badly influenced. So a low mass is favourable.
2. **Friction:** Friction means cable force that is lost, this results in a smaller workspace and friction results in a disturbance on the platform. So low friction is favourable.
3. **Accurate positioning of anchor points / kinematic complexity:** The anchor points should be known as accurate as possible since the cable length calculation depends on this, thus the position of the moving platform depends on this. If this position deviates from the planned position, error is induced.
4. **Fabrication complexity:** The fabrication should be possible with the tools and machines available in the IWS. A less complex design is more favourable.
5. **Lifetime:** The lifetime of the cable depends on friction and the ratio of the cable diameter and the bending diameter of the cable. As friction is already a criterion, this criterion will cover the diameter ratio. For a large lifetime D/d should be large. This criterion is the least strict for our design, since we will not be using the prototype for constant pick and place actions in a factory. Lifetime is also not part of the original requirements of the project. However, to be attractive for application in industry it is nice to have as a criterion.

The criteria of mass, friction and accurate positioning are of equal importance to reach the requirements that are set at the start of the project. The fabrication should be possible and an easy design would be nice, however this is less important than the first three criteria. Finally, the least important criterion is the lifetime since this is already partly covered by the friction requirement and this criteria does not have an effect on the requirements set at the start of this project.

Concepts:



Concept A: Pulleys that guide the cable into the cable loop pulley, inspired by the wheel of a shopping cart.

Concept B: Pulleys that guide the cable into the cable loop pulley.

Concept C: A bearing without an inner ring guides the cable. The cable is in contact with multiple balls that can roll in their groove.

Concept D: A screw eye is guiding the cable into the cable loop, on the perimeter of the screw eye, rollers are placed with springs in between them to space them.

Concept E: Rollers are used to guide the cable into the cable loop, so instead of many rollers as in concept D we only use four in a square shape.

Concept F: Half eyes are used to guide the cable, since the cables will always head up only this half is needed in theory.

Concept G: Screw eyes are used to guide the cables into the cable loop, this saves mass.

Concept H: Rounded eyes are used to guide the cable into the cable loop.

Concept Selection:

Mass/ Inertia:

The exact mass/ inertia of the concepts are not known yet since they need to be designed in detail first. However, based on the number of parts we can make a fair comparison.

Mass	Grade
Very low	5
Low	4
Medium	3

High	2
Very High	1

Concept	Grade	Note
A	2	Compared to the other concepts, this concept has a lot more parts. Therefore the mass / inertia is considered high.
B	1	Compared to the other concepts, this concept has a lot more parts. Therefore the mass / inertia is considered high. Compared to concept A, this concept needs an extra platform which makes the mass even higher.
C	3	The mass and inertia of this concept is considered medium since the mass of a bearing is only a few grams but a plate is needed to support the bearing.
D	5	The mass of this concept is considered very low since only two screw eyes are needed with teflon rings on them.
E	3	The mass of this concept is considered medium since only a couple of rollers are needed but a plate is needed to support the rollers.
F	4	The mass of this concept is low since only half of the plate is needed.
G	5	The mass of this concept is very low since only screw eyes are needed.
H	4	The mass of this concept is low since only sliding bearings are needed these could be inserted in screw eyes as well.

Friction:

Friction Coefficient	Grade
Very low	5
Low	4
Medium	3
High	2
Very High	1

Concept	Grade	Note
A	5	Only the friction of the ball bearings is present.
B	5	Only the friction of the ball bearings is present.
C	2	When the balls roll in the groove the friction is low, however in this case the balls stay in position they slide in the groove. This is steel on steel friction (maybe lubricated). Steel on steel has a high friction coefficient. $\sim 0.4^1$ Therefore the cable will slide over the steel balls \rightarrow friction coefficient max 0.11 (see book by Pott).
D	4	The friction of teflon on steel is between 0.05 and 0.2 and most likely lower than cable on steel and cable on teflon.
E	2	The roller can not be bought with a rolling bearing and space will be an issue then. A sliding bearing might be an option. However most likely the steel roller will be placed in a steel hole so the friction will be steel on steel. This friction is higher than steel on cable such that the cable will slide over the rollers max 0.11.
F	2	The friction coefficient of the cable on steel is maximally 0.11 (see Pott). However this is higher than teflon on steel. And cable on teflon.
G	2	The friction coefficient of the cable on steel is maximally 0.11 (see Pott). However this is higher than teflon on steel. And cable on teflon.
H	3	The friction coefficient of cable on teflon or a ceramic material could not be found but is most likely lower than cable on steel.

The angle of the cable and the y axis is between 10 and 54 degrees for the computed workspace. This results for a friction coefficient of 0.11 (max cable on steel) in a friction force of 2 - 9 % of the tension force in the cable. This is considered to be quite low and in reality the friction might be even lower due to the cable sliding on teflon or a ceramic material.

¹ <https://web.mit.edu/8.13/8.13c/references-fall/aip/aip-handbook-section2d.pdf>

Accurate Positioning:

Accurate Positioning	Grade
Very low	1
Low	2
Medium	3
High	4
Very High	5

Concept	Grade	Note
A	3	The pulley mechanism introduces complexity in the kinematics and also more chance of error in the positioning of the cable anchor point since the computation of the anchor point depends on more parameters like the contact angle of the cable on the pulley and the pulley angle and diameter.
B	3	The pulley mechanism introduces complexity in the kinematics and also more chance of error in the positioning of the cable anchor point since the computation of the anchor point depends on more parameters like the contact angle of the cable on the pulley and the pulley angle and diameter.
C	4	The error in the cable anchor point position only depends on the play of the cable inside the holes.
D	4	The error in the cable anchor point position only depends on the play of the cable inside the holes.
E	4	The error in the cable anchor point position only depends on the play of the cable inside the holes.
F	4	The error in the cable anchor point position only depends on the play of the cable inside the holes.
G	4	The error in the cable anchor point position only depends on the play of the cable inside the holes.
H	4	The error in the cable anchor point position only depends on the play of the cable inside the holes.

Fabrication Complexity:

Friction Coefficient	Grade
Very low	5
Low	4
Medium	3
High	2
Very High	1

Concept	Grade	Note
A	2	A number of small parts need to be fabricated and connected to each other. The parts can not be bought off the shelf.
B	2	A number of small parts need to be fabricated and connected to each other. The part can not be bought off the shelf.
C	3	The inner ring of the bearing needs to be removed and the bearing needs to be placed.
D	3	Teflon rings need to be placed around the eye and a spacing between the rings needs to be fabricated to separate the rings.
E	2	Small rollers need to be fabricated and placed in square holls in the plate.
F	5	Only holes have to be drilled in the side plate and the side plate needs to be cut in half.
G	4	Only screw eyes need to be placed or a side plate and the sliding bearings need to be pushed in these holes.
H	5	Only screw eyes need to be connected to the main body.

Lifetime:

Friction Coefficient	Grade
Very low	1
Low	2
Medium	3
High	4
Very High	5

Concept	Grade	Note
A	5	The pulleys have a larger radius of curvature compared to the other concepts.
B	5	The pulleys have a larger radius of curvature compared to the other concepts.
C	2	The balls of the bearing have a small radius compared to the radius of the cable.
D	3	The radius of curvature is dependent on the design. However, a large radius results in a lower accuracy since the cable anchor points are hard to determine.
E	3	The radius of curvature is dependent on the design. However, a large radius results in a lower accuracy since the cable anchor points are hard to determine.
F	3	The radius of curvature is dependent on the design. However, a large radius results in a lower accuracy since the cable anchor points are hard to determine.
G	3	The radius of curvature is dependent on the design. However, a large radius results in a lower accuracy since the cable anchor points are hard to determine.
H	3	The radius of curvature is dependent on the design. However, a large radius results in a lower accuracy since the cable anchor points are hard to determine.

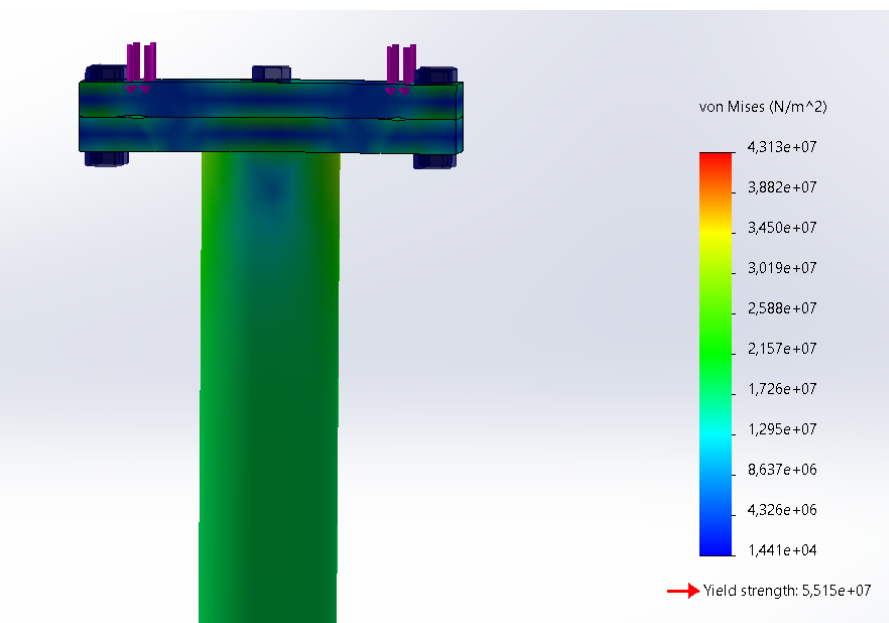
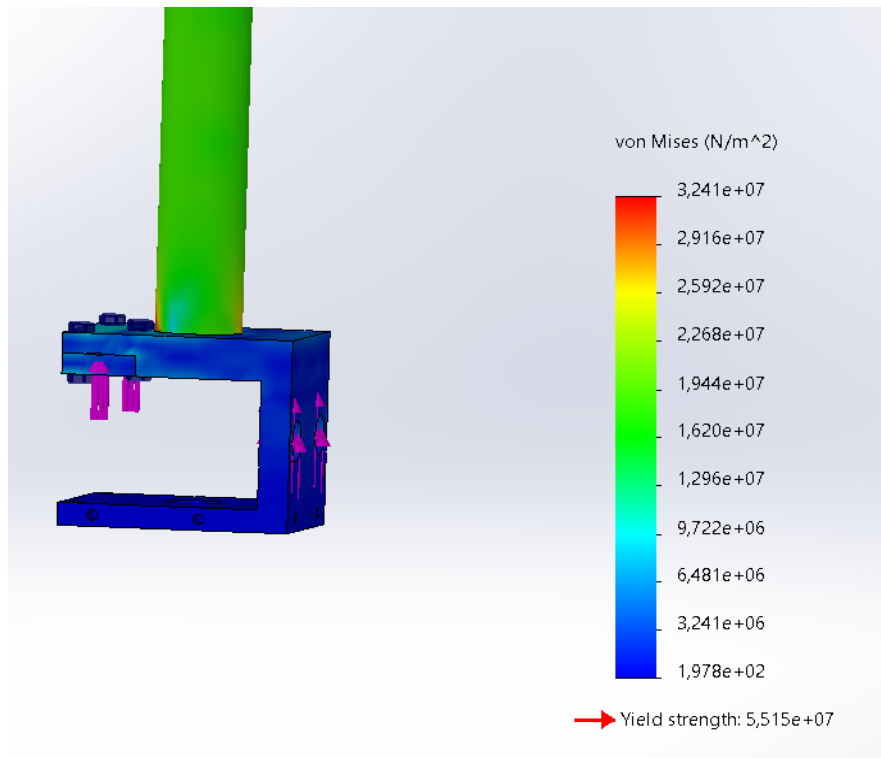
	Mass	Friction	Accuracy	Fabrication	Lifetime	SCORE
A		2	5	3	2	39
B		1	5	3	2	36
C		3	2	4	3	35
D		5	4	4	3	48
E		3	2	4	2	34
F		4	2	4	5	43
G		5	2	4	4	44
H		4	3	4	5	46
weight		3	3	3	2	1

Concepts D and H are graded best. However reconsidering concept D showed that the small rings will be pulled apart by the cable and will obstruct the cable more than it will guide it. Therefore concept H was selected, and a small and quick test was performed to feel if the friction of the eyelet was not too high, as shown in the figure below.

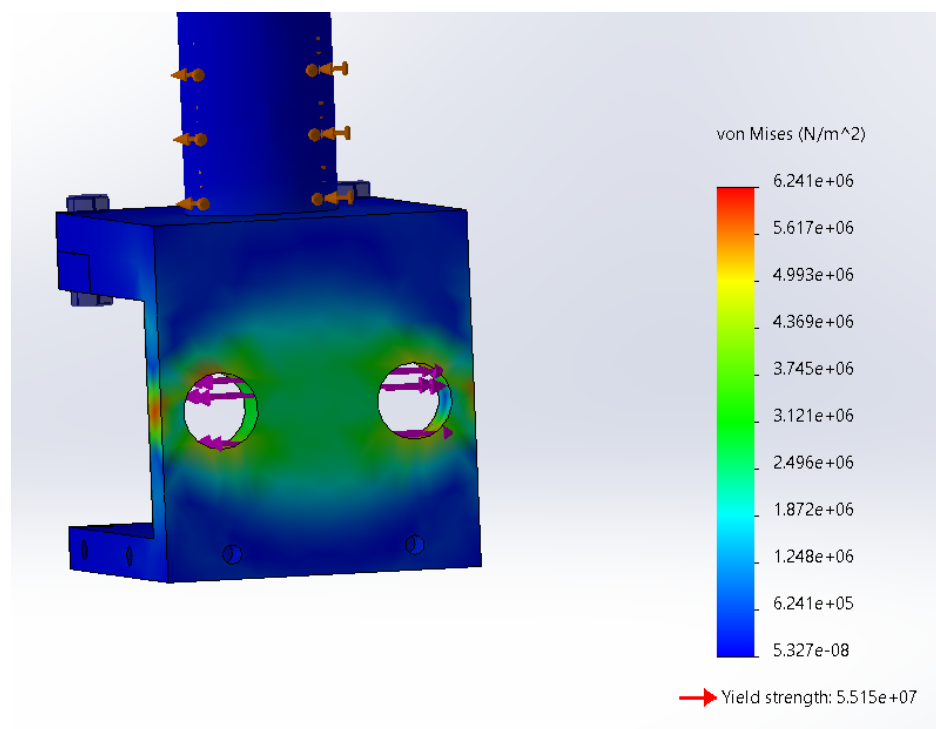
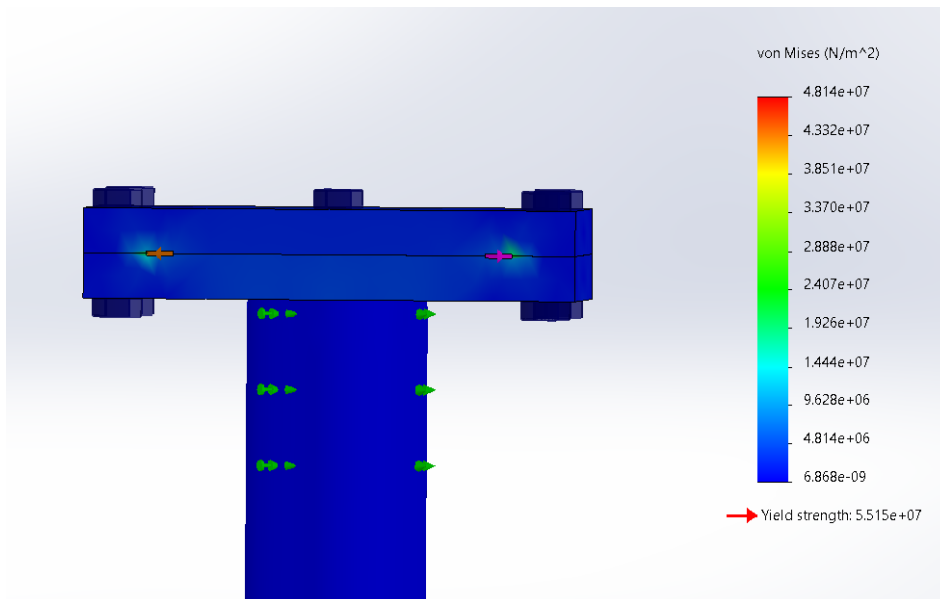


Appendix 6: Strength analysis

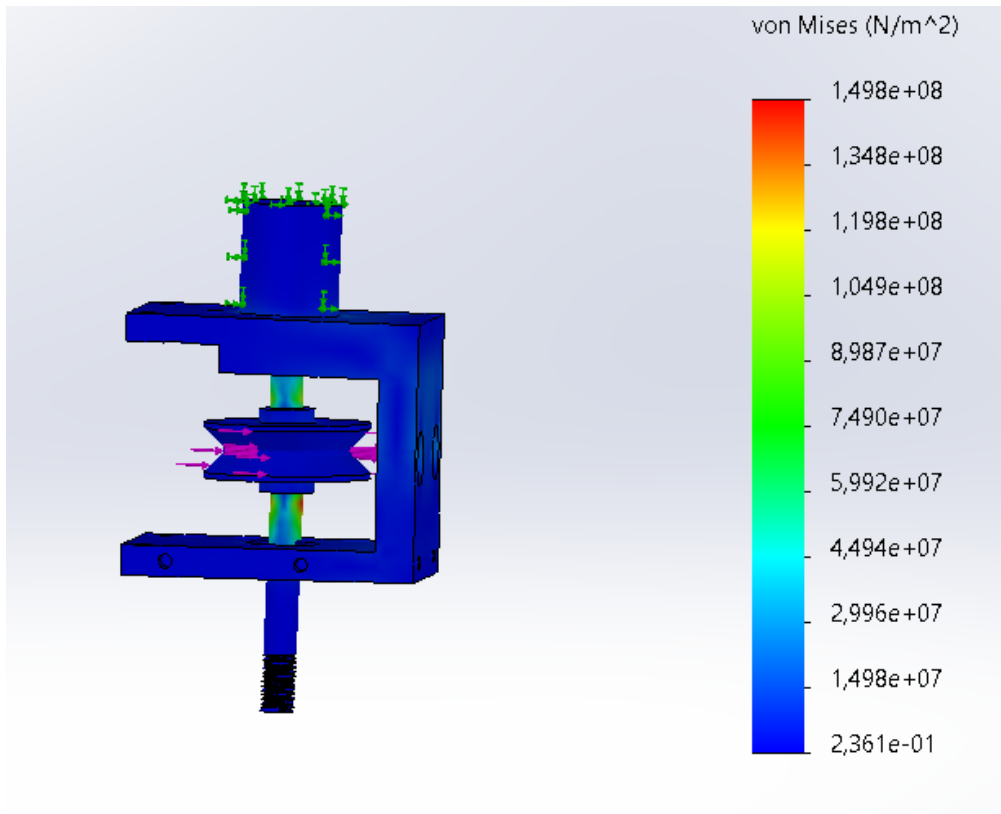
In this appendix a strength analysis is performed on the design by means of a finite element analysis in Solidworks. The cable forces that are imposed at the platform are computed from the maximum motor torque of CaRISA, which is 1.35Nm. The drum (100mm diameter), and the gearbox (1:16) result in a maximum cable force of 432N. Now taking a realistic loss in the system of 10-20% and a maximum cable angle in the workspace of 53 degrees results in a maximum cable force of 300N. This force will be used for the strength analysis and is still a vast overestimation since the cables can not have the maximum angle of 53 degrees at the same time.



These figures show that for the given cable force of 300N, which gives a total vertical force of 1200N, the stress still remains beneath the yield strength of aluminium. Also applying the forces purely horizontally shows that the stress still remains beneath the yield strength of the material.



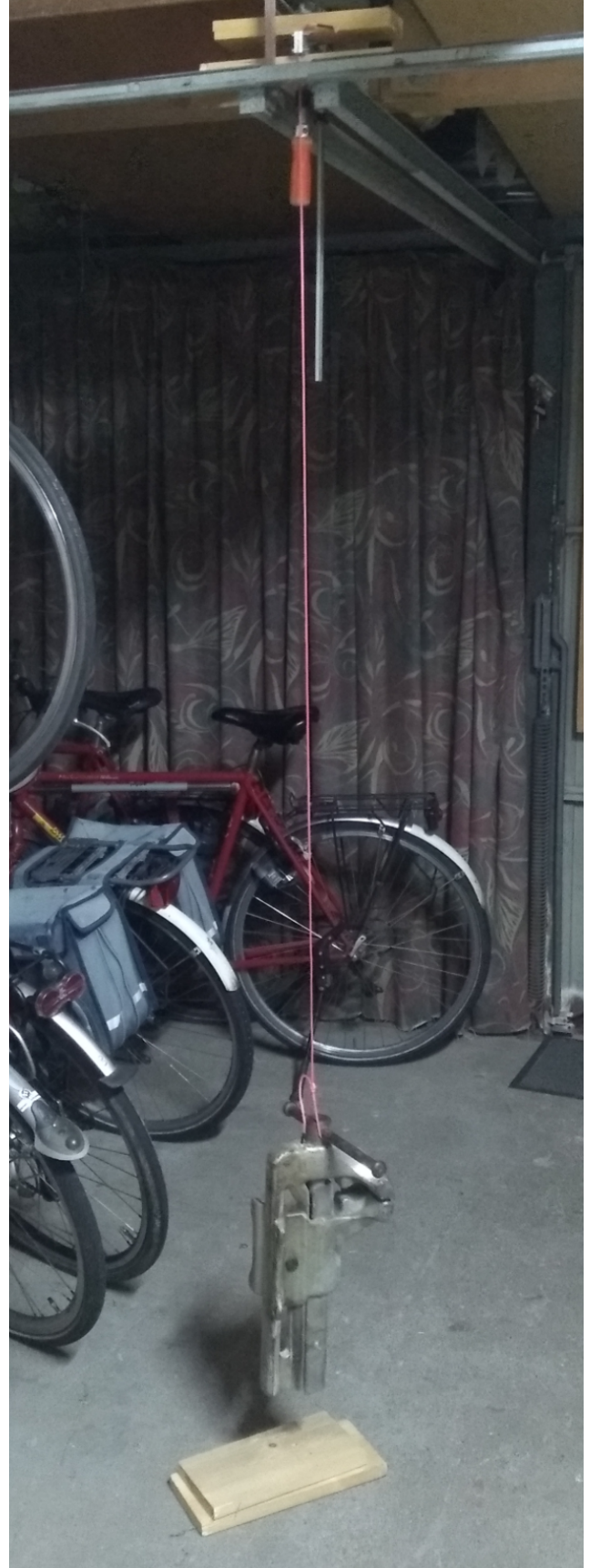
Now applying the cable forces on the pulley and the axis of the moving platform results in the figure as shown below. Here we can see that the maximum stress is 1.5e8 Pa, which is higher than the yield stress of aluminium. However, the maximum stress occurs in the axis which is made of steel with a yield strength of 282e6 Pa. Therefore, the maximum stress is still below the yield strength.



After this analysis the design was considered to be safe and ready for the next stage, which is fabrication.

Appendix 7: Clamping design test

The cable clamping design was tested at an early stage of fabrication to confirm that the cable would not slide through when a force was applied on the cable. A small test was performed as shown in the figures below, where a mass of 15 kg was applied on the cable and the clamping design. The weight was applied for 24 hours and the cable showed no displacement.



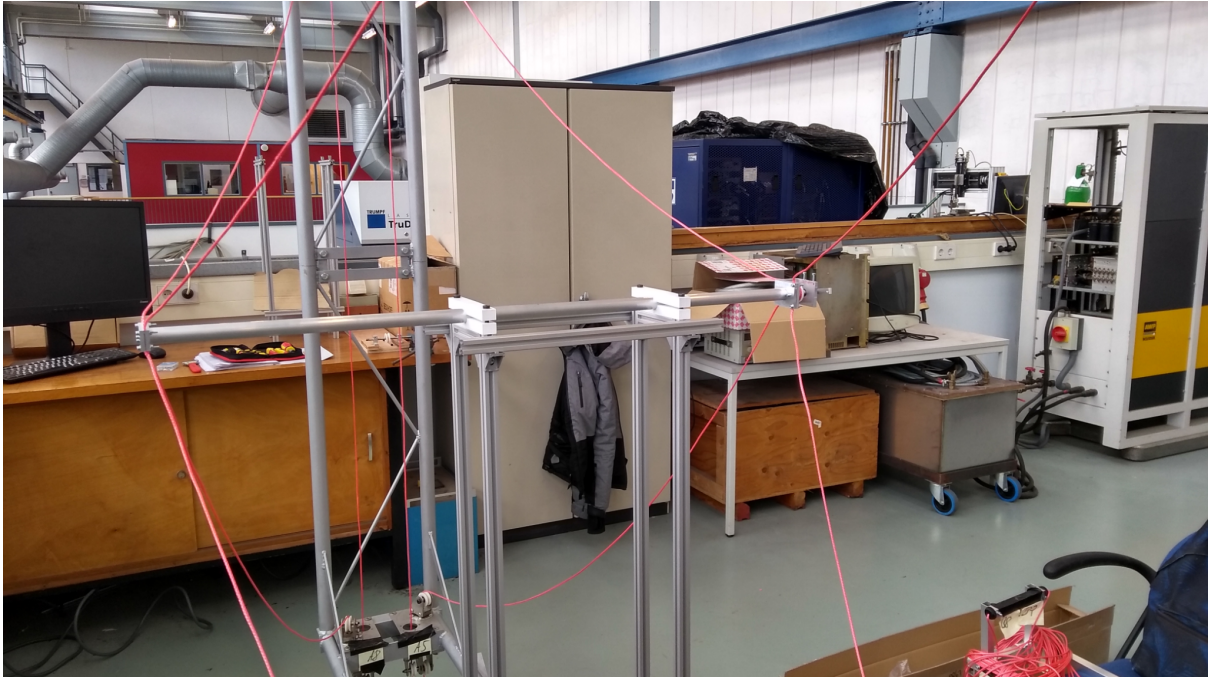
Appendix 8: Calibration of CaRISA

This appendix describes how to calibrate CaRISA. This will be of use for users of the robot. To understand this document, one needs to be at the computer interface of CaRISA.

Calibration:

Calibration should be done before a run → applying the correct tension to the cables

1. Set the calibration frame in position
2. Move the robot to this platform
3. Fix Moving platform to calibration frame:



4. Tension cables one by one like tightening the nuts of a car wheel ;
 - a. Go to manual mode
 - b. Leave trafo OFF
 - c. Click switch axis display ON
 - d. Tighten or loosen every cable until satisfied
 - e. Now every cable shows a value off zero
5. Go to TWINCAT / Microsoft Visual studio
6. Go to: Motion → CNC.dpr → Axes → select winch (double click) → parameter list → P-AXIS-00403
7. Subtract value in HMI (current position) from the Value in P-AXIS-00403
8. Click save at top bar
9. Repeat for every winch
10. Click activate configuration (button top left with the building blocks)
11. Now in HMI click the reset button

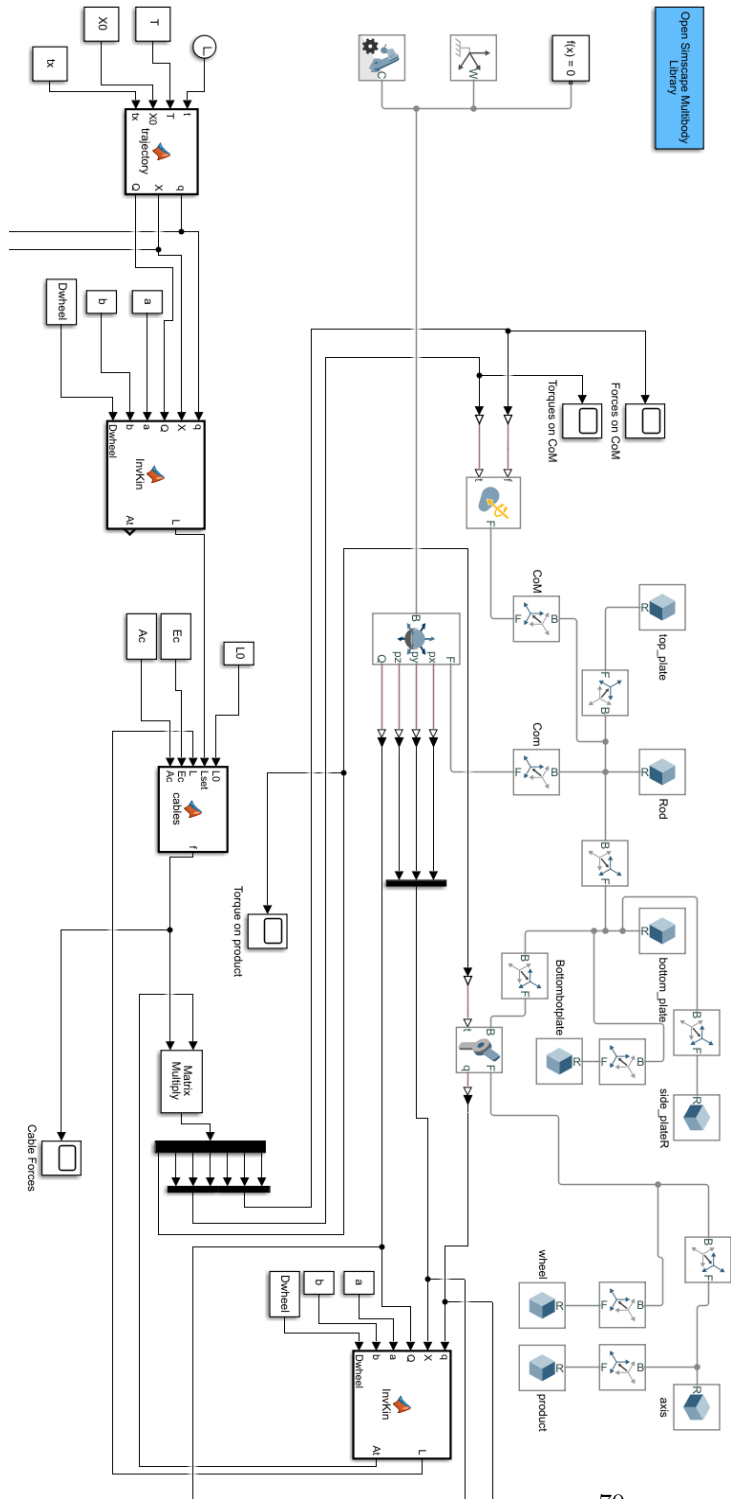
Appendix 10: Repeatability measurements

This appendix shows the measurements values that were taken to compute the repeatability. These values were found halfway the adapt cycle, meaning at the position where the product would be picked. The repeatability is calculated by the standard deviation.

X (mm)	Z (mm)	Angle (°)
147.536	0.979	172.019
147.642	1.013	171.785
146.826	0.994	172.232
147.712	1.001	172.593
146.615	1.018	172.763
147.685	1.145	172.380
147.352	1.026	172.359
147.238	1.057	172.487
147.080	1.127	172.466
147.896	1.067	173.040
147.159	1.013	172.678
147.422	1.018	172.763
147.598	0.983	173.083
147.379	1.018	172.615
148.607	0.970	173.253
147.528	0.981	173.295
147.106	0.979	173.061
147.238	1.016	172.593
147.089	0.981	172.955
147.273	0.964	173.274
148.529	0.977	173.232
147.036	1.033	173.404
147.378	0.966	172.955
147.212	0.951	173.040

Appendix 11: Simulink model of the forward dynamic model

In this appendix, the forward dynamic model is shown in a figure. At the left bottom, the trajectory is inserted into the model. Then trajectory instances are converted to cable lengths by the inverse kinematics function. The cable lengths from the trajectory are then compared with the current cable lengths from the rigid body model which results in cable forces that are imposed on the rigid body model. These forces again result in accelerations of the rigid bodies and a displacement. This loop is repeated till the end of the trajectory.



Appendix 12: Matlab scripts

In this appendix, the most important matlab scripts are shown including comments to be understandable. The first script shows the improved closed form method, which calculates the cable force distribution and feasibility. The second script shows the hull method, which is used to calculate the dynamic workspace. The third script shows how the optimization is built up in matlab, and the fourth script is from the final project phase. This script converts the adept cycle trajectory into cable lengths and G-code such that the robot can perform the adapt cycle.

```

% Improved closed form method for non suspended parallel cable robots
function [f,ex]=impclform(At,w,fmin,fmax)
%{
  INPUTS:
  - minimum and maximum force are scalar inputs and the same for every
    cable
  - At is the transpose of the structure matrix with n rows (DoF) and m
    columns (cables).
  - w is the wrench imposed on the DoF (n*1 vector)
  OUTPUTS:
  - f gives the cable force distribution in a vector, each row stands
    for a
    cable (m*1 vector)
  - ex gives output 0 OR 1, 0 means at least one of the cable forces in f
    is
    out of bounds, 1 means that all cable forces are within bounds
%}
n=size(At,1);
m=size(At,2);
f=zeros(m,1);
ex=0;
%Check for singularities:
if rank(At)<n
    return
end
%Compute redundancy (red):
red=m-n;
%Compute f based on red:
fm=(1/2)*(fmin+fmax);
if red==0
    f=At\(-w);
    if max(f)<=fmax && min(f)>=fmin
        ex=1;
    end
elseif red>0
    Atpseudo=transpose(At)*(At*transpose(At))^( -1);
    fv=-Atpseudo*(w+At*(fm*ones(m,1)));
    f=fm*ones(m,1)+fv;
    if norm(fv)>sqrt(m)*fm
        return
    elseif max(f)<=fmax && min(f)>=fmin
        ex=1;
    end
% Fix the largest or smallest cable force to fmin or fmax and
% execute the improved closed form method for a reduced redundancy:
else
    fvabs=abs(fv);
    [M,j]=max(fvabs);
    if f(j,1)<fm
        wreduced=fmin*At(:,j)+w;
        f(j,1)=fmin;
    else

```

```
wreduced=fmax*At(:,j)+w;  
f(j,1)=fmax;  
end  
Atreduced=At;  
Atreduced(:,j)=[];  
[freduced,exreduced]=impclform(Atreduced,wreduced,fmin,fmax);  
ex=exreduced;  
% Reform reduced cable force vector to original case:  
z=1;  
for i=1:1:m  
    if i==j  
        continue  
    end  
    f(i,1)=freduced(z,1);  
    z=z+1;  
end  
end  
end  
end
```

Not enough input arguments.

*Error in impclform_appendix (line 15)
n=size(At,1);*

Published with MATLAB® R2018b

```

% Perform Hull method:

% First triangulation of the unit sphere as an octahedron
% Setting up the vertices of the initial octahedron:
va=[0;0;1];
vb=[0;1;0];
vc=[-1;0;0];
vd=[0;-1;0];
ve=[1;0;0];
vf=[0;0;-1];
F1=[va,vb,vc];
F2=[va,vb,ve];
F3=[va,ve,vd];
F4=[va,vd,vc];
F5=[vf,vb,vc];
F6=[vf,vb,ve];
F7=[vf,ve,vd];
F8=[vf,vd,vc];
F=[F1,F2,F3,F4,F5,F6,F7,F8];

% Splitting each triangle in four triangles (ni times):
for i=1:1:ni
    Ntbef=2^(2*(i-1)+3);
    Ntaf=2^(2*i+3);
    Fnew=zeros(3,Ntaf*3);
    for j=1:1:Ntbef
        Fnew(:,(12*j-11):(12*j))=onetofourtri(F(:,(3*j-2):(3*j)));
    end
    F=Fnew;
end

F=transpose(F);
F=unique(F,'stable','rows');
F=transpose(F);

%Perform line search to find the workspace boundary
parfor unit=1:1:size(F,2)
    F(:,unit)=linesearch(F(:,unit),...);
end

%Plot and compute volume of convex workspace hull:
F=transpose(F);
[k,V] = convhull(F);
trisurf(k,F(:,1),F(:,2),F(:,3),'FaceColor','cyan')

% Functions:
function [F]=onetofourtri(F)
Fn=zeros(3,3);
Fn(:,1)=(F(:,1)+F(:,2))/norm(F(:,1)+F(:,2));
Fn(:,2)=(F(:,2)+F(:,3))/norm(F(:,2)+F(:,3));
Fn(:,3)=(F(:,3)+F(:,1))/norm(F(:,3)+F(:,1));
Vec1=[F(:,1),Fn(:,1),Fn(:,3)];

```

```
Vec2=[F(:,2),Fn(:,1),Fn(:,2)];  
Vec3=[F(:,3),Fn(:,2),Fn(:,3)];  
Vec4=[Fn(:,1),Fn(:,2),Fn(:,3)];  
F=[Vec1,Vec2,Vec3,Vec4];  
end
```

```
Error using dbstatus  
Error: File: C:\Users\pimst\Documents\Master tu\Year 2\Paper  
\hullmethod_appendix.m Line: 38 Column: 36  
Invalid use of operator.
```

Published with MATLAB® R2018b

```

%Optimization:

% Load the accelerationset so the wrench set can be created
load('acceleration_set')
rdd=acceleration_set(1:3,:);
thetadd=acceleration_set(4,:);
amax=max(acceleration_set(1,:));

% Specs of the load/product
mass_ee=0.1;
I_theta=2.8e-4;

% Setting remaining constant values for the hull method and line
search
fmin=10;
fmax=100;
lambdamin=0;
lambdamax=3;
maxiter=100;
ebs=0.01;
lcablemax=4;
ni=4;           % #of subdividing the triangles into 4 smaller
               triangles

S=3;           % safety factor for the constraints

% Concept specific parameters
n_constr=5; % number of constraints that are applicable to this
           concept

% Performing optimization
nvars=6;           % number of variables
lb=[0.5,0.05,0.02,0.02,0,0]; % lower bounds of the variables
ub=[2,1,0.2,0.2,0.05,0.05]; % upper bounds of the variables

OPTIONS= optimoptions('particleswarm','Display','iter');
[X,fval] = particleswarm(@(X)
    obj_conc2(X,rdd,thetadd,mass_ee,I_theta,fmin,fmax,lambdamin,lambdamax,maxiter,ebs

% At every paricleswarm evaluation the workspace volume is computed
with
% the hull-method for given variables, finding the variables with the
% largest workspace.

Error using load
'acceleration_set' is not found in the current folder or on the MATLAB
path, but exists in:
    C:\Users\pimst\Documents\Master tu\Year 2\Dynamic Cable Robot
Models\optimization2.0\concept2\constraint_optim
    C:\Users\pimst\Documents\Master tu\Year 2\Dynamic Cable Robot
Models\optimization2.0\concept2
    C:\Users\pimst\Documents\Master tu\Year 2\Dynamic Cable Robot
Models

```

```

% Adept cycle in G-Code
clear all
close all

% INPUTS:
%Cycle time:
T=3;

%Sample rate:
rate=40;

%Pause time at start and end of code
pausetime=3;

%Geometry:
a1=[-1.17275;0.06025;0.938535];
a2=[1.17275;0.10425;0.938535];
a3=[1.22275;-0.10425;0.938535];
a4=[-1.22275;-0.06025;0.938535];
a5=[-1.22275;0.10425;-0.938535];
a6=[1.22275;0.06025;-0.938535];
a7=[1.17275;-0.06025;-0.938535];
a8=[-1.17275;-0.10425;-0.938535];
a=[a1,a2,a3,a4,a5,a6,a7,a8];
b1=[-0.0275;0.493;0.0145];
b2=[0.0185;0.475;0.021];
b3=[0.01875;-0.475;0.0125];
b4=[-0.01875;-0.475;0.0125];
b5=[-0.0275;0.493;-0.0145];
b6=[0.0185;0.475;-0.021];
b7=[0.01875;-0.475;-0.0125];
b8=[-0.01875;-0.475;-0.0125];
b=[b1,b2,b3,b4,b5,b6,b7,b8];
Dwheel=0.0265;

% Generate trajectory:
[x,z,theta]=adeptcycle_coordinates(T,rate);
x=x*-1;
y=-z;
z=zeros(1,length(x));
X=[x;y;z];

% Convert to cable lengths / cable rates:

% Determine cable lengths at the workspace centre:
X0=[0;0;0];
theta0=0;
L0=pos2length(theta0,X0,a,b,Dwheel);

% Determine cable length for each sample along the trajectory
m=size(a,2);
L=zeros(length(x),m);

```

```

dL=zeros(length(x),m);
for i=1:1:length(x)
    L(i,:)=pos2length(theta(:,i),X(:,i),a,b,Dwheel);
    dL(i,:)=(L(i,:)-L0)*1000;% cable length in mm compared to zero
    position
end

% Determine cable speed for each sample along the trajectory
dL_speed=zeros(length(x),m);
max_speed=zeros(length(x),1);
max_speed(1,1)=100; %mm/min max speed for going to initial
    position
for j=2:1:length(x)
    dL_speed(j,:)=60*abs(dL(j,:)-dL(j-1,:))*rate;
    % cable length change in mm/min
    max_speed(j,1)=max(dL_speed(j,:));
    if max_speed(j,1)<=0.001
        max_speed(j,1)=0.001;
    end
end

% Convert to G-Code:
Tms=T*1000;
filename = sprintf('adeptcycle_ T%.0f_rate%d.txt', Tms,rate);
formatSpec= ...
'G90 G01 X=%+.3f Y=%+.3f Z=%+.3f A=%+.3f B=%+.3f C=%+.3f U=%+.3f W=%
+.3f F%.3f\n';

fileID = fopen(filename,'w');
fprintf(fileID,'G04 %u\n',pausetime);
fprintf(fileID,'#FGROUP WAXIS\n');
for k=1:1:length(x)
    fprintf(fileID,formatSpec,dL(k,1),dL(k,2),dL(k,3),dL(k,4),dL(k,5), ...
        dL(k,6),dL(k,7),dL(k,8),max_speed(k,1));
end
fprintf(fileID,'G04 %u\n',pausetime);
fprintf(fileID,'M30');

Undefined function 'adeptcycle_coordinates' for input arguments of
    type 'double'.

Error in G_code_generation_adeptcycle_appendix (line 37)
[x,z,theta]=adeptcycle_coordinates(T,rate);

```

Published with MATLAB® R2018b